Republic of Iraq
Ministry of Higher Education
and Scientific Research
University of Babylon

EXPERIMENTAL INVESTIGATION OF THE STABILITY OF CELLULAR COFFERDAMS

A Thesis
Submitted to the College of Engineering
of the University of Babylon in Partial
Fulfillment of the Requirements
for the Degree of Master
in Water Resources
Engineering

By
Hayder Sami Mohammed Al-Khyatt
(B.Sc. Civil Engineering)

October, 2009

بِسْمِ اللَّهِ الرَّحْمَنِ الرَّحِيمِ

عَلَّمَ الْإِنْسَانَ مَا لَمْ يَعْلَمْ (العلق: ٥)

صَدَقَ اللهُ العليُّ العظيمْ

Dedication

TO

MY FAMILY

AND

EVERYONE WHO'S

WISHING US TO LIVE IN PEACE

Examining Committee Certificate

We certify that we have read this thesis entitled **"Experimental Investigation of the Stability of Cellular Cofferdams"**, and as an examining committee, examined the student **"Hayder Sami Mohammed AL-Khyyat"**, in its contents and what related to it, and that in our opinion it meets the standard of a thesis for the degree of Master of Science in Civil Engineering in field of specialization is **Water Resources Engineering.**

Signature:
Name: **Asst. Prof. Dr. Saleh I. Khassaf**
(Member)
Date: 26 / 10/ **2009**

Signature:
Name: **Asst. Prof. Dr. Abdul-Hassan K. Al-Shukur**
(Member)
Date: 28 /10/ **2009**

Signature:
Name: **Asst. Prof. Kadhim N. AL-Ta'ee**
(Supervisor)
Date: 25 / 10/ **2009**

Signature:
Name: **Prof. Dr. Abdul-Hadi A. Al-Delewy**
(Supervisor)
Date: 25/10 / **2009**

Signature:
Name: **Prof. Dr. Nameer A. Alwash**
(Chairman)
Date: 1 / 11 / **2009**

Approval of the Civil Engineering Department

Signature:
Name: **Prof. Dr. Ammar Y. Ali**
Head of the Civil Engineering Department.
Date: / / **2009**

Approval of Deanery of the College of Engineering

Signature:
Name: **Prof. Dr. Adil A. Alwan**
Dean of the College of Engineering.
Date: / / **2009**

CERTIFICATION

We certify that the preparation of this thesis entitled **"Experimental Investigation of the Stability of Cellular Cofferdams"**, was prepared by **"Hayder Sami Mohammed AL-Khyatt"**, under our supervision at Babylon University in partial fulfillment of the requirements for the degree of Master of Science in Civil Engineering with field of specialization in Water Resources Engineering.

Signature: K. N. Al taee

Name: **Asst. Prof. KADHIM N. AL-TAEE**

Date: 22/ 2/ **2009**

Signature: A- Hadi Delewy

Name: **Prof. Dr. Abdulhadi A. Al-Delewy**

Date: 22/ 2/ **2009**

ACKNOWLEDGMENTS

I wish to express my deepest gratitude to my supervisors: **Prof. Dr. Abdul-Hadi A. Al-Delewy** and **Asst. Prof. Kadhim N. Al-Ta'ee** for their continued valuable guidance and encouragement during the preparation of this work.

Many thanks to the head of civil engineering department **Dr. Ammar Yaser** and to the staff of laboratory of soil for their help and advice.

Thanks are also presented to the library staff of the college of engineering for their assistance through the course of this work.

Hayder Sami Mohammed
2009

ABSTRACT

In this research models of circular cellular cofferdams were constructed and tested in the laboratory of soil of the Civil Engineering Department, aiming at investigating the stability of cellular cofferdams. This has been achieved through testing the models for three cases of isolated circular cofferdams with different width (b) to height (H) ratio $(\frac{b}{H})$, with five types of soil fill. The evaluation of Cummings design method has also been studied in this research.

The tests indicated the following:

The cells filled with subbase were more stable against sliding at different $(\frac{b}{H})$ ratio, the cells filled with sand passing No.8 were more stable against overturning at different $(\frac{b}{H})$ ratio.

Minimum percentage of decreasing in resistance of the cell if the $(\frac{b}{H})$ ratio decreasing from (1.0 to 0.85) is nearly (28%) when the cell filling with subbase, if the $(\frac{b}{H})$ ratio decreases from (0.85 to 0.75). The minimum percentage of decreasing in resistance is nearly (28%) when the cell filling with sand passing No.8, and if the $(\frac{b}{H})$ ratio decreases from (1.0 to 0.75) the minimum percentage of decreasing in resistance of the cell is nearly (36.25%) when the cell is filled with clayey sand.

CONTENTS

LIST OF FIGURES

LIST OF TABLES

LIST OF SYMBOLS

Symbols	Notations
b	Equivalent width of the cell
F.S	Factor of safety
$F.S._{hs}$	Factor of safety against horizontal shear
$F.S._{SL}$	Factor of safety against slippage failure
$F.S._{vs}$	actor of safety against Vertical shear
f	Coefficient of friction of cell fill
f_{ss}	The coefficient of friction of steel on steel
H	Height of the cell
K_a	Active earth pressure
K	Coefficient of lateral earth pressure
M	Moment due to external force
M_{max}	Maximum resisting moment
M_o	Overturning moment
M_r	Resisting moment
M_t	Total resisting moment
P	Lateral load
P_a	Active pressure
P_p	Passive pressure

Symbols	Notations
r	Radius of circular cell
S_1	Shearing resistance along the center of the cell
S_2	Shearing resistance on the neutral plane per unit length
t	Interlock tension
t_{max}	Maximum interlock tension
V_{max}	Maximum vertical shear stress
W	Effective weight of cell fill
y	Height of lateral load above the ground surface
y_{cr}	Critical height
ø	Angle of internal friction of soil
$\bar{\gamma}$	Unit weight of the soil
δ	Friction angle between the fill and the sheetpile

CHAPTER ONE

INTRODUCTION

CHAPTER ONE INTRODUCTION

1.1 GENERAL

There are many construction projects to be executed inside the water such as piers of bridges or weirs, or close to water such as docks. Such an execution is relatively difficult because of the expected seepage of water unless the area of construction is protected against water.

There are many ways of a such protection. One of these ways is by using a temporary structure, called cofferdam. A cofferdam serves through surrounding the area of construction to prevent water from access. One type of cofferdams is the cellular cofferdam.

The purpose of the cofferdam is to retain a hydrostatic head of water or to provide a lateral support to the mass of soil behind it. However, the cofferdam is subjected to unbalanced lateral forces acting at different heights. These unbalanced forces will tend to produce a resultant moment which tends to overturn the cofferdam or to produce a resultant force which tends to slide the cofferdam on its base. The resisting forces and moments against the sliding and overturning vary in magnitude from soil to soil depending on the unit weight and the coefficient of friction of the soil. A clayey soil forms a critical case in this respect, **[Al- Chalabi, (1959)]**.

The cellular cofferdam was first developed as a temporary structure to exclude water from an excavation and allow construction in the dry. It is now used with increasing frequency as either a temporary or permanent structure retaining soil, water, or both. Cellular cofferdams are used lieu of earth or rock

fill cofferdams when the width of the structure must be small, when a vertical face is required, or when stability against scour is required. Permanent cellular cofferdams are performing well as dock walls, piers, and retaining walls **[Bowles, (1997)]**.

Meanwhile, a cellular cofferdam is usually constructed of steel sheetpiles and used primarily as a water-retaining structure. However, its stability depends on the interaction of the soil used to fill the cell and the steel sheetpiling, whereas either material, if used alone, would be unsatisfactory. Both materials in combination provide a satisfactory means to develop a dry work area in water-covered sites such as construction projects areas close to ocean, lakefront, or a river. One of the most common shapes of a cellular cofferdam is the circular, as shown in Fig. (1-1).

1.2 OBJECTIVE OF THE RESEARCH

The main objective of this research is to study a more stable circular cellular cofferdam (materials and dimensions) to withstand sliding and overturning.

1.3 METHODOLOGY OF THE RESEARCH

The methodology of research can be summarized as follows:

1- The research will be based on laboratory testing of models of circular cellular cofferdams with different depth to radius ratio.

2- The tested models will be built with different types of soil, aiming at finding the best case that offers the more resistance against sliding and overturning forces.

Fig.(1-1): Circular cellular cofferdam.

CHAPTER TWO

LITERATURE REVIEW

CHAPTER TWO
LITERATURE REVIEW

2.1 HISTORICAL BACKGROUND

Cofferdams, in their simplest form, were found in ancient times. The Mesopotamian rivers, for example, were edged in many places with wooden box cofferdams filled with soil to protect the land from the floods. Beside the simplicity of the structure they were basically functioning to retain a hydrostatic head of water.

The first cellular cofferdam was built in the United States of America in 1908-1909 at Black Rock Harbor, Buffalo, New York. This cofferdam was a rectangular type and it consisted of 70 cells of (9×9 m). It was built on rock foundation. This idea led Major-General Harley B. Ferguson, Corps of Engineers, U.S. Army to use the circular cells in constructing the cofferdam for raising the battleship "Maine" which had been sunk in the harbor of Havana, Cuba in 1910. This was the first recorded application of a circular cellular cofferdam; the cells were filled with clay and rested on a stratum of soft silt and clay underlain by a stratum of medium clay. The first diaphragm type cellular cofferdam was built in Troy, New York. It was built for constructing Troy's dam and lock. In this cofferdam the inner and outer walls of the cofferdam were arcs; **[Al-Chalabi, (1959)].**

Fourteen cofferdams were built by the Tennessee Valley Authority (TVA) for their various projects. The first of these projects requiring cellular cofferdams was the Pickwick Landing Dam. In this case a circular type was used. It was successful and economical. Since then the circular type was adopted by the TVA in all the Tennessee River projects; **[TVA, (2003)].**

2.2 LABORATORY STUDIES

A popular approach to investigate the behavior of cellular structures has been explained through model studies. In general, these studies have consisted of relatively small scale models loaded to failure. Cell stability, i.e., determination of the force or moment required for failure, has been of primary concern.

Polivka, (1945) involved a series of tests on a five-cell model of cofferdam during Polivka preliminary investigation on cellular cofferdams in the Kaiser shipyards at Richmond, California. The testing set-up consisted of five circular cells, (75mm, 100mm, 125mm, 150mm, and 175 mm) in diameter, (150 mm) high and arranged in an arc shaped wall. The cell walls consisted of a continuous cylinder, made from (0.1 mm) thick sheet metal. In this study, Polivka attempted to correlate the model test results with field data and Terzaghi's theory of vertical shear. Polivka found that the coefficient of earth pressure decreases with an increase of H/R ratio, where H is the height and R is the radius of the cell, and the total resistance against slippage increases with increasing the radius.

Cummings, (1957) contained the results of model studies of cofferdams on rock. It is probably the best known model study and forms the basis for his theory of internal cell failure by horizontal shear. Cummings' model consisted of (612.5 mm) diameter, (600 mm) high circular cells and equivalent rectangular cells with (487.5 mm× 612.5 mm). Wood staves, (7.8 mm× 37.5 mm), were used as model sheetpiles. These staves were held together by a thin wire threaded through screw-eyes located at the top, middle, and bottom of the sheetpiles. Each cell was threaded together loosely, with little contact between the wood staves, so that very little friction could be developed between model

sheetpiles. All the cells rested on a rough concrete base (25 mm) thick. The fill consisted of crushed rock. Lateral loads were applied by a wire loop at (⅓ H) [where (H) is the height of the cell]. Cable loads were measured with proving rings. Cummings was also concerned with the change in the state of stress in the fill resulting from lateral loads. Pullout tests of wood staves buried in the cell fill were conducted before and after application of the lateral load to provide data for calculation of the aforementioned stresses in the fill.

Cummings found that pullout tests conducted on laterally loaded cells indicated an increase in lateral pressure occurred within the cell fill at the loaded side of the cell. He found that the plane of rupture goes from the top of the pressure side to the bottom inner corner (toe of cofferdam). The cell fill in the rupture region acts essentially as a surcharge and only the soil below the failure plane will develop shear resistance, as shown in Fig. (2-1).

Burki and Richards, (1975) developed a method to determine elastic stresses inside the soil mass of a cofferdam by using photoelastic technique. A cofferdam model was fabricated simulating the soil mass with gelatin and the

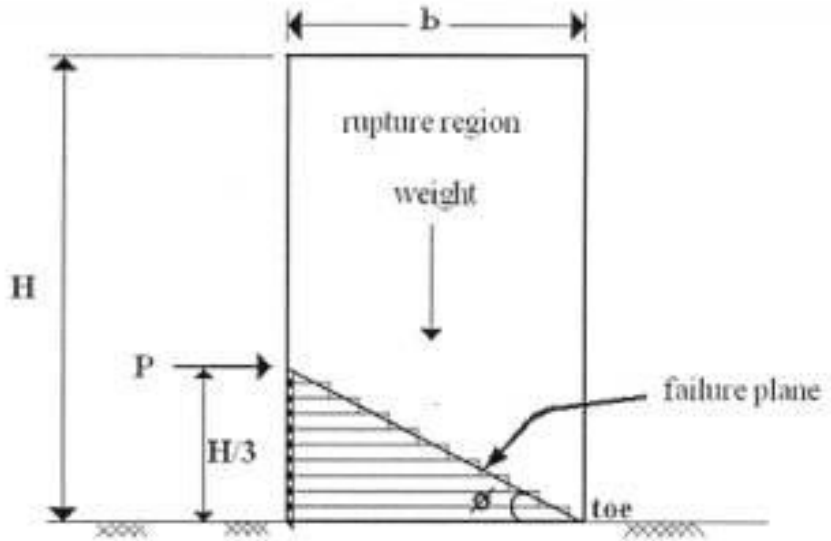

Fig. (2-1): Cell fill resistance to lateral force; **[Cummings, (1957)].**

steel sheetpiles with urethane rubber. This model was tested in a state of plain strain, and, from the photoelastic data, elastic stresses within the fill material were found due to both gravity loading and water pressure. In the gravity loading case, normal stresses agreed with the standard theory of soil mechanics for geostatic stresses. Water pressure introducing bending was found to affect the stresses appreciably causing a nonlinear distribution of stresses and pressure on the base of the cofferdam. Contrary to many theories, shear stresses were found to be higher near the sheet pile walls than the midplane. New failure surfaces, in accordance with the elastic stress state, were postulated.

Maitland and Schroeder, (1979) performed a series of model tests. The process involved four large model circular cells and three smaller cells. The larger models consisted of a single circular cell (1225 mm) in diameter and constructed of 58 interlocking sheetpiles and two connecting arcs (525 mm) in diameter, each constructed with 12 sheetpiles. Total sheetpiles lengths from (1200 mm to 1800 mm) with embedment depth below the dredgeline ranging from (0 mm to 600 mm). The smaller cells were (600 mm) in diameter. The proportions of embedment depth to cell height corresponded to those used for the larger cells.

A uniformly graded subangular sand was used during the study. Loads were applied incrementally and continued until large cell deflections had occurred by a steel cable loop (200*100 mm). Timber was used as a loading yoke. Deflections of the front sheets, sheetpile strains, and cable force were monitored throughout cell failure. The model test results were related to field data and with Terzaghi's theory of vertical shear. Terzaghi found that the ultimate overturning capacity of the model cellular structures was best predicted by:

$$M_{max} = \frac{1}{3}\,\bar{\gamma} * b * k * H^2 * (\tan \emptyset + f) \qquad (2\text{-}1)$$

where:

M_{max} = maximum resisting moment $(\frac{N.m}{m})$;

$\overline{\gamma}$ = effective unit weight of cell fill $(\frac{N}{m^3})$;

b = equivalent width of cell (m);

k = coefficient of lateral earth pressure;

H = height of cell (m);

$\emptyset$ = angle of internal friction of cell fill;

f = coefficient of interlock friction for sheetpiles.

Al-Taee, (1990) studied the design and construction of cellular cofferdams through test models to observe their stability. Series of laboratory tests have been carried out on one, two, and three diaphragm cells of different width to depth ratios, as well as a rectangular and an isolated circular cell. The tests included the study of the following factors: effect of height, width, length, embedment depth, and loading height. Additional tests were carried out on an instrumented diaphragm cell to determine the distribution of the bending moments and hoop tensions.

Many conclusions had been drawn from this study. Among these are the load capacity in sliding failure is greater than that of overturning failure, and the embedment depth is greatly affected the stability of cells.

Horiuchi et al., (1992) studied the construction of a man-made island using a cofferdam and fill, considering the problems which are often encountered in this regard, such as sliding failures of a soft seabed or ruptures of the cofferdam. A new filling method, underwater placement of light and self hardening slurry, presents great advantages that were confirmed by theoretical analysis. Appropriate slurry for this new method, containing fly ash, volcanic ash, and a small amount of cement, was developed from experimental

investigations. This light, self-hardening slurry greatly reduces the earth pressure and increases the safety factor of the island, and it also makes subsequent construction work easier. Strength development of the slurry is inhibited by low temperature, but this can be compensated for by a small increase in the cement content. Practical slurry compositions were also proposed based on laboratory studies, which included test-tank tests. It was concluded that underwater placement of fly-ash slurry was a viable method for man-made island construction.

Mohammod et al., (2001) behavior of double sheetpile wall cofferdam on sandy soil subjected to high water was studied through a series of centrifuge model tests. Model ground and fill of the cofferdam were made by fine silica sand in a rectangular model container. The model double sheetpile wall cofferdam consisted of two aluminum sheetpile walls, tie rods at the top and also at ground level. Various factors affecting stability of the cofferdam were examined. Under 70g, water was fed into the upstream of the cofferdam to simulate high floodwater until the water level reached nearly to the top of the cofferdam or large deflection of the cofferdam was observed. Test results imply that: (i) the shear deformation of the fill dominates the failure mechanism of the cofferdam, (ii) as the width of the cofferdam increase, the water height at failure increases, (iii) to a certain depth the embedment does not appreciably increase the resistance against high water, (iv) the relative density of the fill and the friction between the walls and the fill contribute to the resistance of the cofferdam against the shear deformation of the fill, (v) the sheetpile wall at the downstream is subjected to higher stresses than the sheetpile wall at the upstream and (vi) double layers of tie significantly increase the lateral resistance of the cofferdam against high water.

2.3 FIELD STUDIES

White et al., (1963) contained the results of a comprehensive field investigation of a 33- circular cell bulkhead at pier E in Long Beach Harbor, California. Tests were conducted on bulkheads (18.6 m) in diameter with connecting arcs (4.87 m) in radius and retain a (16.5 m) height of fine silty sand fill. Sheetpiles were instrumented to measure hoop stress in the steel. Piezometers and settlement plates were used to observe the generation of pore water pressure and settlements in the fill. The deflections of sheetpiles were measured by a driftmeter. The free water level in the cell and tidal fluctuations were also monitored. From this study, it was found that the maximum hoop tension occurred at level 4 as shown in Fig. (2-2), approximately at the original ground level. The coefficient of lateral earth pressure was found to be equal to (0.66) during the filling of the cell, dropped to (0.54) shortly after the cell was filled, and to (0.53) two years after construction; the soil in the cell required 10 days after completion of filling to reach approximately (90%) consolidation.

Alizadeh, (1973) studied the site investigations, dewatering, design, construction procedures and observations, and stress measurements during construction of a circular land cofferdam for a (24.0 m) deep excavation for construction of a car dumper structure for Oak Creek Power Plant in Oak Creek. The cofferdam consisted of wood lagging, four levels of concrete ring beams, and a lower caisson section. The concrete ring beams were instrumented with mechanical strain gages. Apparent earth pressure diagram computed from the results of the instrumentation was presented. Design and construction of the caisson section and the dewatering system were also examined.

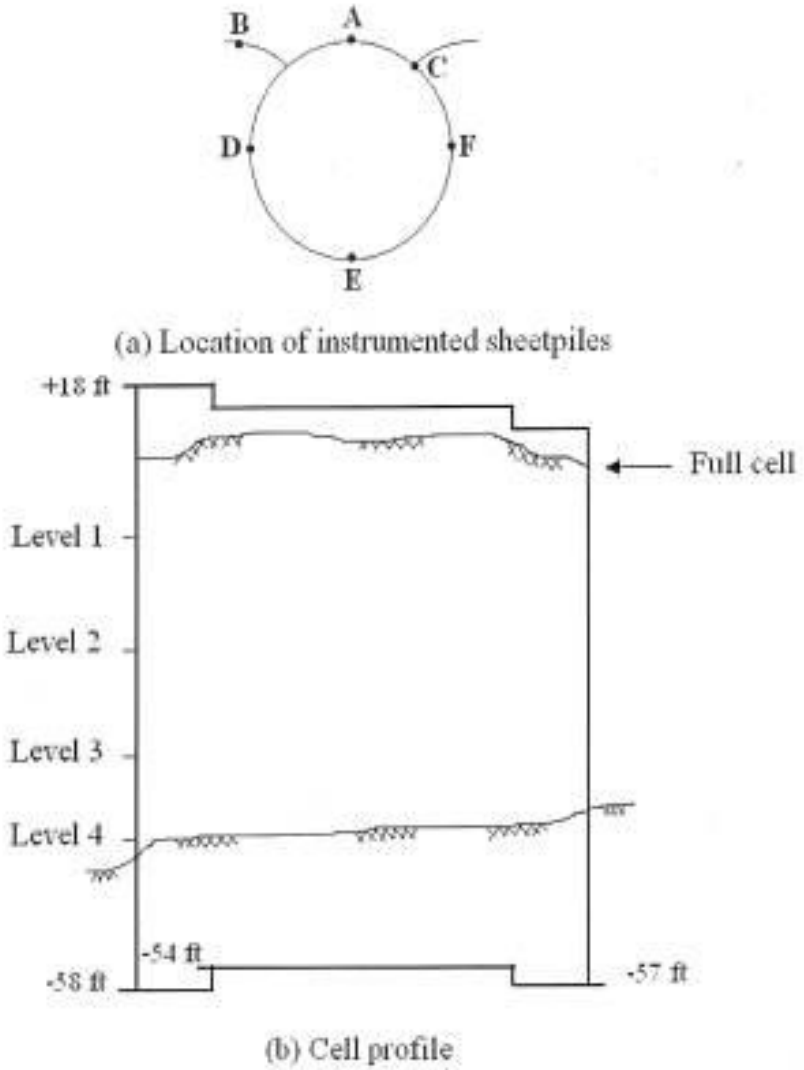

Fig.(2-2): Long beach cell [After White et al., (1963)]

Thomas et al., (1975) studied the failure that happened in the cofferdam around the uniontown locks and dam on the Ohio River, ten days after dewatering the project area during a rising river period. The configuration of the failure in the highly faulted shale foundation occurred as a block transition, sliding horizontally on a relatively soft underclay. There were no relief drains within the cofferdam nor piezometers to monitor uplift forces. The design of the pier foundation was changed from open cut on three shales to drilled caissons on the most competent of the three shales.

Schroeder et al., (1977) performed investigation on 12-cell wharf at Terminal No.4 along the Willamette River in Portland, Oregon. Figure. (2-3) shows the general layout of the project. Individual cells are (19.74 m) in diameter, spaced (25.74 m) center to center, a freestanding height of (20.1 m), and connecting arcs which have a radius of (4.32 m). Vibrating wire strain gages were used to monitor strains at four elevations on eight different sheetpiles as shown in Fig. (2-3). Besides, inclinometer casings were attached to the outside of instrumented sheetpiles to measure horizontal deformations, while land-based surveys measured cell crest movement and sheetpile settlement during construction. The free water level in the cell was also monitored and compared with the adjacent river level. From this study, it was found that the maximum interlock force in the cell was also near the dredgeline and the lateral earth pressure values recommended by Terzaghi are adequate for design.

Schroeder and Maitland, (1979) made field and laboratory research on cellular sheetpile structures. Design for both internal stability and overall stability were considered. It was proposed that for cellular bulkheads embedded in sands, neither sliding nor overturning can occur before a cell fails by tilting in the vertical shear mode. Guides for interlock force analysis and selection of lateral earth pressure coefficients for a newly proposed vertical shear model were given.

Sorota and Kinner, (1981) presented a description of design of a steel sheetpile cellular cofferdam that was required for construction of a graving drydock. The cofferdam was constructed approximately (168 m) offshore within the Hood Canal of Washington State and was required to retain (24 m) of water after basin dewatering. Interlock tensions associated with the required cell diameter in this deep water location resulted in one of the first United States cofferdam applications of high strength steel sheetpiling and extruded wye

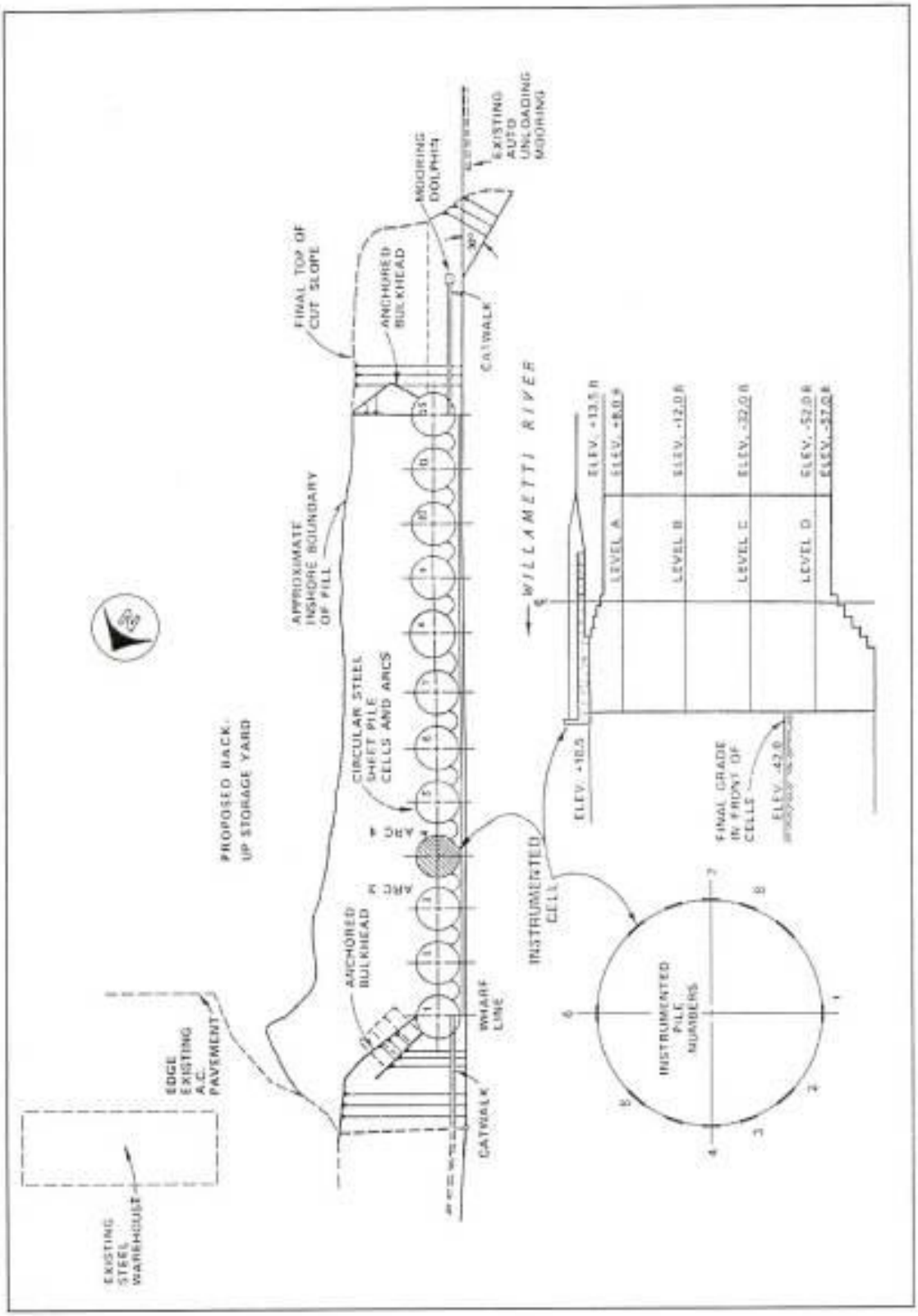

Fig. (2-3): Terminal No.4 [After Schroeder et al., (1977)]

connections. Much of the cofferdam was designed to be permanent to provide in-service laydown areas adjacent to the completed drylock. Items discussed include the need for two pumped dewatering systems, the need for vibratory probe compaction of the cell fills, site soil conditions, dredging, and steel sheetpile corrosion protection.

2.4 THEORETICAL STUDIES

Esring, (1970) performed examination on the case of failure of cellular cofferdams by sliding along vertical planes (vertical shear). The Terzaghi and Krynine approaches to evaluate stability against vertical shear led to conclusions that were shown to be contrary to engineering expectations and difficult to accept. No reasonable failure mechanism that permits sliding along vertical planes was uncovered in the examination. It was suggested that if a measure of stability against failure by vertical shear was desired then the cellular cofferdam should be assumed to fail in simple shear. Failure by simple shear implies a near-vertical failure surface and a ratio of horizontal to vertical stress equal to one. However, it was also suggested that it may be better to ignore vertical shear entirely.

Rossow, (1984) proposed a method for calculating the interlock tensions in the sheetpile walls of a circular cellular cofferdam. A horizontal strip of unit width of wall was considered and the governing equations were derived from equilibrium and compatibility requirements for the strip. The pressure of the cell fill against the sheetpile walls was assumed known. Numerical examples were presented in which interlock tensions in the arc cell, main cell, and common-wall were calculated for various pressures. Bulging of the cell walls and rotation

of the legs of the connecting Y were also found. The calculations provided theoretical justification for using of the equation for estimating the force in the common wall and led to a generalization of that equation. Rossow stated that the method may be applied to other sheetpile wall configurations beside those of a circular cofferdam.

Al-Shamkhi, (1992) the investigation concerns the analysis and behavior of cellular cofferdams under lateral loadings involving, backfilling, water pressure, and fillings.

The analysis process is conducted by development of computer program using finite element method. The triangular axisymmetric ring element has been employed to represent the soil fill, and cylindrical shell element to represent the sheetpile wall.

The computer program is applied to solve the full scale circular cofferdams. Comparison with field observations and evaluation of the current methods of analysis which have been involved in this study.

The results indicate that, the maximum radial displacement and maximum hoop tension are taking place at $(\frac{1}{6})$ of the height above the ground surface.

During loading, the settlement is maximum at the cell center and decrease as the distance from that center increase.

Peng et al., (2007) based on the hydraulic computation theory, a hydraulic numerical model describing an overflow cofferdam during multi - phase diversion is presented to achieve the discharge capacities, stream wise water levels, velocities of both overflow cofferdam and narrowed river. The validity of the model was checked with the observed data of the Xiangjiaba Project in 2005. The calculated values are in good agreement with the observed data.

Chen et al., (2008) during the dam construction, it is possible that a transnormal flood occurs, and then the cofferdam will be broken down, which will cause an enormous effect on the security of the construction and the cities along the lower course. On the basis of the hydraulic model test and numerical computation of the coffer-dambreak, the effect of the cofferdam-break on the lower reach of Jinghong Hydroelectric Station is analyzed. And the result shows that: (1) the gradual breaking of the downstream cofferdam has a tiny effect on the region along the lower course while the breaking of the upper cofferdam will cause a greats effect, and the effect will be vast when the instantaneous breaking happens; (2) the results of numerical computation and observed data from indoor model test are approachable.

Zhang et al., (2008) prestressed anchorage cables in some import cofferdam will be unloaded before the import cofferdam is removed, which can ensure the safe and successful removal of the cofferdam. It involves the order and technique problems of anchorage cable unloading. The anchorage cable unloading order is analyzed by FLAC-3D and optimized. A safe and feasible anchorage cable unloading order scheme is obtained and its technique is studied. The removal of the anchorage cable is implemented by this optimum unloading scheme. At the same time, the deformation of the cofferdam is monitored during the anchorage removal. The measured results show that the deformation of the cofferdam is very small according to the above optimum scheme, namely, the influence of the removal of anchorage cable on the stability of the cofferdam is very little. So it can ensure the subsequent removal of the cofferdam to conduct smoothly.

CHAPTER THREE

TESTING INSTRUMENTS OF THE CELLULAR COFFERDAM STRUCTURES

CHAPTER THREE
TESTING INSTRUMENTS OF THE CELLULAR COFFERDAM STRUCTURES

3.1 GENERAL

A cellular cofferdam is a gravity retaining structure formed from series of interconnected straight web steel sheetpile cells filled with soil, usually sand or sand and gravel. The interconnection provides water-tightness and self-stability against the lateral pressure of water and earth.

3.2 TYPES OF CELLULAR COFFERDAMS

Cellular cofferdams are usually classified according to the configuration and arrangements of the cells. As shown in Fig. (3-1), the three basic types of cellular cofferdams are:

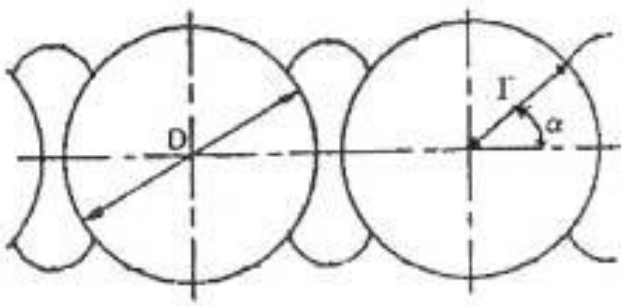

(a) CIRCULAR CELLS

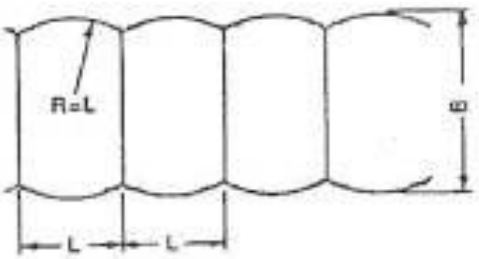

(b) DIAPHRAGM CELLS

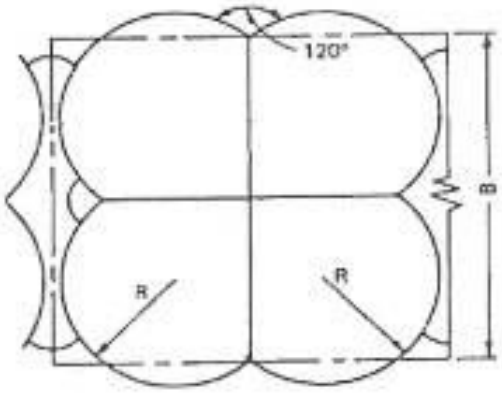

(c) CLOVERLEAF CELL

Fig. (3-1): Cellular cofferdams; [After USS, (1970)].

3.2.1 Circular cells

This type consists of individual large diameter, (D), circles connected together by arcs of smaller diameter. These arcs generally intercept the circles at a point making an angle, (α), of (30 or 45) degrees with the longitudinal axis of the cofferdam, as shown in Fig. (3-1-a). The prime feature of the circular type cofferdam is that each cell is self-supporting and independent of the next. The circular type requires fewer piles per linear foot of cofferdam as compared with a diaphragm type of equal design, as shown in Fig. (3-2), **[TVA, (2003)].**

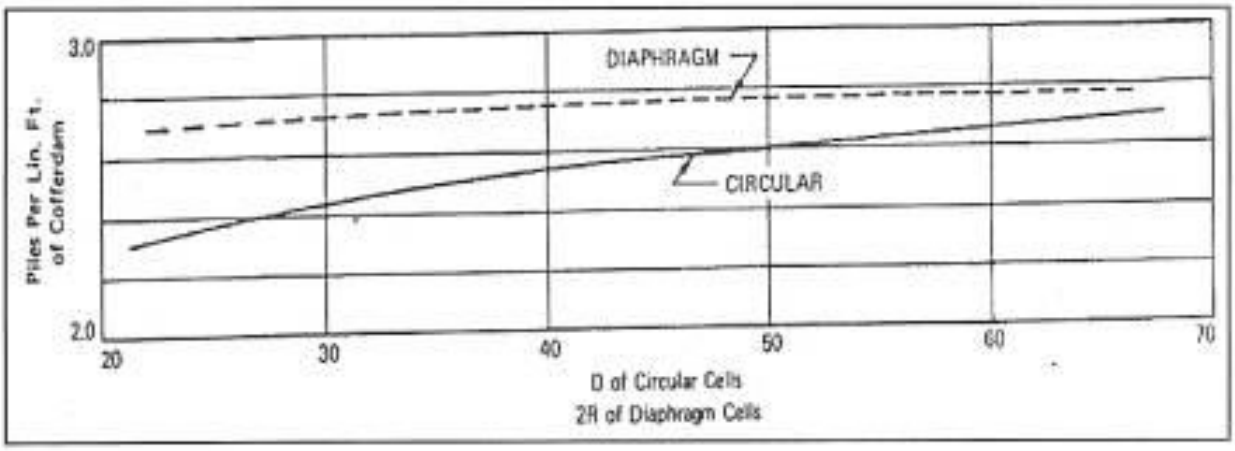

Fig. (3-2): Piling required per linear foot of Cofferdam; [After TVA, (2003)].

3.2.2 Diaphragm cells

This type of cell consists of two series of circular arcs connected together by diaphragms perpendicular to the axis of the cofferdam. It is a common practice that the radii of the arcs and the diaphragm make angles of 120 degrees with each other, as shown in Fig. (3-1-b).

The diaphragm type cofferdam can easily be widened by increasing the length of the diaphragms. This increase will not raise the interlock stress, which is a function of the radius of the arc portion of the cell. At any given level, there is a uniform interlock stress throughout the section. The stress is smaller than that at the joint of a circular cell of an equal design, **[USS, (1970)]**.

3.2.3 Cloverleaf cells

This type of cell is a modification of the circular cell. It is generally employed for cases of large head where the large diameter required by stability would result in excessively high interlock stress if diaphragms were not added. As illustrated in Fig. (3-1-c). The cloverleaf cell uses more steel than circular or diaphragm types cells. It is adaptable to greater heights, **[USS, (1970)]**.

3.2.4 Modified types

In a few cases where stability is not a problem, it may be possible to eliminate or change certain arcs in the circular or diaphragm arrangements, as shown in Fig. (3-3), **[Bowles, (1997)].**

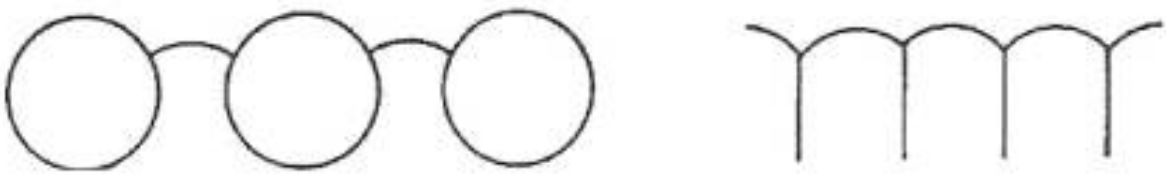

(a)Modified circular type. (b) Modified diaphragm type

Fig. (3-3): Modified cellular cofferdams; [After Bowles, (1997)].

3.3 CONNECTION TYPES

The major components of cellular cofferdams are the steel sheetpiling for the cells, the cell fill, and the earth berms (that are often used to increase stability).

Straight sheetpile sections permit a maximum deflection angle of (10) degrees. When larger deflection angles are required for small diameter cells, standard bent piles are available as shown in Fig. (3-4-a). Junction points in cellular cofferdams require special prefabricated pieces, commonly (90) degree (T's) and (30) and (120) degree (Y's). These standard connections are also shown in Fig. (3-4), (b, c, and d), **[USS, (1970)].**

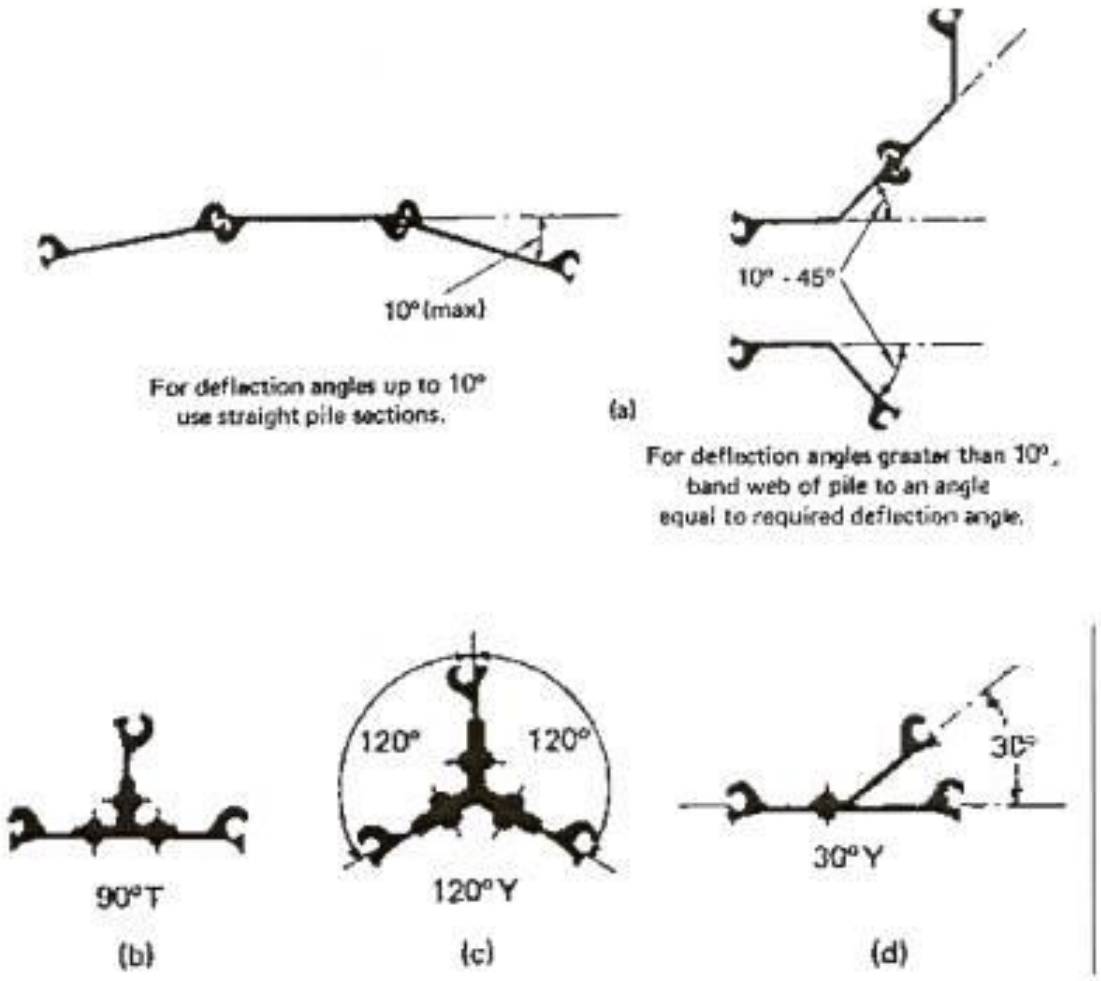

Fig. (3-4): Types of steel sheetpile and connections for cellular cofferdams; [After USS, (1970)].

3.4 EQUIVALENT RECTANGULAR DIMENSIONS

For the purpose of analysis, the cellular structure is replaced by an equivalent rectangular shape. The width, (b), has either the same cross-sectional area or section modulus as the actual cofferdam. TVA engineers have indicated that results of analysis using either method are practically identical, **[TVA, (2003)]**.

TVA engineers have suggested that for a cell of radius (r), the equivalent width, (b), as shown in Fig. (3-5), is given by:

$b = 1.57\,r$ ..... with 90 degree T connection (3-1)

$b = 1.75\,r$ ..... with 60 degree T connection (3-2)

However, Terzaghi recommended, **[Terzaghi, [1945]**:

$b = 1.7\,r$ ..... for circular cells (3-3)

$b = 1.8\,r$ ..... for diaphragm cells (3-4)

The length of the equivalent rectangular circular cofferdam, 2L, is the distance between alternative two centers of arcs.

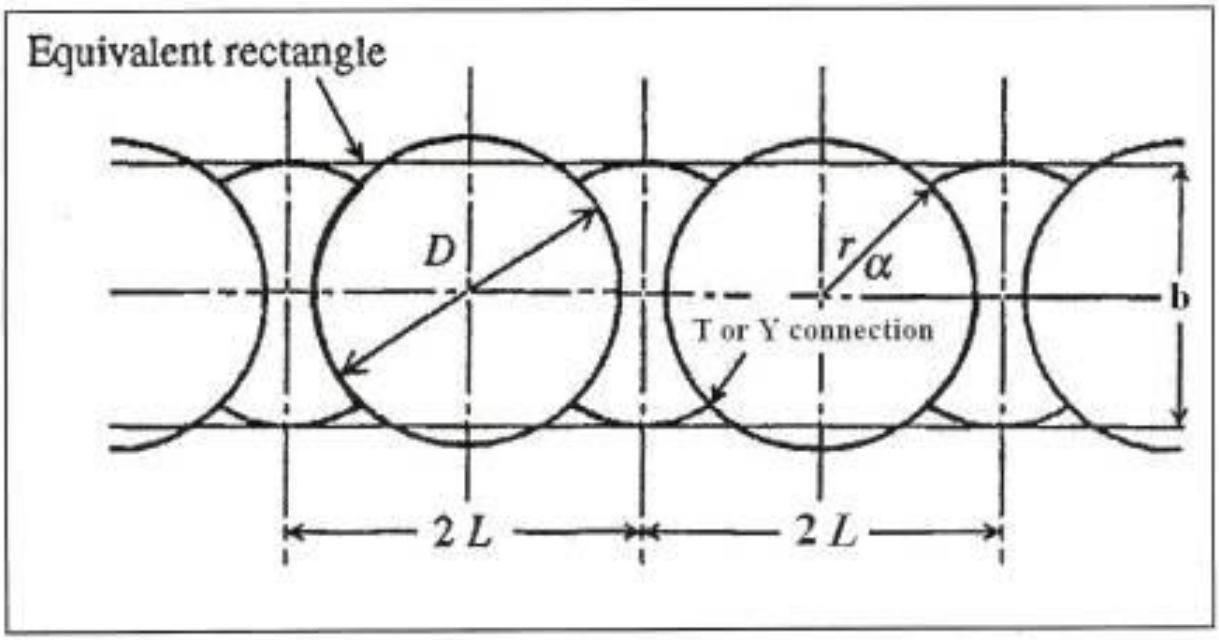

Fig. (3-5): Approximate dimensions of circular cells; [After Bowles, (1997)].

3.5 FAILURE MODES

Under lateral loads, cellular cofferdams may fail in one or more of the following modes:

1- General failure.

2- Local failure.

3.5.1 General failure

In this case the cell is assumed to behave as a unit. General failure includes:

3.5.1.a Sliding failure

This failure takes place when the cofferdam is subjected to unbalanced forces due to water head; these forces cause the cell to slide as a unit along a horizontal plane located under the cell, as shown in Fig. (3-6). That means a shear stress at the base exceeds the shearing resistance, **[Al- Chalabi, (1959)]**.

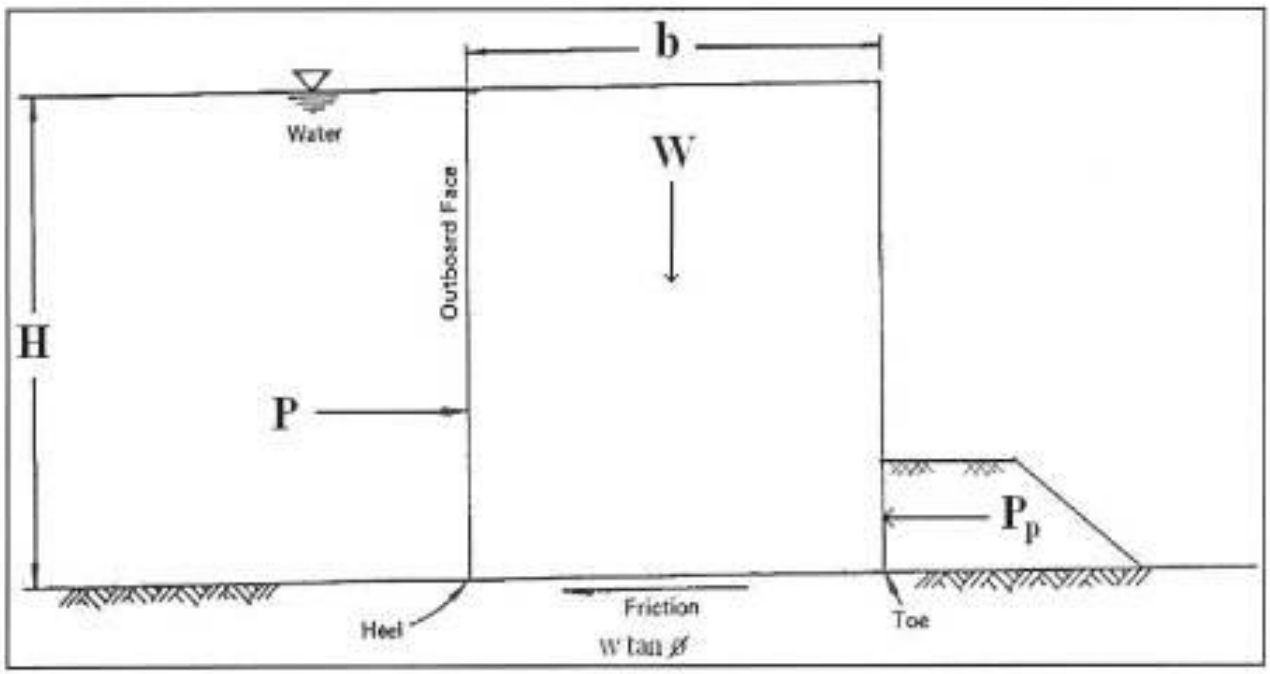

Fig. (3-6): Sliding stability of cell; [After Al-Chalabi,(1959)].

A cofferdam must provide adequate resistance to sliding on the base caused by the unbalanced hydrostatic pressure; a factor of safety against sliding ($F.S_s$) should range between (1.10 to 1.25), **[Bowles, (1997)]**. This number is defined as the ratio of lateral force to potential resisting forces per unit length of the wall which can be calculated as:

$$F.S_s = \frac{f.W+P_p}{P} \qquad (3\text{-}5)$$

where: f =coefficient of friction between the cell fill and foundation at the base of the cell. This is usually taken as $\tan\phi$, where ϕ, is the friction angle of the cell fill.

W = effective weight of cell fill.

P_p = effective passive resistance which depends on the depth of embedment of sheetpiling.

P = total lateral force.

3.5.1.b Overturning failure

Usually the cofferdam is subjected to unbalanced lateral forces at different heights. These unbalanced forces will tend to produce a resultant moment which tends to overturn the cofferdam, **[Al-Chalabi, (1959)]**.

The cell is assumed to rotate about toe. To provide the stability against overturning, the resultant normal force should lie within the middle third of the base as shown in Fig. (3-7), **[Dismuke, (1975)]**.

The cofferdam must be stable against overturning and the factor of safety against overturning ($F.S_{ot}$) should range between (1.1 to 1.25), **[Bowles, (1997)]**. This number is defined as the ratio of resisting moment, (M_r), to the overturning moment, (M_o), which is calculated as follows:

$$F.S_{ot} = \frac{M_r}{M_o} = \frac{\frac{W.b}{2}}{\frac{P.H}{3}} \qquad (3\text{-}6)$$

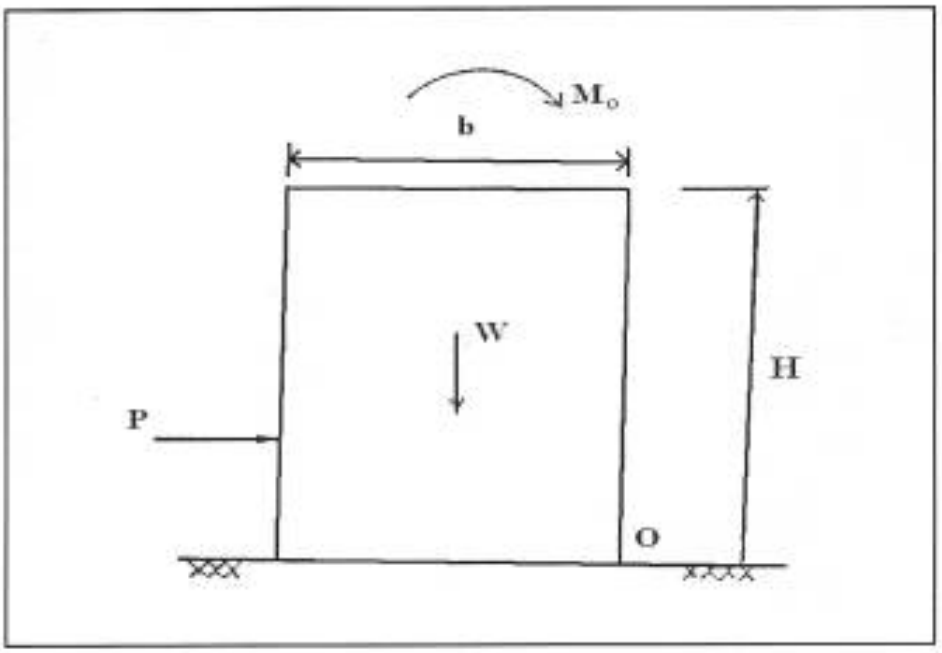

Fig. (3-7): Overturning stability of cell. [After Dismuke, (1975)].

where:

W = weight of cell fill.

b = width of the cell.

P = horizontal pressure, and

H = height of the cell.

3.5.2 Local failure

In this case the failure takes place in the cellular cofferdam parts during its construction or during the overturning or sliding failure taken place, and includes:

3.5.2.a Excessive interlock tension failure

A cell must be stable against bursting pressure. The pressure exerted against the sheets by the fill inside the cell must not exceed the allowable interlock tension. The interlock tension is developed in a cell as a function of the internal cell pressure. The internal horizontal pressure (P) at any depth in the cell

fill is the sum of the earth and water pressures. The earth pressure is equal to the effective weight of the cell fill above that depth times the coefficient of horizontal earth pressure (K). The coefficient is dependent upon the type of cell fill material, **[USACE, (1989)].**

In 1945, Terzaghi showed that (K) must have the value between (0.4) and (0.5). He suggested the empirical value of (0.4), **[Terzaghi, (1945)].**

Krynine suggested the following equation to determine (K), **[Krynine, (1945)]**:

$$K = \frac{\cos\phi}{2-\cos\phi} \qquad (3\text{-}7)$$

where:

ϕ = friction angle of the soil in the cell.

The observations of the deformation of cellular cofferdams indicate that the maximum bulging of the cell occurs in a zone between ($\frac{1}{4}$ to $\frac{1}{3}$) of the height of the exposed portion of the sheetpile above the embedded part of the cell. For design purpose the maximum pressure assume at a point ($\frac{1}{4}$) of the exposed height of the cell above the dredgeline, **[Lacroix et al., (1970)].**

The factor of safety (F.S) against excessive interlock tension is defined as the ratio of the interlock strength as guaranteed by the manufacturer to the maximum computed interlock tension.

Interlock tension is also proportional to the radius of the cell. The maximum interlock tension in the main cell is given by:

$$t = P * r \qquad (3\text{-}8)$$

where:

P = Maximum guaranteed inboard sheeting pressure.

r = radius.

The interlock tension at the connections between the main cells and the connecting arcs is increased due to the pull of the connecting arcs, **[USACE, (1989)]**, as illustrated in Fig. (3-8), and can be approximated by:

$$t_{max} = \frac{P.L}{\cos\phi} \qquad (3\text{-}9)$$

where:

t_{max} = interlock tension at connection.

P = maximum inboard sheeting pressure.

L = as shown in Fig. (3-8).

The factor of safety against interlock failure should be at least 2 **[USS, (1970)]**.

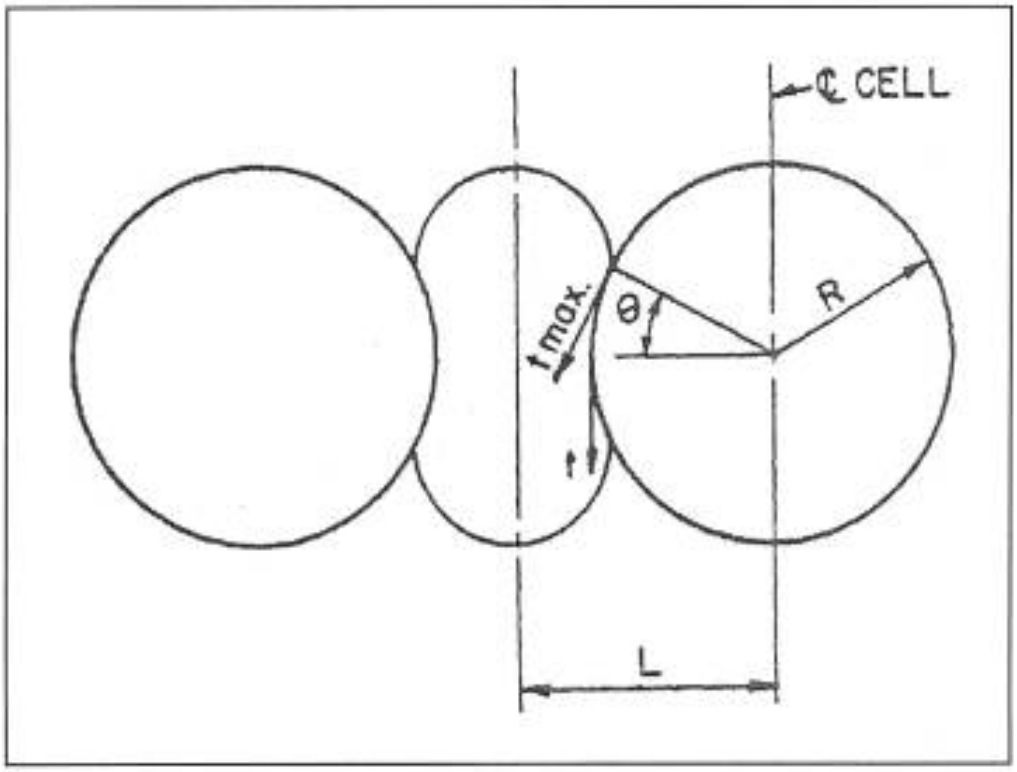

Fig. (3-8): Interlock stress at connection, [After USACE, (1989)].

3.5.2.b Slipping failure between sheeting and cell fill

This mode of failure is frequently takes place between the sheetpiles and surrounding soil. When a cellular cofferdam was subjected to a large overturning moment, there is a tendency for the sheet sheel to rotate about the toe. As the sheet rotates, failure can occur by lifting the outboard piling and losing the cell fill as it runs out the heel of the cell. In such cases slipping occurs between the sheetpiles on the outboard face and the cell fill. The resisting moment with respect to the inboard toe is due to the frictional forces is assumed to be equal to the applied lateral load, (P), times the coefficient of friction between the cell fill and sheetpiles, as shown in Fig. (3-9).

The factor of safety against slippage can be taken as, **[Teng, (1962)]**:

$$F.S._{SL}=\frac{(P\tan\delta)\,b}{P\,(\frac{H}{3})} \qquad (3\text{-}10)$$

where:

$F.S._{SL}$= factor of safety against slippage failure.

δ = friction angle between the fill and the sheetpiles.

Since slippage occurs between the cell fill and sheetpiles, the fill weight does not contribute in the resisting moment. A factor of safety against slippage of at least (1.25) has been recommended, **[Teng, (1962)]**.

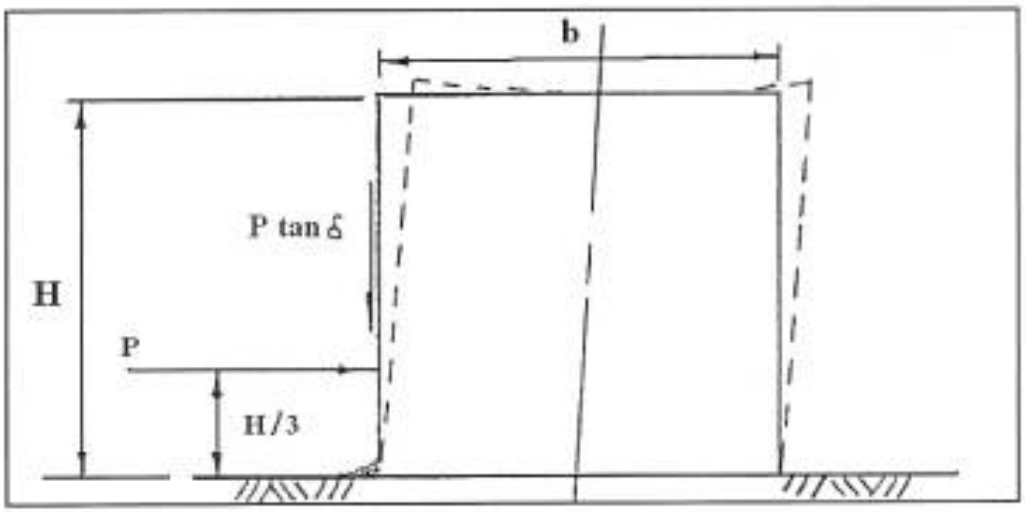

Fig. (3-9): Slipping stability of a cell, [After Teng, (1962)].

3.5.2.c Vertical shear failure

As any structural member acted upon by lateral forces, the cofferdam is subjected to shearing stresses. The magnitude of this shear force is maximum along the center of the cell, as shown in Fig. (3-10), and may be determined as follows, **[Esring, (1970)]**.

$$V_{max} = \frac{3\,M}{2b} \qquad (3\text{-}11)$$

where:

$\boldsymbol{M}$ = true moment due to external lateral force above base (or above any horizontal section under consideration).

$\boldsymbol{b}$ = width of the cofferdam.

Shearing resistance on the plane along the center of the cell, (S_1), is computed from the lateral, (P_a) as

$$S_1 = P_a \,.\, \tan\phi \qquad (3\text{-}12)$$

where:

$\boldsymbol{P_a}$ = active horizontal pressure.

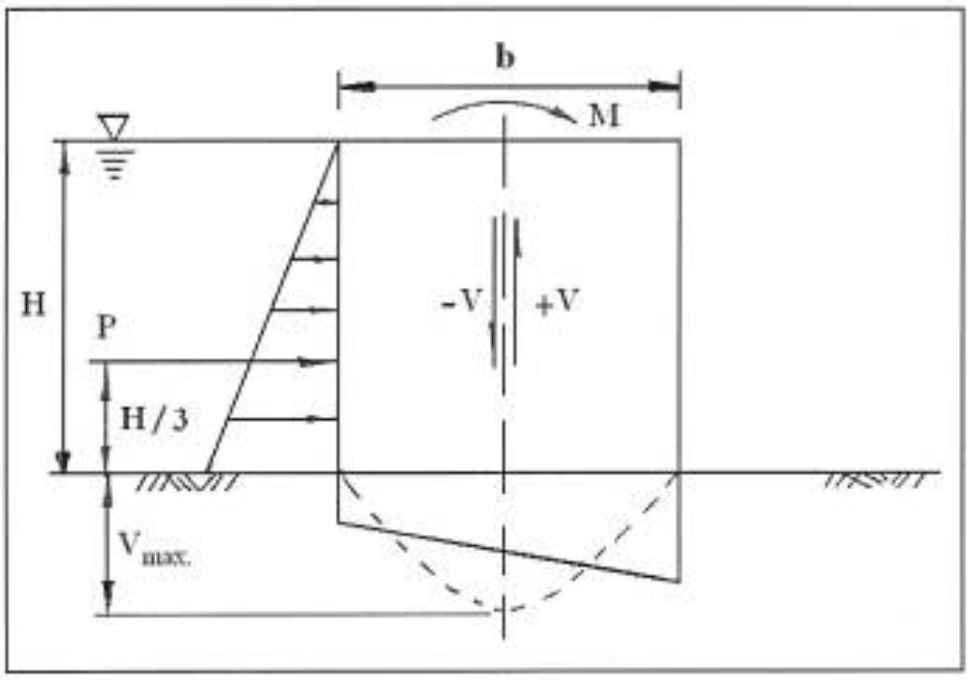

Fig. (3-10): Vertical shear in cell; [After Esring, (1970)].

where:

ϕ = the angle of internal friction of the fill material, and

$$P_a = \frac{1}{2}\gamma * h_a^2 * K_a \quad (3\text{-}13)$$

where:

h_a = height of the active side, and

K_a = active earth pressure coefficient can be calculated as

$$K_a = \frac{1-\sin\emptyset}{1+\sin\emptyset} \quad (3\text{-}14)$$

Therefore

$$S_1 = \frac{1}{2}\gamma . H^2 . K_a . \tan\phi \quad (3\text{-}15)$$

In addition to this shearing resistance, the friction in the sheetpiling interlocks at both ends of the diameter, through which the normal plane passes, also provides resistance, the tension in the interlocks will be:

$$t = P_a . r \quad (3\text{-}16)$$

where:

r = radius of the cell. So the friction in the interlocks is:

$$S_2 = P_a . r . f_{ss} \quad (3\text{-}17)$$

where:

f_{ss} = the coefficient of friction of steel on steel.

Since there are two interlocks in a unit length, (2L), of fictitious cell, the total available interlock friction on the neutral plane per unit length of cofferdam is:

$$S_2 = \frac{2*\frac{1}{2}\gamma*H^2*K_a*r*f_{ss}}{2L} = \frac{\gamma*H^2*K_a*r*f_{ss}}{2L} \quad (3\text{-}18)$$

Therefore, the total available shearing resistance per unit length is:

$$S = S_1 + S_2 \quad (3\text{-}19)$$

The factor of safety against this type of failure is:

$$F.S._{vs} = \frac{S}{V_{max}} \quad (3\text{-}20)$$

Where:

$F.S._{vs}$= factor of safety against Vertical shear.

For temporary cofferdam structures the factor of safety against vertical shear is (1.25), and (1.5) for permanent cofferdam structures, **[USS, (1974)].**

3.5.2.d Horizontal shear failure

In 1957, Cummings proposed a method of analyzing cofferdams based on his experiments on model cofferdams on rock. When the lateral force, (P), is applied to the cell, a resistance from the cell will be develop as a triangle, (hij), as shown in Fig.(3-11), forming an angle (ϕ) with the horizontal. The soil in triangle (hij) is in the passive state. The rest of the fill acts as a surcharge and stabilizes the soil in triangle (hij). This part of the fill is termed (W1). Its weight can be calculated as

$$W_1 = \gamma(a+Y)Y\ cot\,\emptyset \tag{3-21}$$

The shearing resistance along the plane (gf) becomes:

$$S_1 = W_1\ tan\emptyset = \gamma(aY + Y^2) \tag{3-22}$$

When $Y=c$, S_1 is maximum. Hence:

$$S_{1\,max} = \gamma(ac + c^2) \tag{3-23}$$

But:

$$c = b\ \ \tan\phi \tag{3-24}$$

and:

$$a = H - c \tag{3-25}$$

therefore:

$$S_{1\,max} = \gamma * H * b * tan\emptyset \tag{3-26}$$

From equation (3-22), (S_1) can be represented by a rectangle and triangle as shown in Fig.(3-11). The resisting moment computed for (R_1) and (R_2) is:

$$M_r = M_1 + M_2 = R_1\frac{c}{2} + R_2\frac{c}{3} = \gamma(\frac{a*c^2}{2} + \frac{c^3}{3}) \tag{3-27}$$

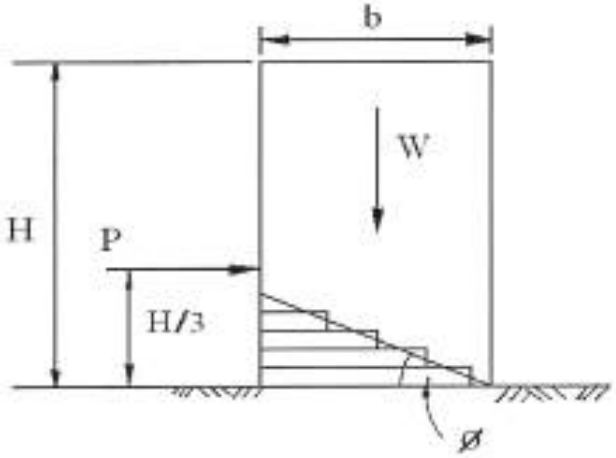

a) Cell fill resistance to lateral force

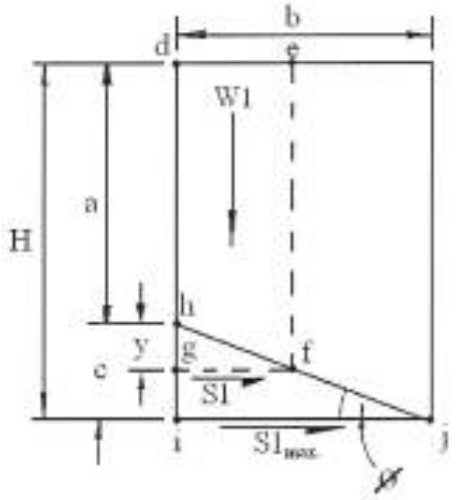

b) Forces in tilting failure mode

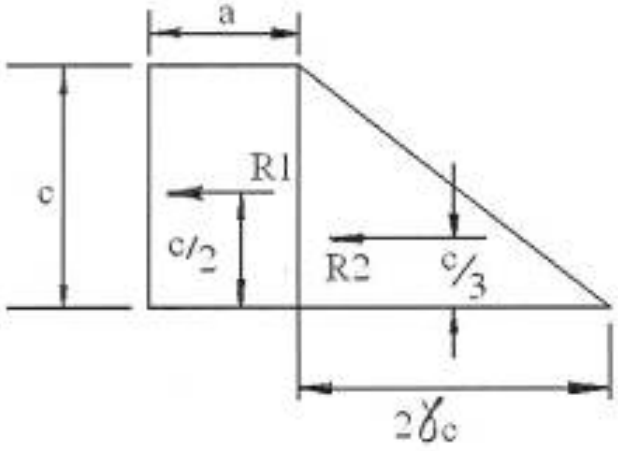

c) Pressures provided by cell fill

Fig. (3-11): Tilting analysis; [After Cummings, (1957)].

If the resisting moment due to interlock friction is considered, then the expression for the total resisting moment, (M_t), is given by:

$$M_t = \gamma.\left(\frac{a.c^2}{2}+\frac{c^3}{3}\right)+ P.f.b \qquad (3\text{-}28)$$

The factor of safety ($F.S._{hs}$) against horizontal shear is defined as the ratio of resisting moment, (M_t) , to the overturning moment, (M_o), or

$$F.S._{hs}=\frac{M_t}{M_o} \qquad (3\text{-}29)$$

The factor of safety should range between (1.25) and (1.5), **[Lacrox et al., (1970)]**.

3.6 TESTING APPARATUS

The testing apparatus used in this research to check the general stability of cellular cofferdam, consists of:

1- the steel frame.

2- the loading system.

3- the pulley system.

4- the soil box.

5- the circular model cells.

6- the dial gages.

3.6.1 The steel frame

A steel frame was used to carry the soil box and its content, as illustrated in Fig. (3-12), with dimensions (1400 mm) length, (1050 mm) width, and (800 mm) height. At the middle of its width was fastened knee-braced frame. A knee-braced frame was made of two angles (50*50) mm and (500 mm) length are welded vertically, at their bottom end, to the steel frame. The upper side of the angles is connected to a steel beam of (135 mm) length, (50 mm) width and (3 mm) thickness. A space of (35 mm) is provided between the two angles to allow to pass the steel cable load, on each side of knee-braced frame, two steel angles

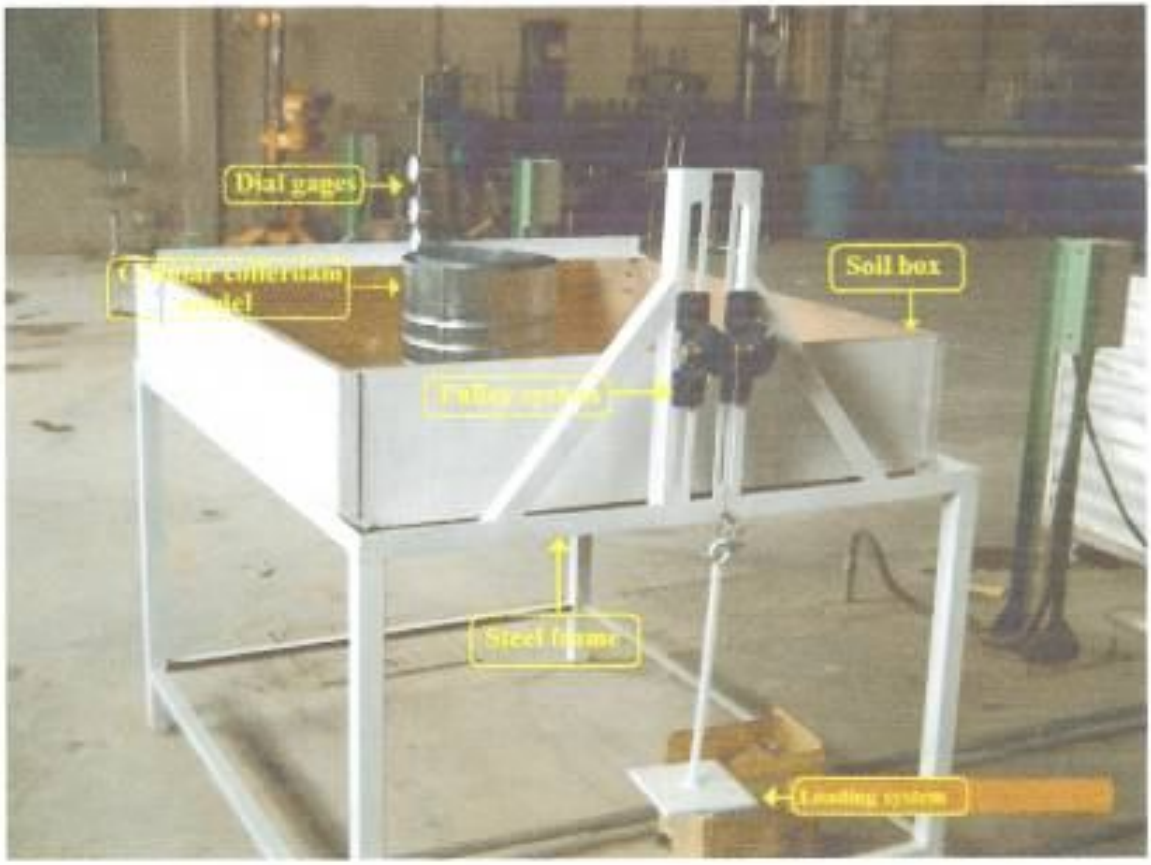

Fig. (3-12): The steel frame

(50*50) mm of (470 mm) length, are welded at (350 mm) height from knee-braced to support it.

In each angle, a slit-like opening with dimensions of (400 mm) height and (15 mm) width is made at (50 mm) height from the knee-braced base. This slit is use to fix the pulley system. The set-up described above it was designed to permit testing of the circular cells under lateral loading at different elevations.

3.6.2 The loading system

The load is applied to the cell by a steel cable loop (4 mm) in diameter hold around the cell tightly from one end and connected to the weight holder from the other and after passing over a system as shown in Fig. (3-13), the loading system consist of:

a) The dead weight holder comprises of two parts, the first is a steal beam with dimensions (330 mm) length, and (10mm) width with square section, the second part is a square steel plate of (100 mm) length and (8 mm) thickness, the first part is welded vertically to the second part.
b) The dead weight of (0.5, 1, 2, 4, 8, 10) kg is used as a loading units.

3.6.3 The pulley system

The pulley system as shown in figures. (3-13), and (3-14) consist of a round steel shaft (30 mm) in diameter and (200 mm) length, a pulley (50 mm) in diameter is fixed in the middle of the shaft, and two brackets each one surrounding ballbearing (60 mm) and internal diameter (30 mm), the two brackets provided with two holes that was used to fix the pulley set to the knee-braced frame.

3.6.4 The soil box

A wooden container with inner dimensions (1250 mm) length, (1040 mm) width, and (250 mm) height, as shown in Fig. (3-12), was used as a container for a foundation to the circular cells of cellular cofferdams.

Fig. (3-13): the loading system.

Fig. (3-14): The pulley system

At (200 mm) distance from the end of the box fastened steel angle beam of (1080 mm) length, (50 mm) width and (50 mm) height by screws above the two sides of the box. There is one hole in the middle of the beam to support a steel screwed shaft, (15 mm) diameter, and (800 mm) length. The steel shaft was used to support four dial gages, as shown in Fig. (3-15).

3.6.4.1 General requirements for cell fill

The general requirements for a fill material for cellular steel sheetpile cofferdams, **[TVA, (1989)]**, are:

1. High coefficient of internal friction.
2. Free draining.
3. Resistance to scour. and
4. High weight in mass to resist sliding and overturning.

3.6.5 The circular model cells

Consists of three continuous circular cells, with (300 mm, 255mm,225mm) diameter, and (300 mm) height, as shown in Fig. (3-16). The

load exerted by the steel cable incrementally at (100 mm) from the base of the models and that is corresponding to one third of the cells height, and at (150 mm, 300 mm) from the base.

Fig. (3-15): Steel shaft carry four dial gages

Fig. (3-16): Circular cell models

3.6.6 The dial gages

Dial gages were used to monitor the displacements of models throughout the entire testing program, four dial gages of (0.01 mm) accuracy and (25 mm) travel were employed, they are mounted to vertical steel shaft as shown in Fig. (3-15), and Fig. (3-17)

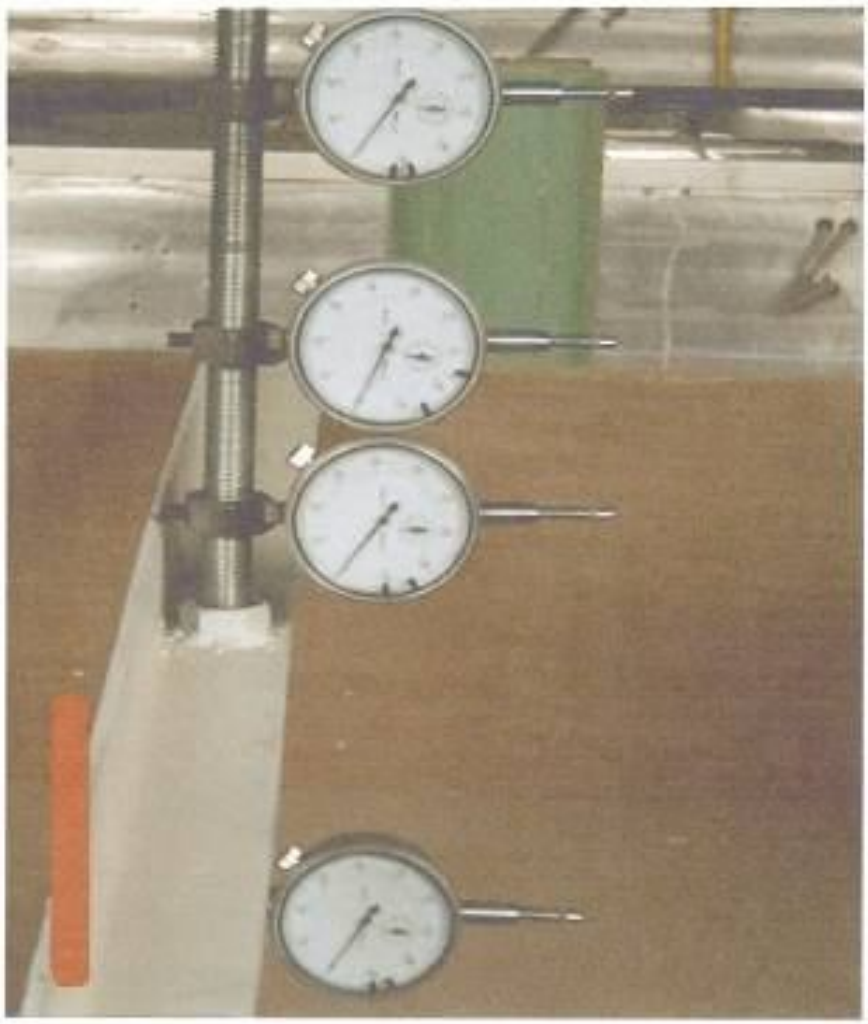

Fig. (3-17): Dial gages

3.7 THE PROPERTIES OF SOIL

Five different types of soil used in all tests, the dry density and angle of friction for all soils are illustrated in table (3-1):

Table (3-1): the properties of the soils used in the cells fill.

Type of soil	Dry density (γ) (kN/m^3)	Angle of friction (ϕ)
Subbase	16.67	38
Sand sieved on No.4	17.82	33.5
Sand sieved on No.8	18.57	32
River sand	14.86	31.5
Clayey sand	14.35	21

3.8 TESTING PROCEDURE

In all tests the soil bed on wooden box of (150mm) height, placed by means of raining technique. The cells then placed in the middle width of soil box at (100mm) distance from the support of dial gages. In all cases, the cells put on ground surface. The models are then filled carefully to minimize disturbance.

The raining technique has been used successfully in providing uniformly dense soil bed for model studies, **[Kelly, (1969)].** Basically, the technique involves raining soil through a single or series of sieves with a constant height of the drop and raining intensity, weight of soil raining per unit area; the raining technique could be used to provide a uniform dense soil fill with good density control, angle of internal friction. A height of (500mm) was kept between the sieve that was used in the raining technique and the top surface of the soil. After the cell was filled, the cell level checked by handy level, as shown in Fig. (3-

18), the loading system and dial gages were adjusted. Then, the load is applied incrementally and continued until a general failure in the model was occurred, as shown in Fig. (3-19). At any load exerted, the dial gages recorded the magnitude of displacement in the tested model, as shown in Fig. (3-20) . There are five typed of soil used in the test, each type of soil was used as cell fill and foundation to the model at the same time. Some test repeated to assurance from its result.

3.9 TESTING PROGRAM

The test program consist of five stages of tests. At any stage, three different type of circular cell was tested, the first type has (b/H =1.0), the second type has (b/H =0.85), and the third (b/H =0.75). all types of circular cell tested

Fig. (3-18): Handy level.

Fig.(3-19): General failure in the tested model cell.

under three loading heights, (100 mm), (150 mm), and at the top point of model (300 mm), so that the different between sliding and overturning failure can easily be clarified. At the first stage sand was sieved on No.4 was used as fill and foundation for these cell models, in the second stage, a sand was sieved on No.8 used as fill and foundation of the cells, at the third stage the subbase was used in tests, the fourth stage the river sand was used as fill and foundation for the cell, and at the last stage the clayey sand used in the test as fill and foundation. At any stage of test, the load was applied at different elevation (100mm, 150mm, 300mm), In all tests the cells put on the ground surface, and embedment depth equal to (0).

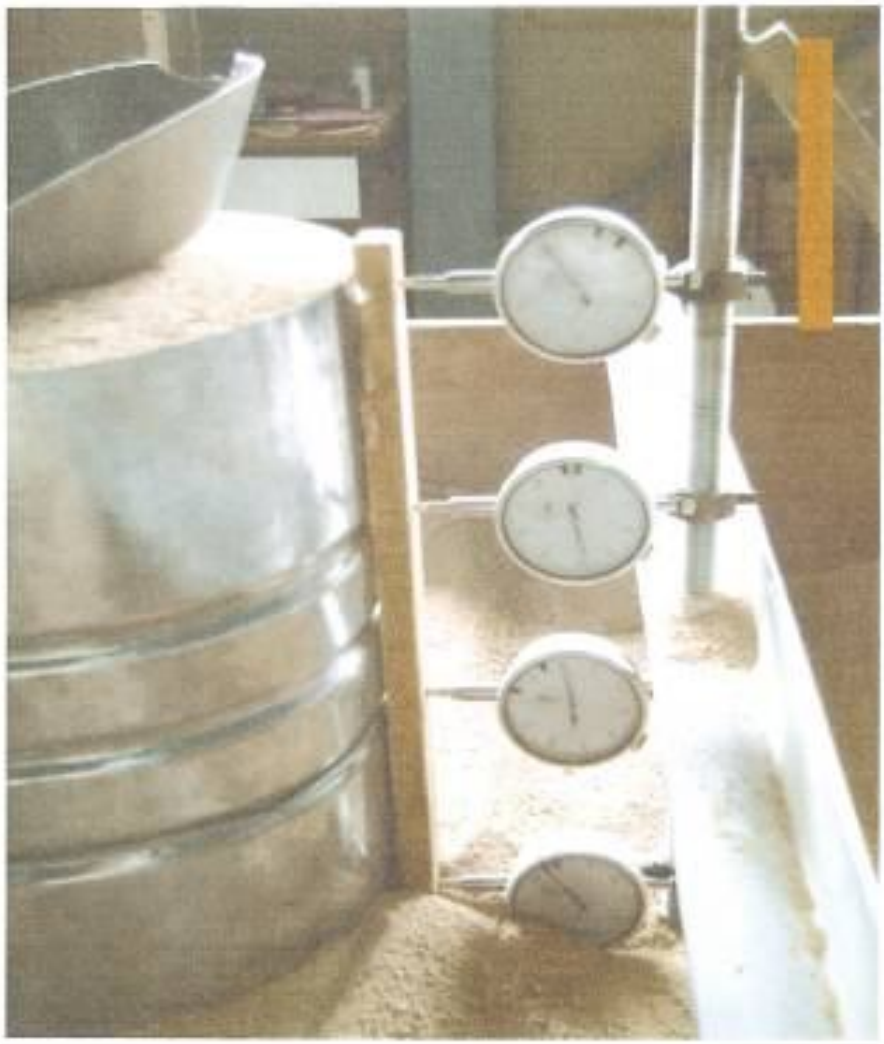

Fig. (3-20): The dial gages recorded the displacement magnitude of model cell.

CHAPTER FOUR

RESULTS AND DISCUSSION

CHAPTER FOUR
RESULTS AND DISCUSSION

4.1 INTRODUCTION

This chapter presents the results obtained experimentally according to the testing program which was previously mentioned in chapter three. The tests results reported in this chapter concern of three circular cells with ratios of width to height, $(\frac{b}{H})$ of, (0.75, 0.85, and 1.0) It is worth mentioning that the displacement term in this research indicates both translation and rotation of the top point of the cell unless it is otherwise stated.

4.2 LOAD-DISPLACEMENT BEHAVIOR

A survey on the load-displacement behavior of all model cells have shown that they are similar and characterized by three distinguish stages, as shown in Figs. (4-1) through (4-3) for models with loading height (y=100 mm), Figs. (4-4) through (4-6) for models with loading ay (y=150 mm), and Figs.(4-7) through (4-9) for models with loading at (y=300 mm), these figures represent the displacement at the top of the cell. Figs. (4-10) to (4-24) shown the load-displacement behavior at the base point of cell. The first stage (a-b), the load is linearly proportional to displacement. After that, a curved relationship (b-c) was obtained, which represent the second stage, the load-displacement relationship become, linear (c-d) until failure but with much flatter slope compared with that of the first stage. The curve form vary from cell to others according to the (b/H) ratio and type of soil used in the filling. The mode of failure was found to be either translation of displacement or overturning failure as that described later in the mechanism of failure. Thus the failure loading or cell resistance was defined as the critical loading above which a general failure in the cell is taken place.

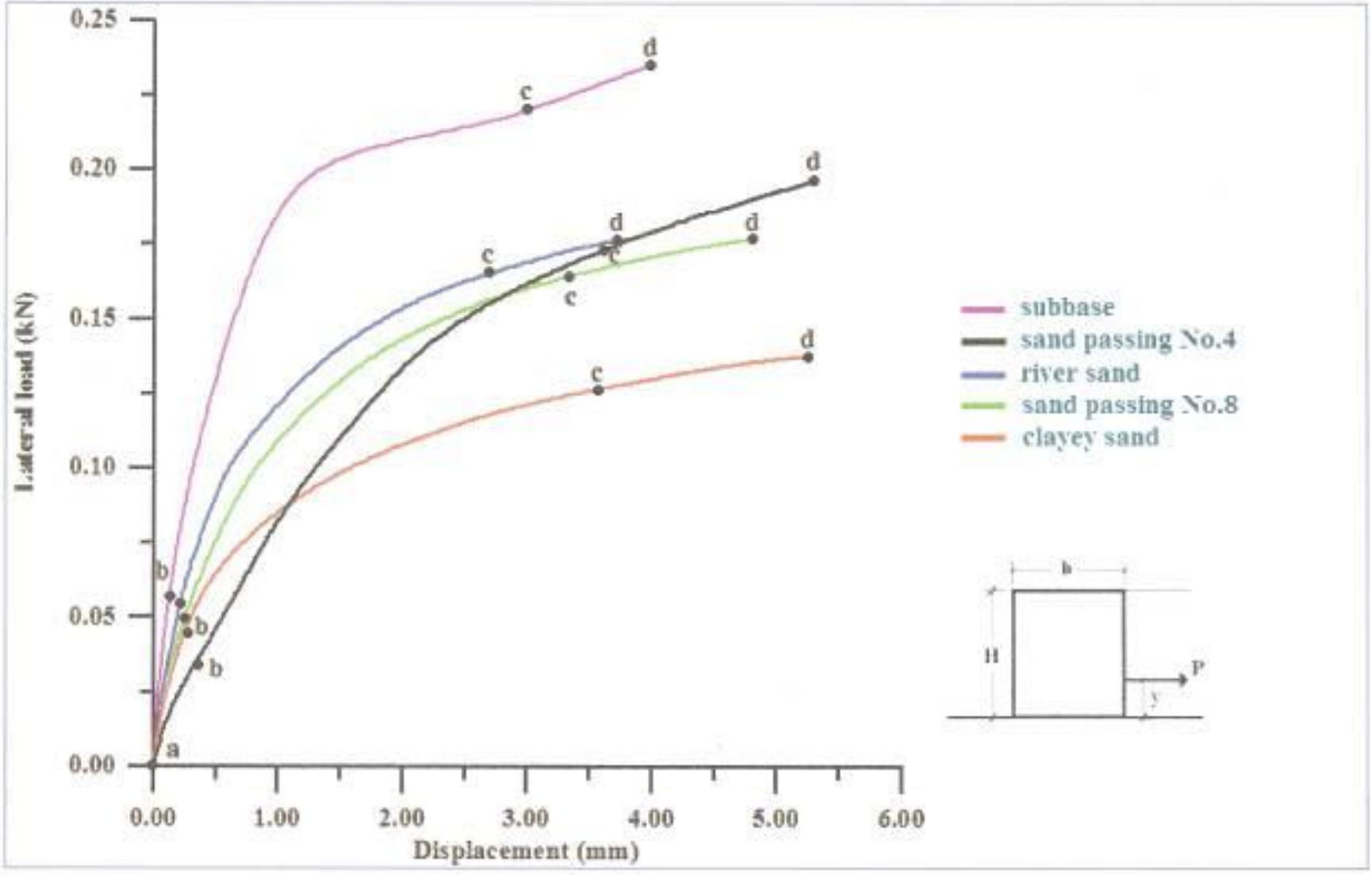

Fig.(4-1): Displacement vs. lateral load curve,

$\frac{b}{H}$=1.0, y=100mm

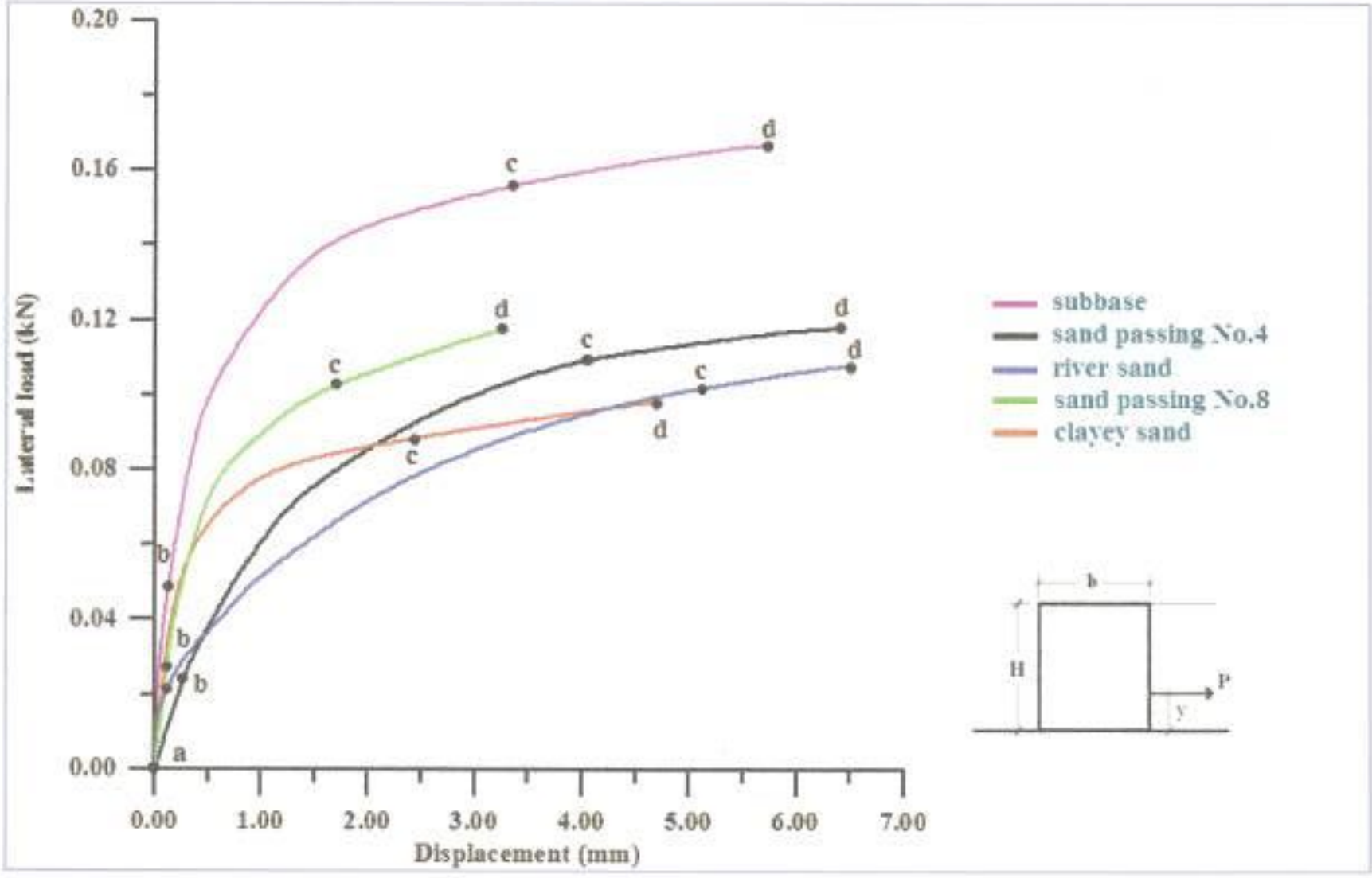

Fig.(4-2): Displacement vs. lateral load curve, $\frac{b}{H}$=0.85, y=100mm

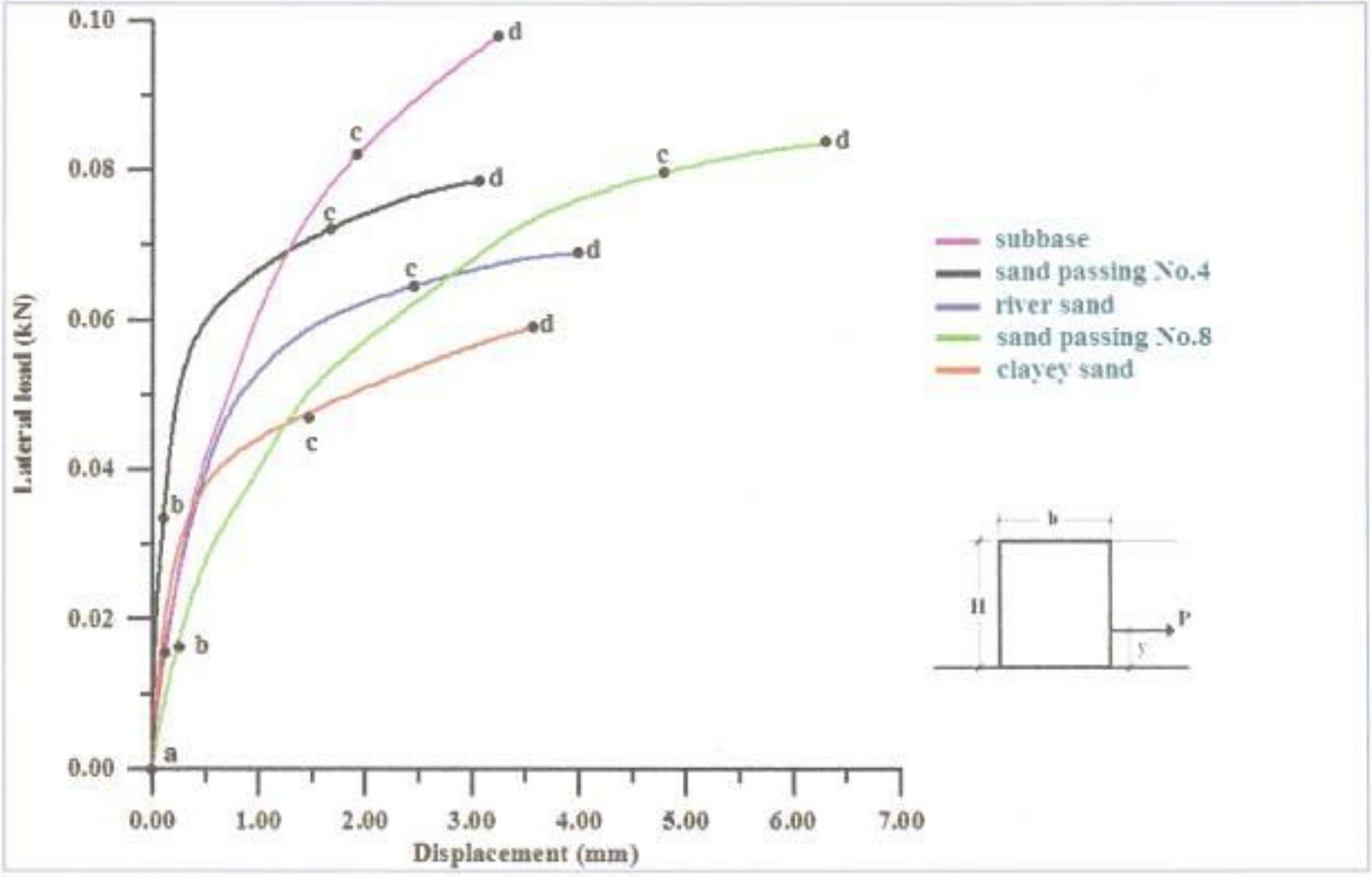

Fig.(4-3): Displacement vs. lateral load curve,

$\frac{b}{H}$ =0.75, y=100mm

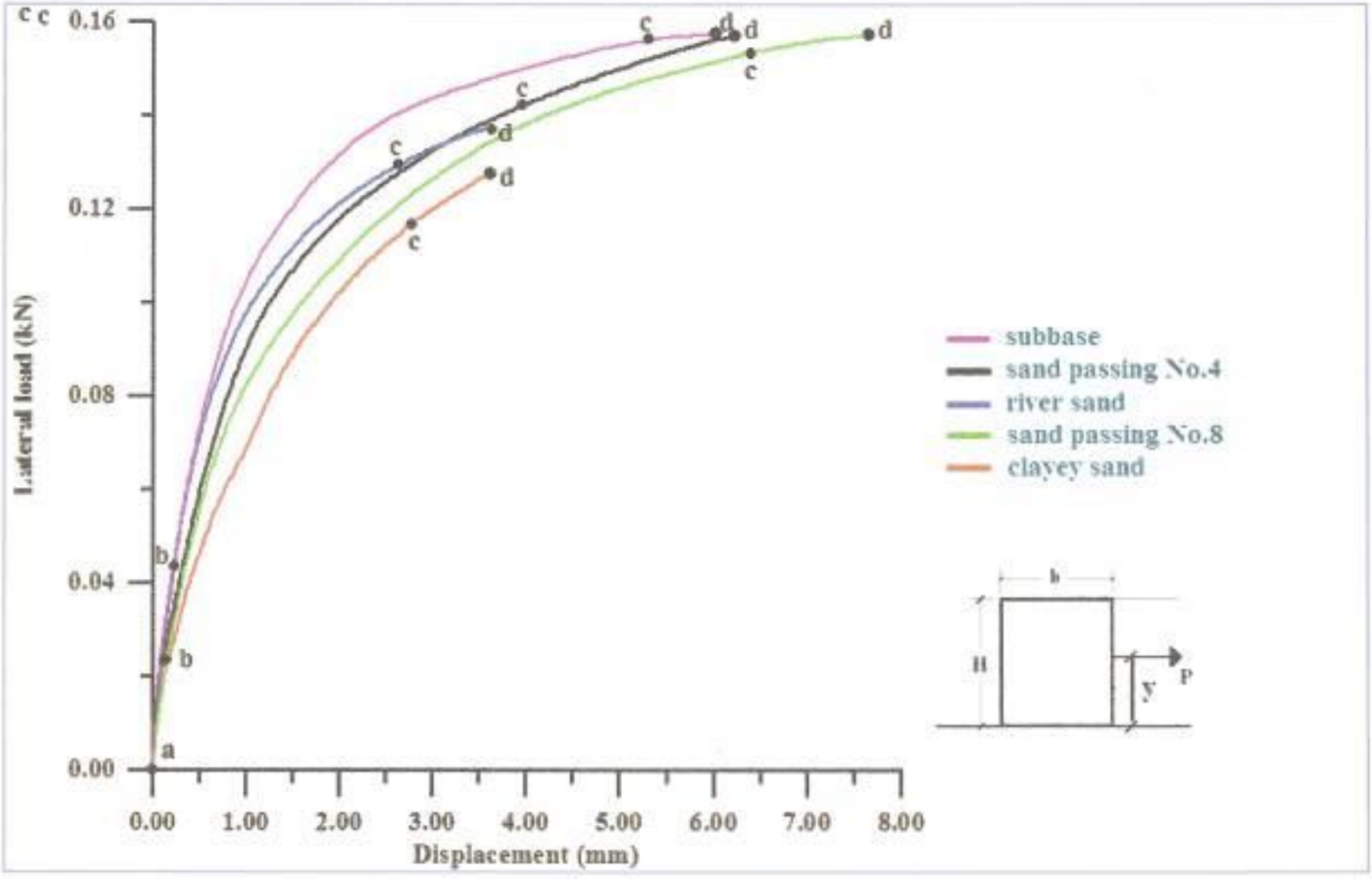

Fig.(4-4): Displacement vs. lateral load curve,

$\frac{b}{H}$=1.0, y=150mm

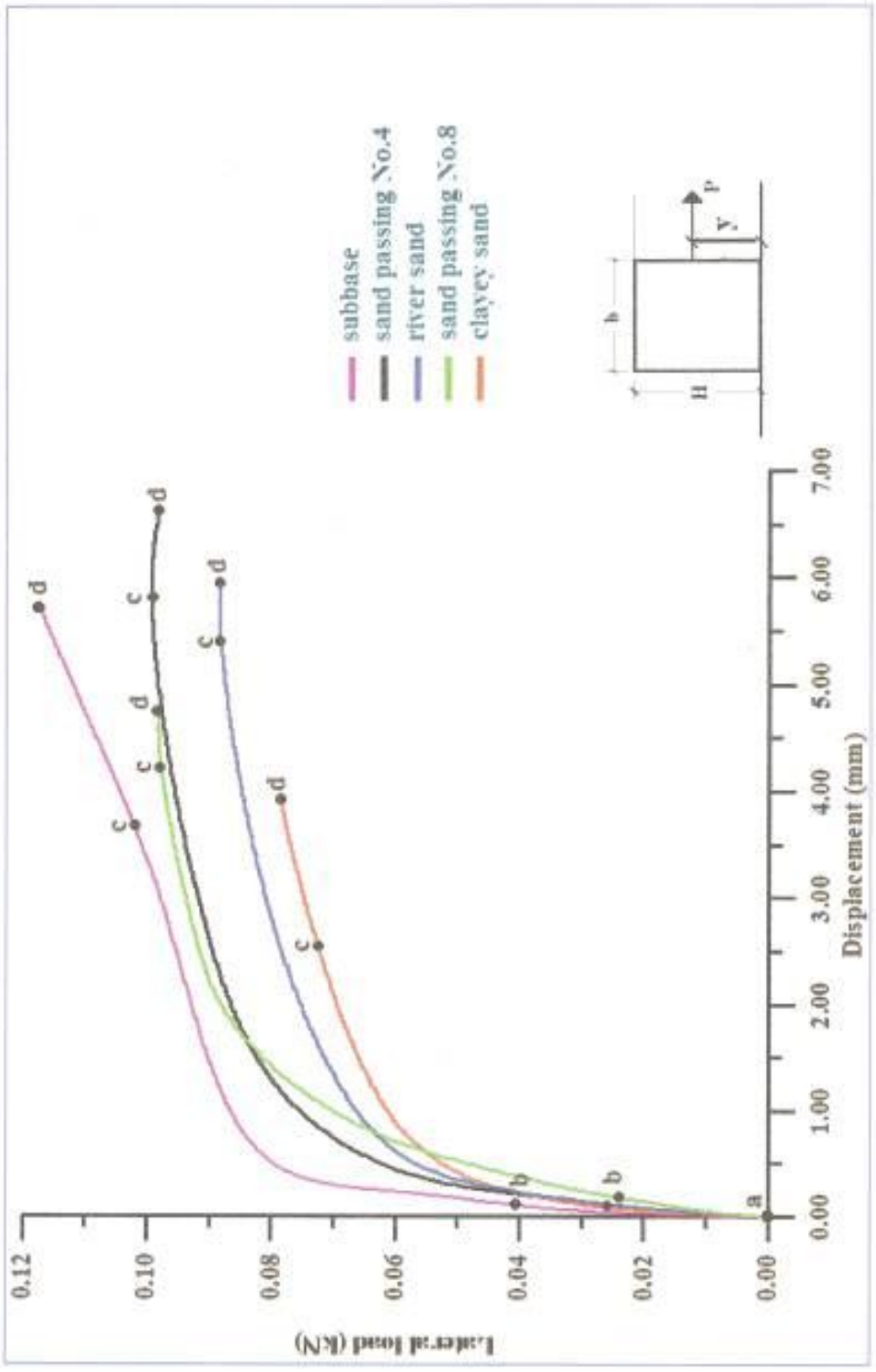

Fig.(4-5): Displacement vs. lateral load curve, $\frac{b}{H}$=0.85, y=150mm

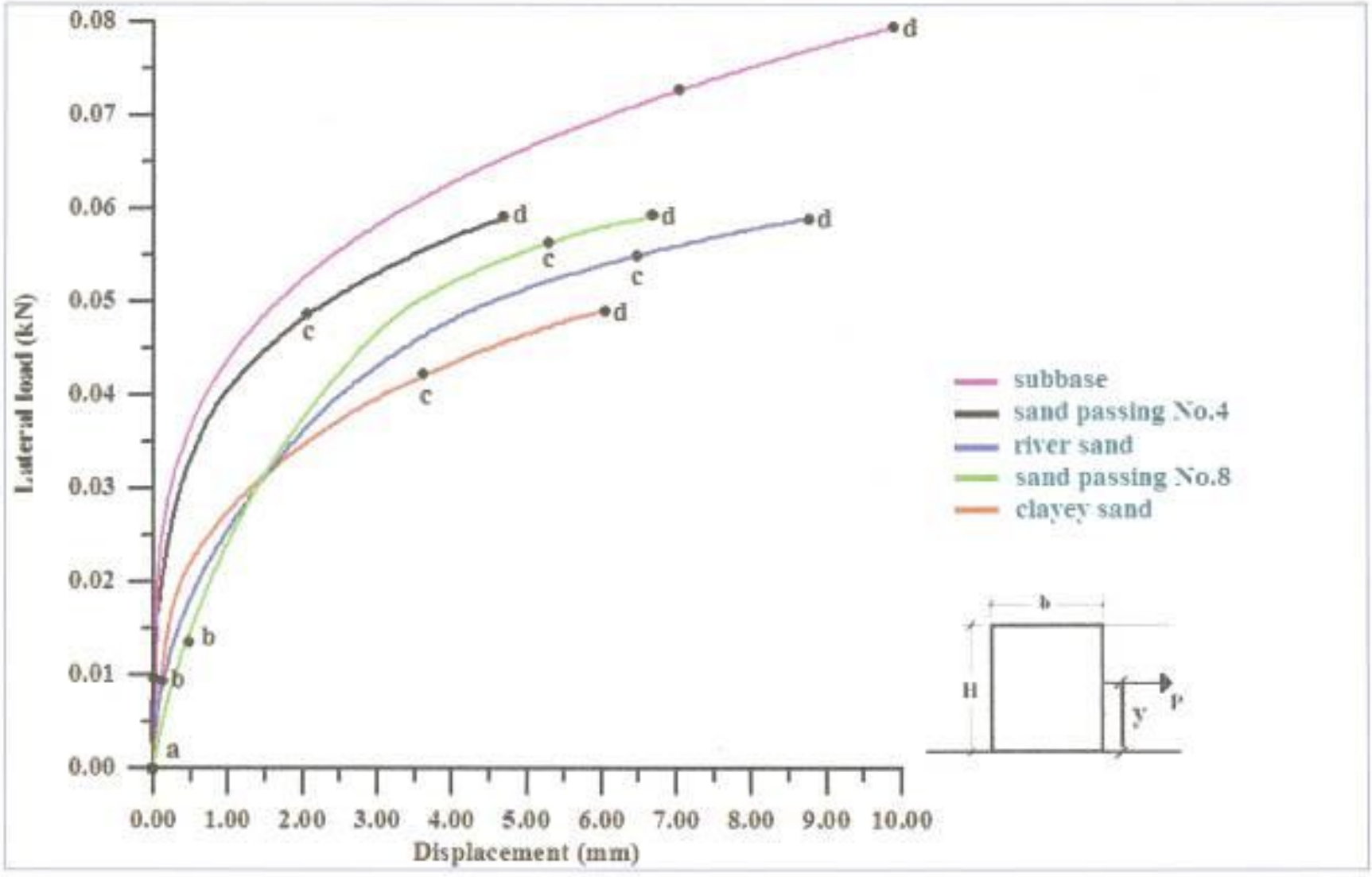

Fig.(4-6): Displacement vs. lateral load curve,

$\frac{b}{H}$ =0.75, y=150mm

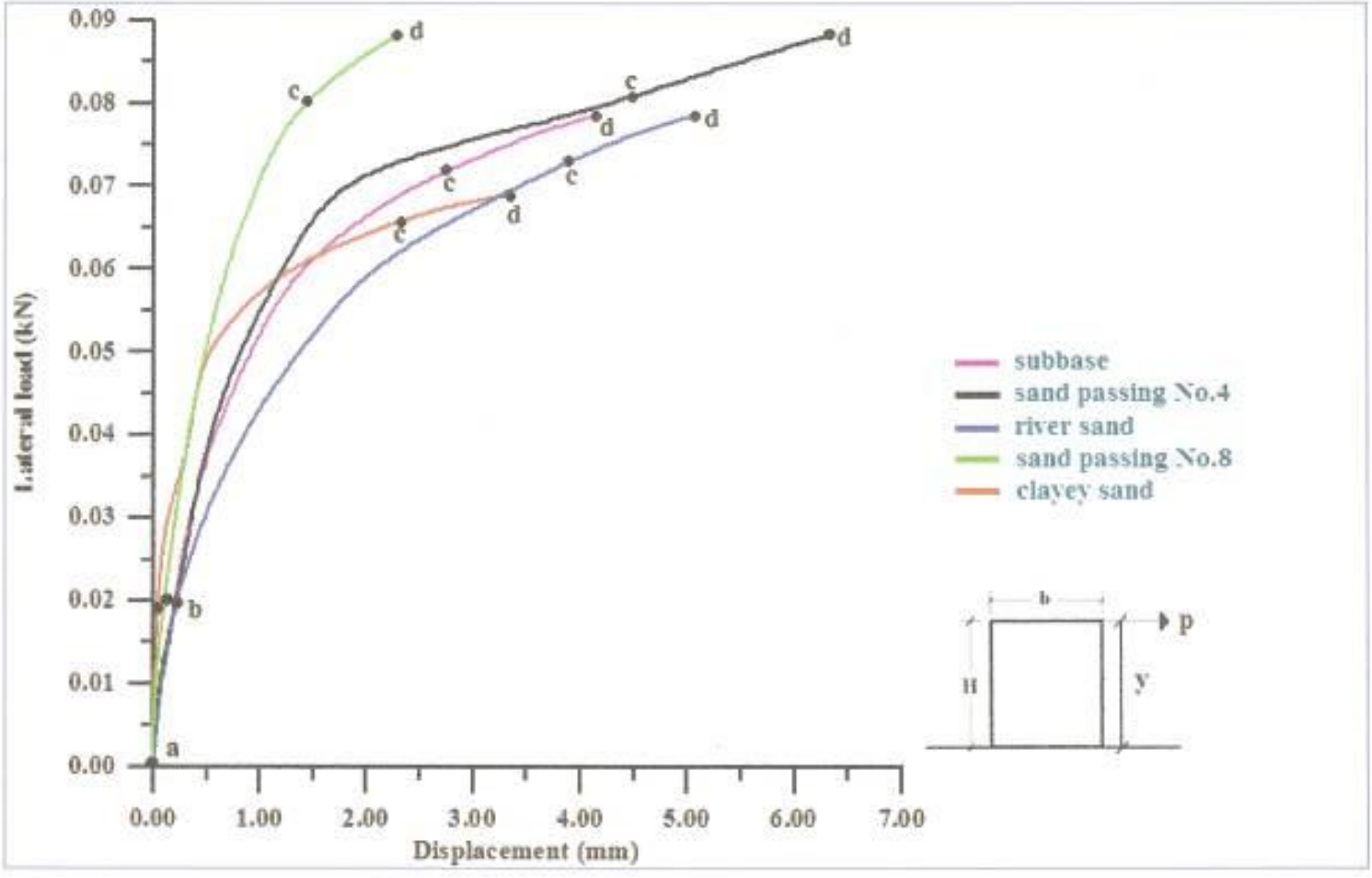

Fig.(4-7): Displacement vs. lateral load curve,

$\frac{b}{H}$ =1.0, y=300mm

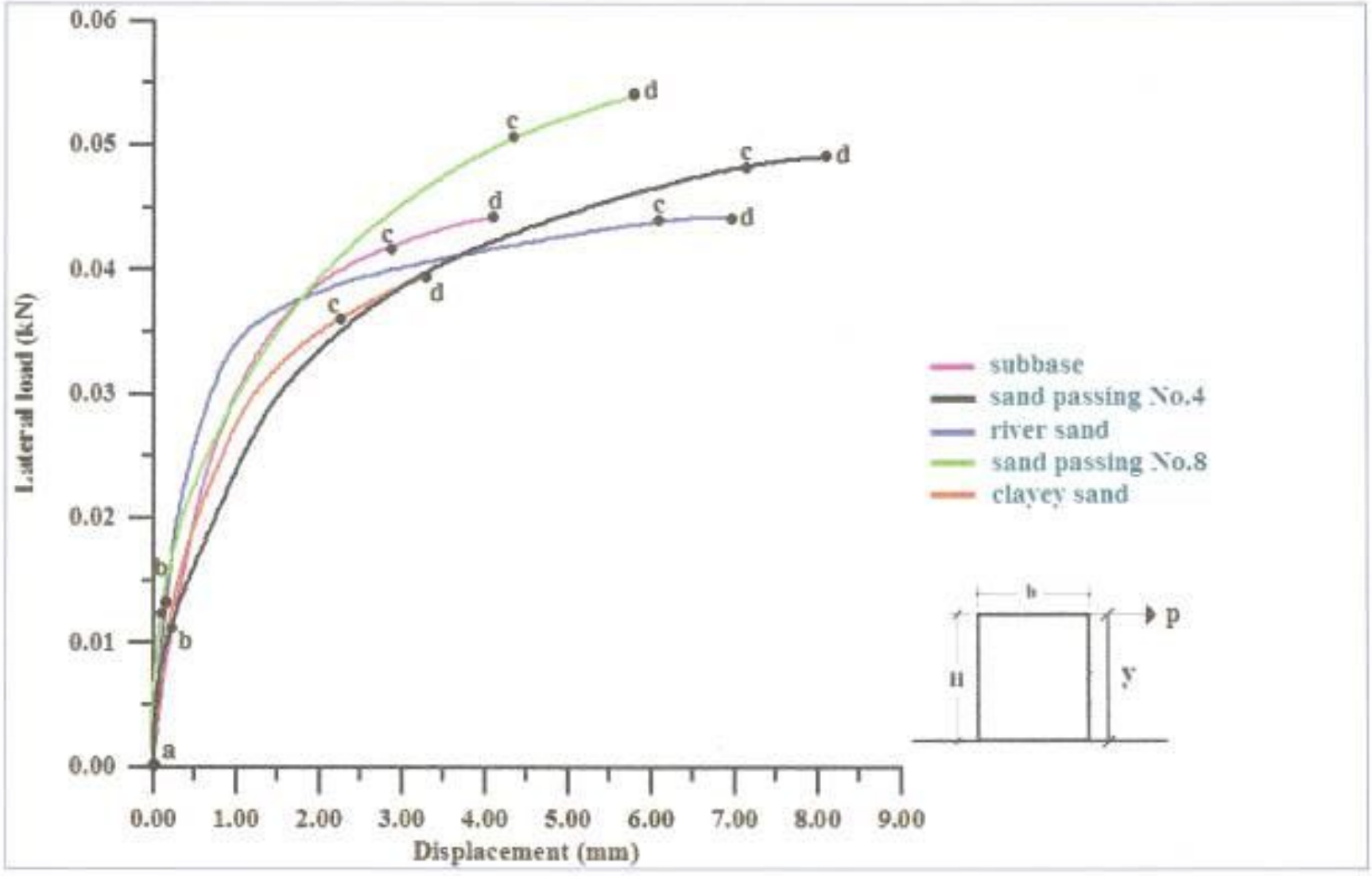

Fig.(4-8): Displacement vs. lateral load curve,

$\frac{b}{H}$ **=0.85, y=300mm**

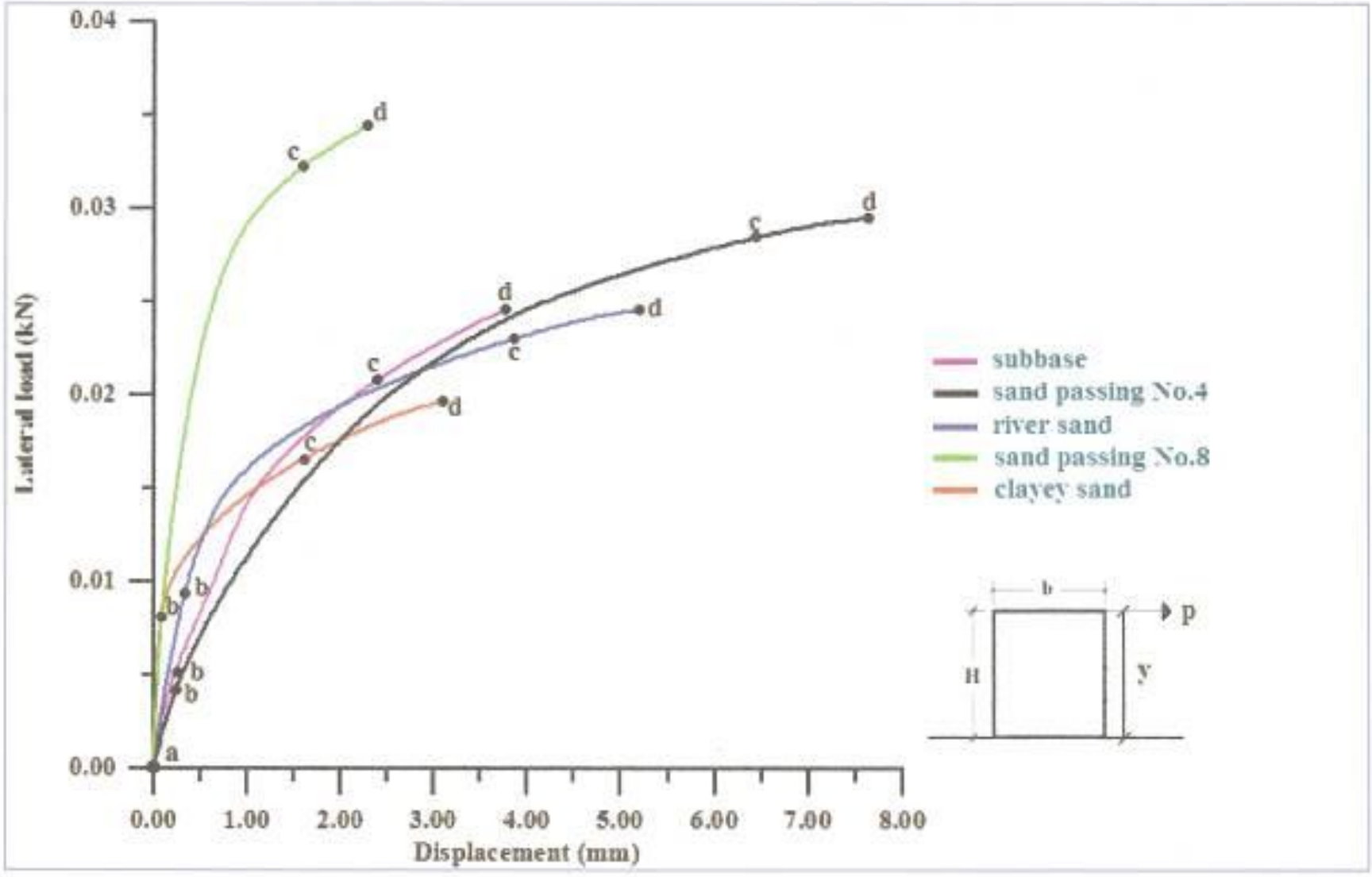

Fig.(4-9): Displacement vs. lateral load curve,

$\frac{b}{H}$ =0.75, y=300mm

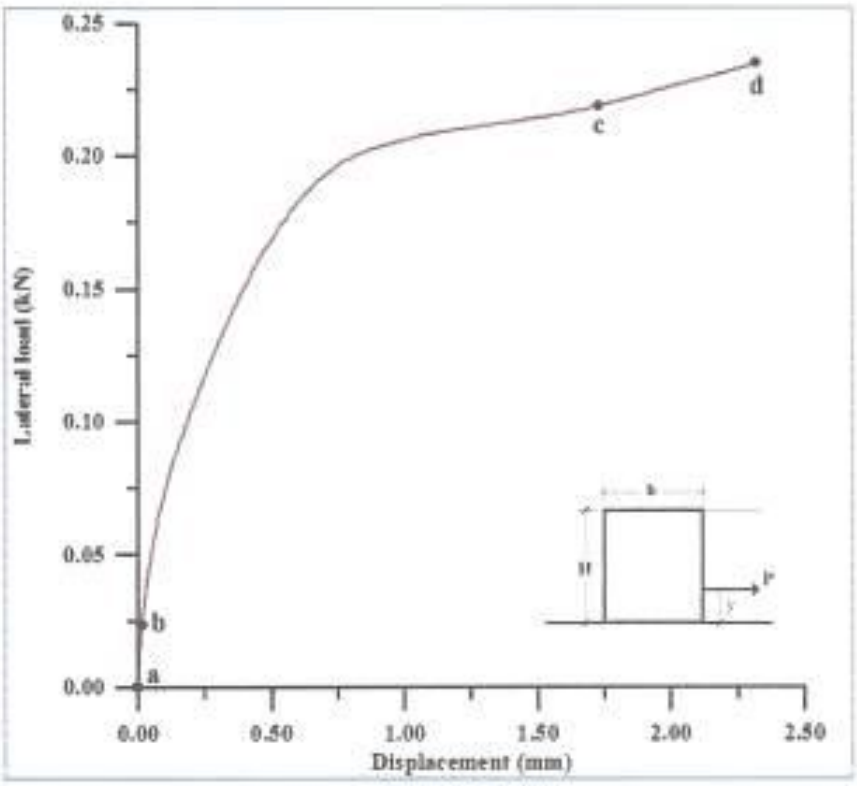

Fig.(4-10):Displacement vs. lateral load curve for cell filled with subbase, $\frac{b}{H}$ =1.0, and y=100mm .

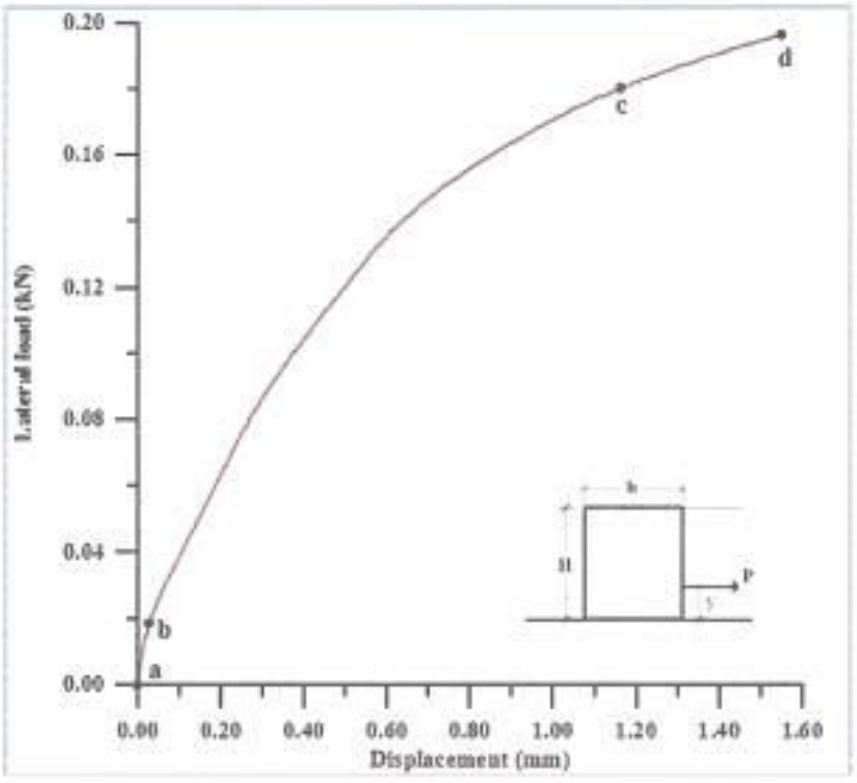

Fig.(4-11):Displacement vs. lateral load curve for cell filled with sand passing No.4, $\frac{b}{H}$ =1.0, and y=100mm .

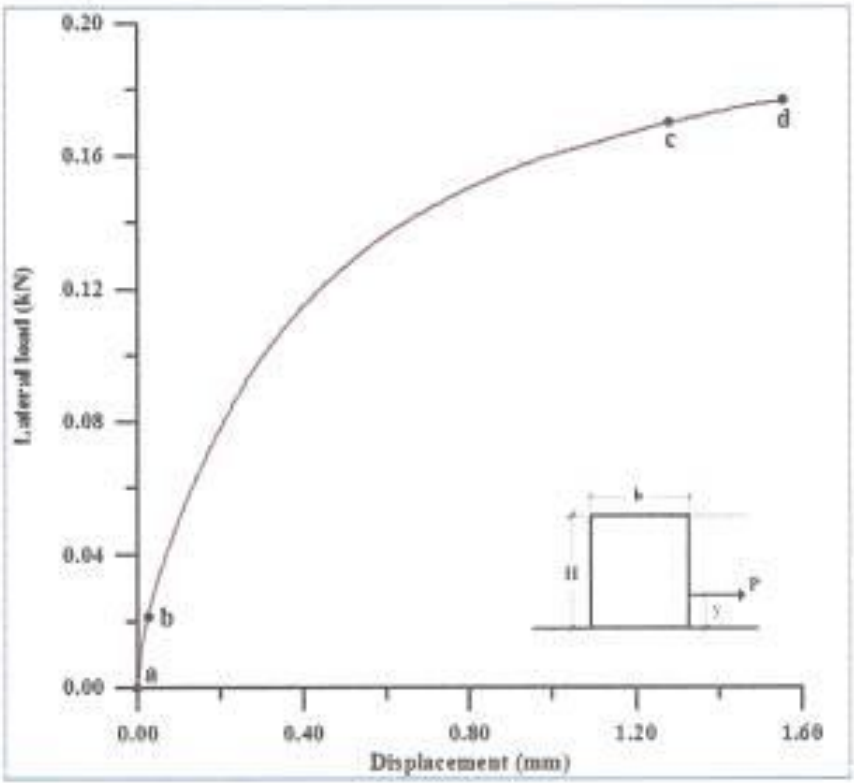

Fig.(4-12):Displacement vs. lateral load curve for cell filled with sand passing No.8, $\frac{b}{H}$ =1.0, and y=100mm .

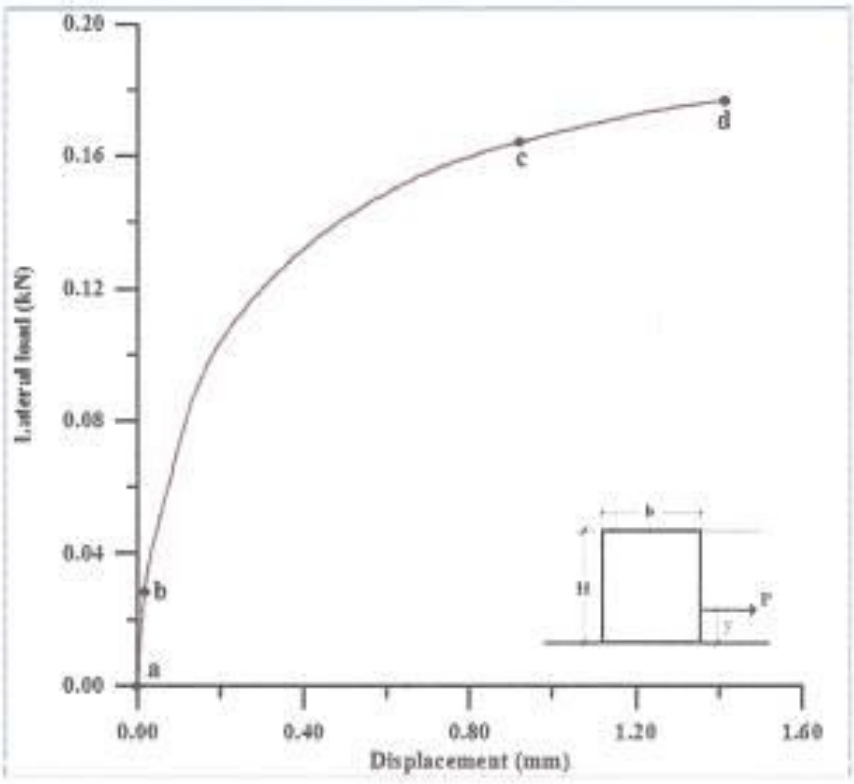

Fig.(4-13):Displacement vs. lateral load curve for cell filled with river sand, $\frac{b}{H}$ =1.0, and y=100mm .

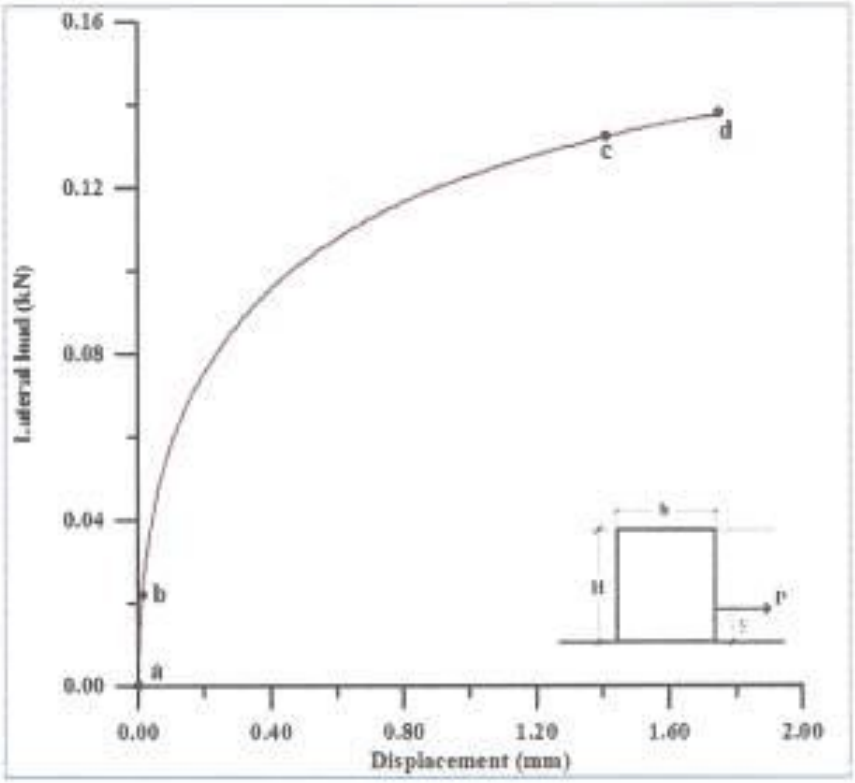

Fig.(4-14):Displacement vs. lateral load curve for cell filled with clayey sand, $\frac{b}{H}$ =1.0, and y=100mm .

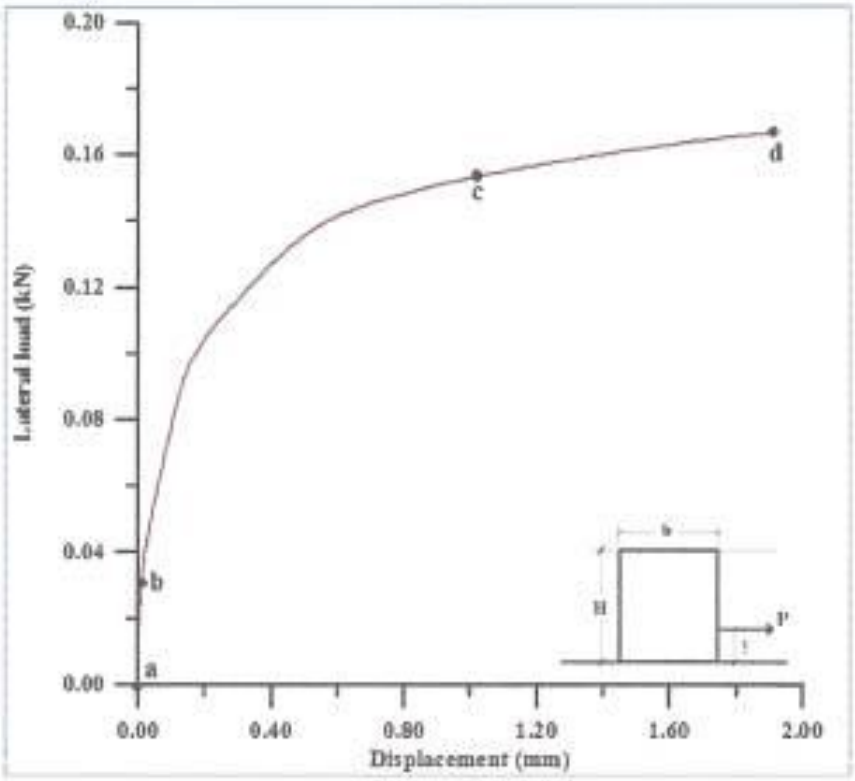

Fig.(4-15): Displacement vs. lateral load curve for cell filled with subbase, $\frac{b}{H}$ =0.85, and y=100mm .

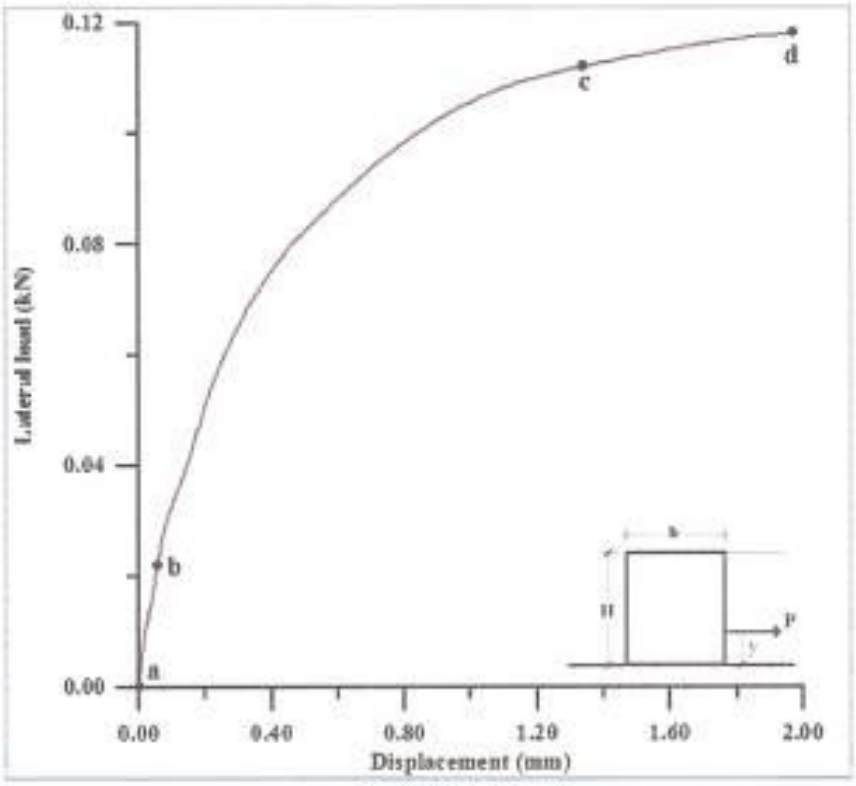

Fig.(4-16): Displacement vs. lateral load curve for cell filled with sand passing No.4, $\frac{b}{H}$ =0.85, and y=100mm .

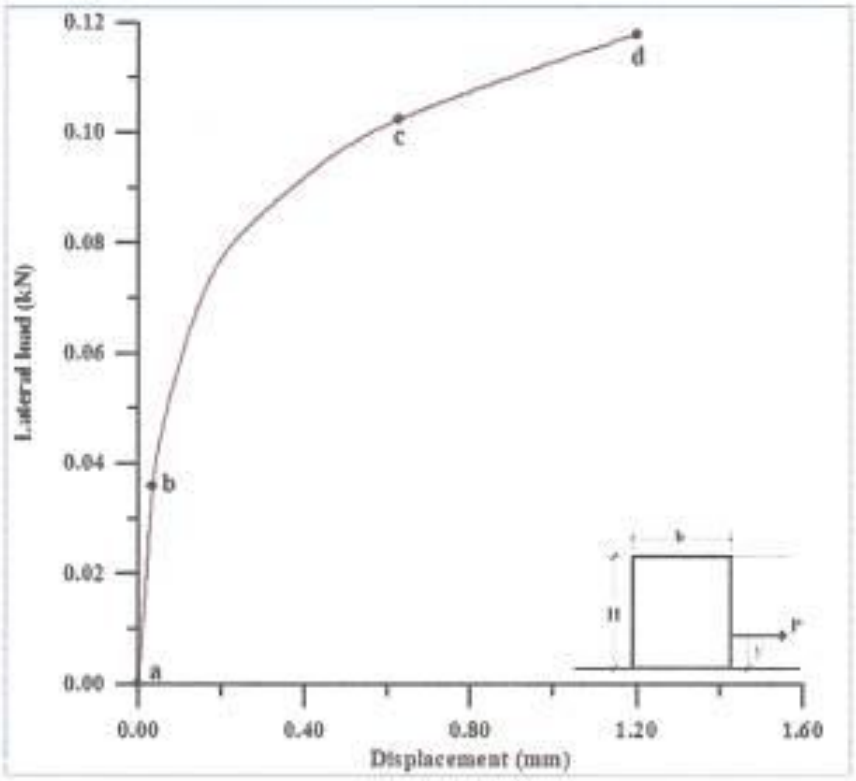

Fig.(4-17): Displacement vs. lateral load curve for cell filled with sand passing No.8, $\frac{b}{H}$ =0.85, and y=100mm .

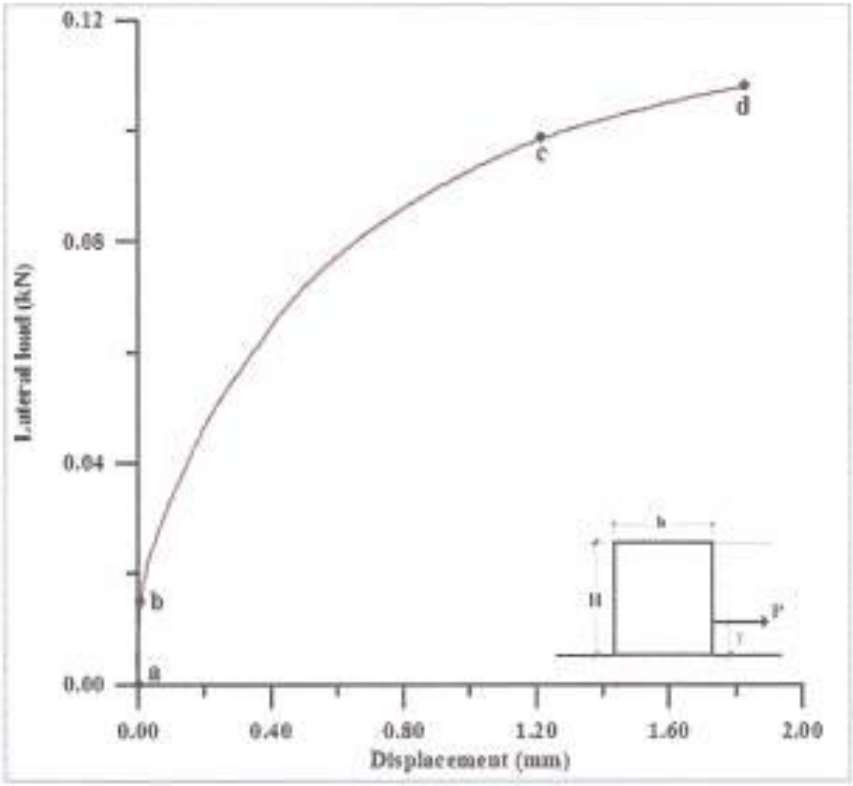

Fig.(4-18): Displacement vs. lateral load curve for cell filled with river sand, $\frac{b}{H}$ =0.85, and y=100mm .

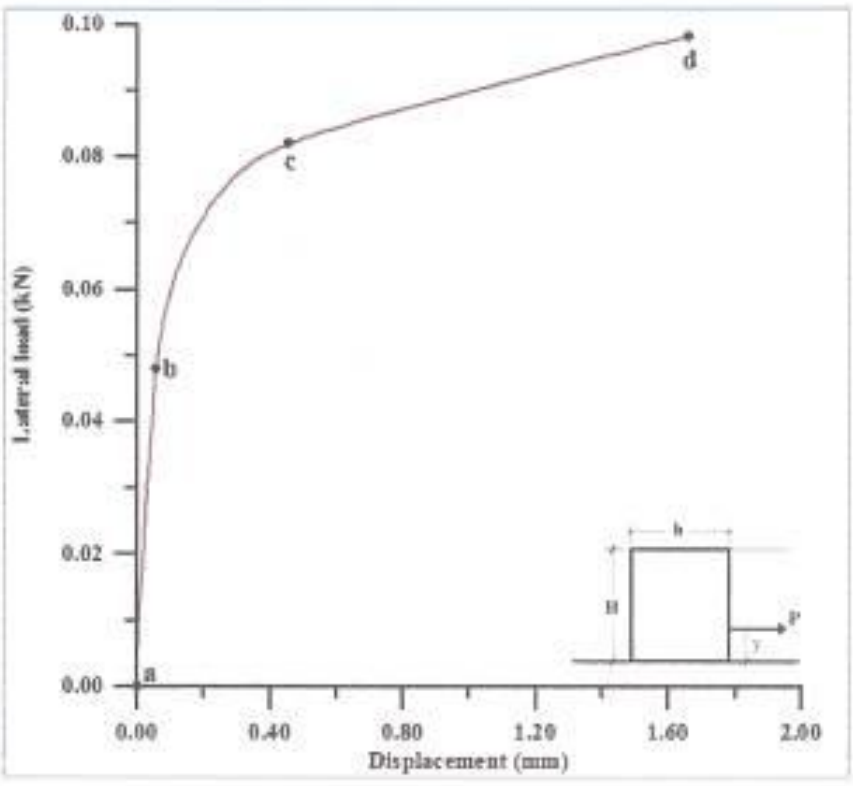

Fig.(4-19): Displacement vs. lateral load curve for cell filled with clayey sand, $\frac{b}{H}$ =0.85, and y=100mm .

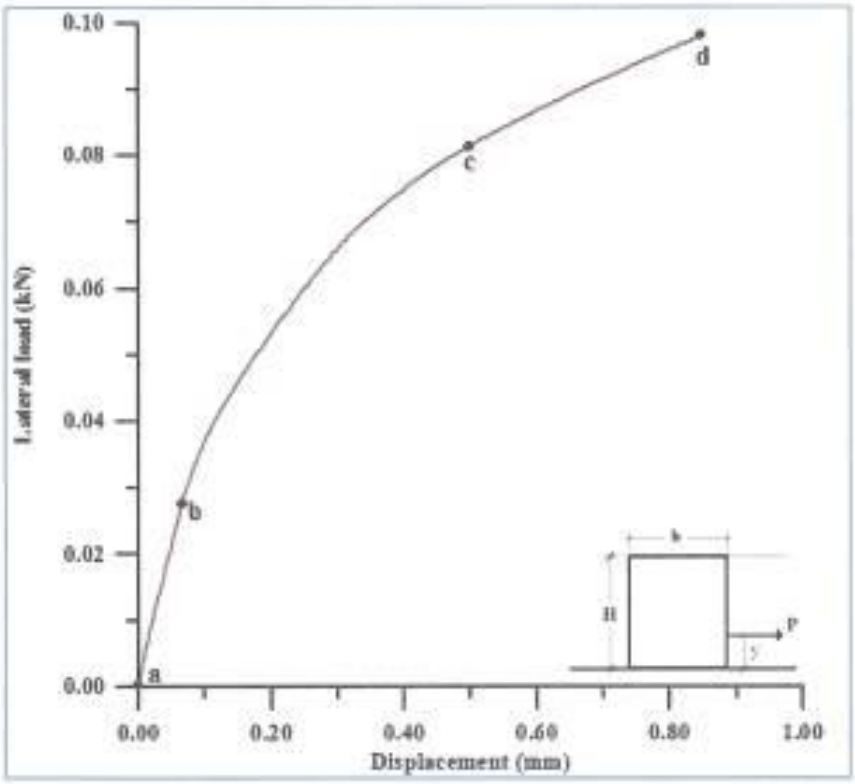

Fig.(4-20): Displacement vs. lateral load curve for cell filled with subbase, $\frac{b}{H}$ =0.75, and y=100mm .

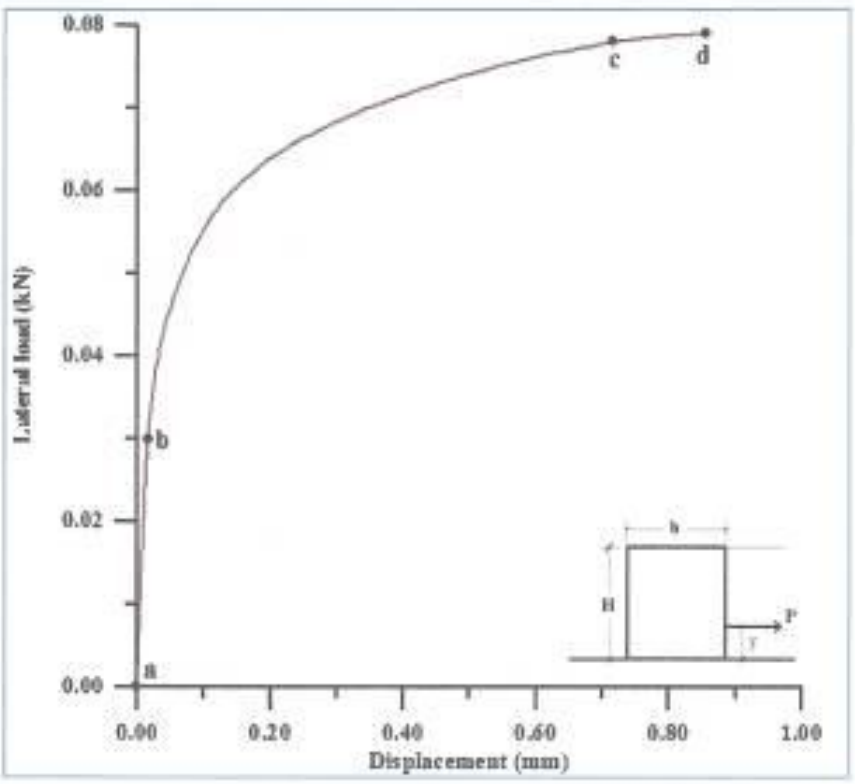

Fig.(4-21): Displacement vs. lateral load curve for cell filled with sand passing No.4, $\frac{b}{H}$ =0.75, and y=100mm .

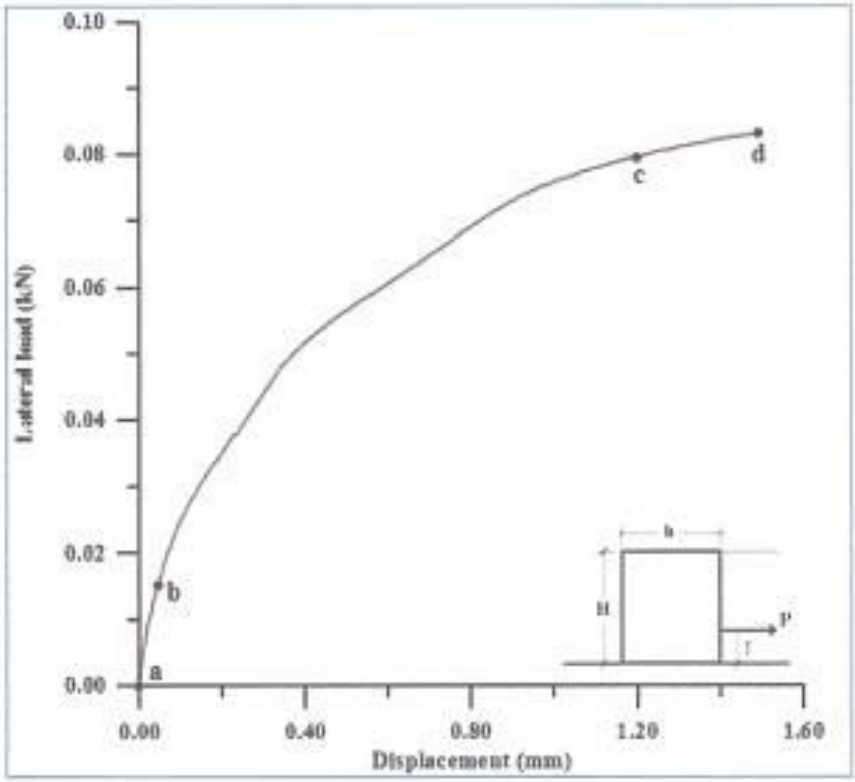

Fig.(4-22): Displacement vs. lateral load curve for cell filled with sand passing No.8, $\frac{b}{H}$ =0.75, and y=100mm .

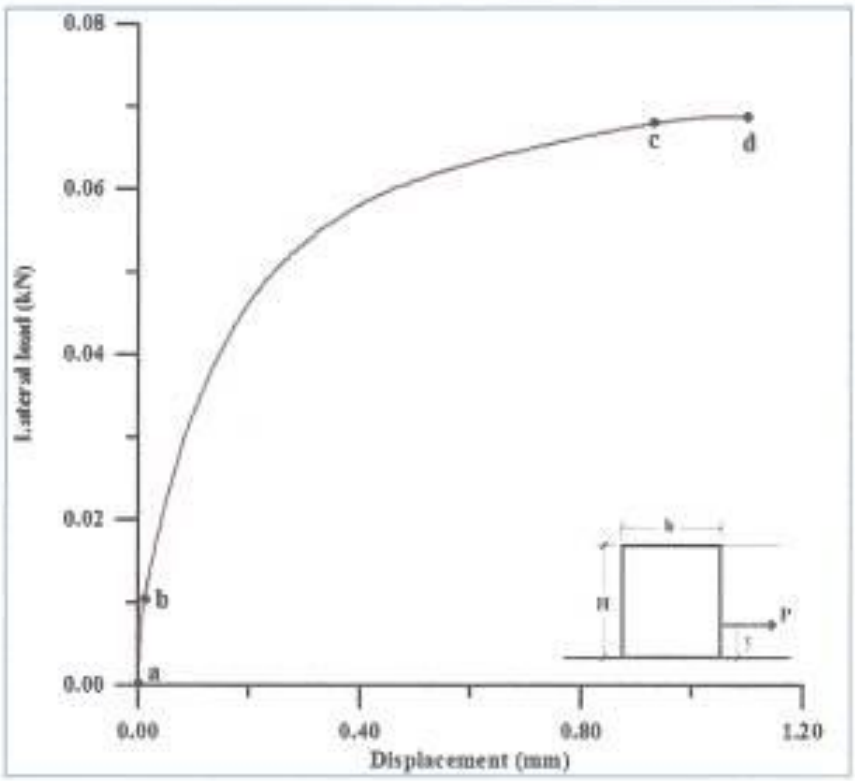

Fig.(4-23): Displacement vs. lateral load curve for cell filled with river sand, $\frac{b}{H}$ =0.75, and y=100mm .

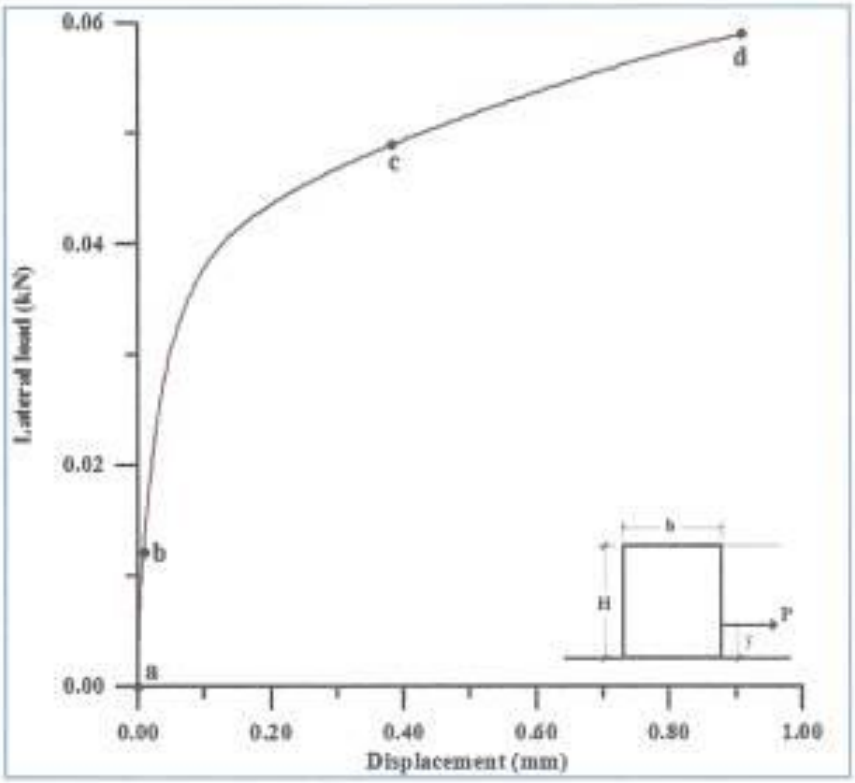

Fig.(4-24): Displacement vs. lateral load curve for cell filled with clayey sand, $\frac{b}{H}$ =0.75, and y=100mm .

4.3 MECHANISM OF CELL FAILURE

As previously mentioned, all cells were loaded until failure. It was noticed that under any loading level below failure, the displacement of any point along the height of tested cell consists of two components, translation and rotation. The translation resulted mainly from the shear distortion that take place along the foundation level. The rotation, which resulted from the applied bending moment, cause a compression on the back side and tension along the front side of the cell. Thus, the sheetpiles of the front side tend to rise while those of the back side tend to sink down into the ground, as shown in Fig. (4-25). Consequently, shear stresses along the soil/sheetpile interface surfaces are then generated. The amount and direction of these stresses depending on the magnitude and direction of the relative displacement. The soil may therefore slips along the sheetpile wall or sticks to that wall, depending on weather the

(a) Sink in the back side of the cell.

(b) Rise in the front side of the cell.

Fig. (4-25): Effect of bending moment on cell.

Shear stress exceeds the resisting shear or not. Besides, relative displacement along the sheetpile elements that caused by an even vertical shear also occur. General shear failure in the foundation may be taken place when the ultimate bearing capacity is exceeded. **[Swatek, (1967)]**.

Figures (4-26) and (4-27), indicates a possible bulkhead failure due to the presence of a weak soil beneath the cell. A general bearing capacity failure or a partial at the toe may be occurred causing the cell to sink or rotate excessively.

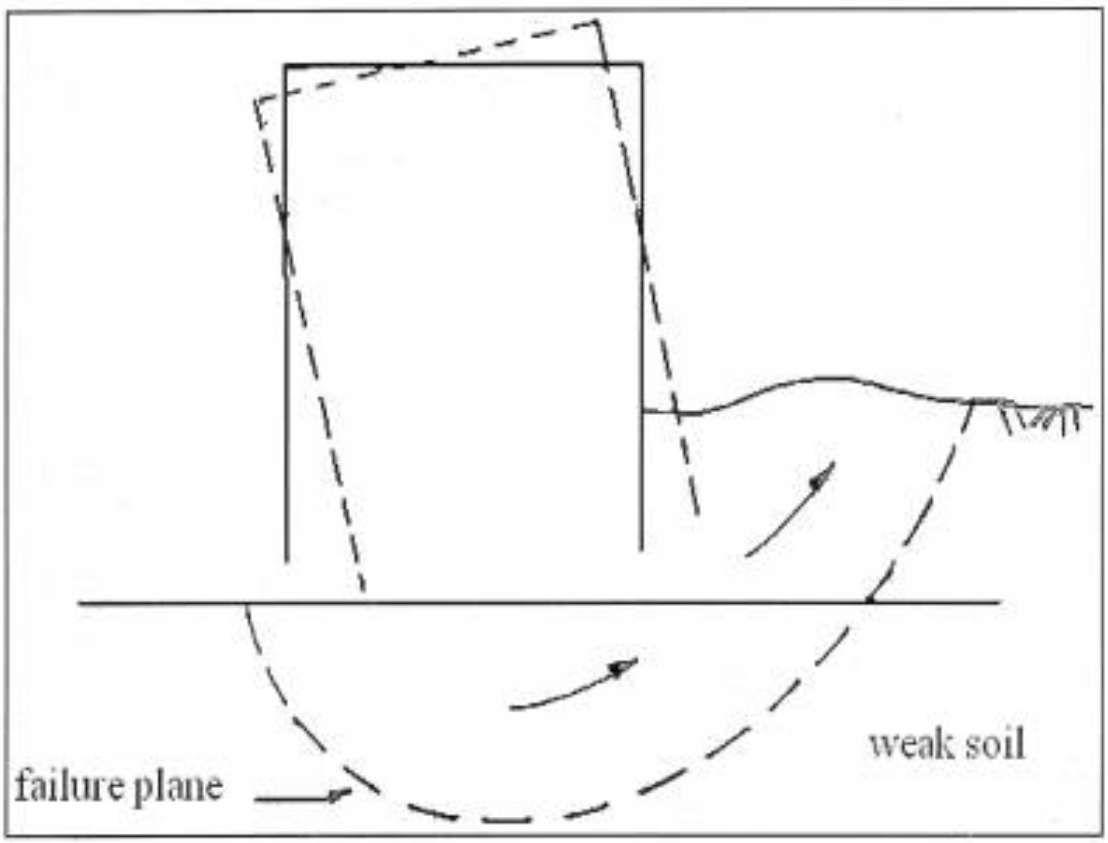

Fig. (4-26): Bearing capacity failure; [After Swatek, (1967)].

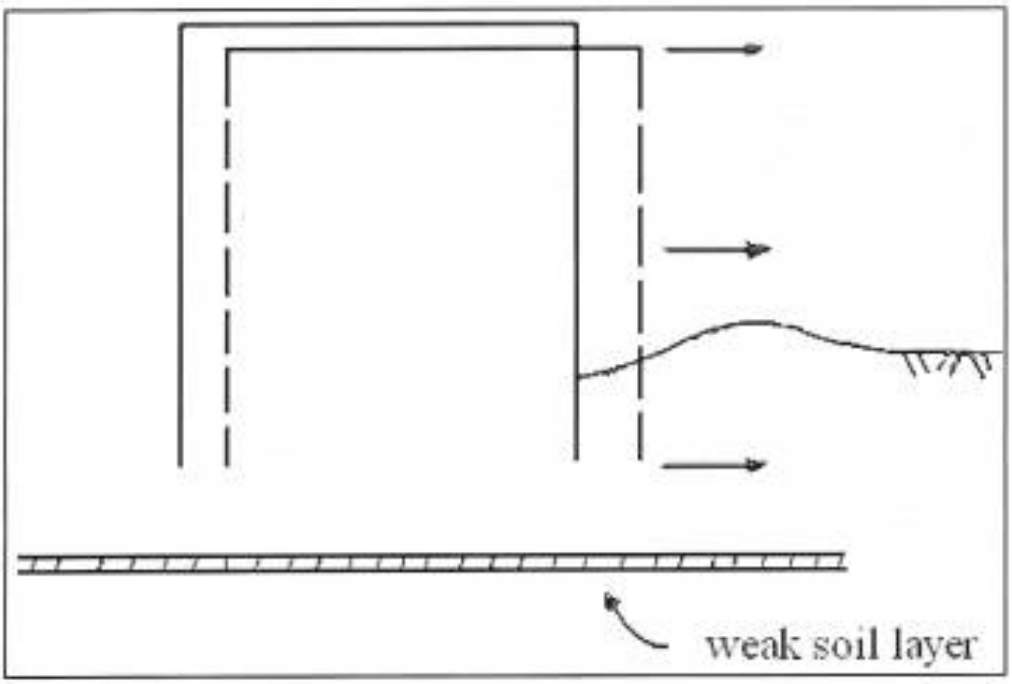

Fig. (4-27): Sliding due to zone of weakness; [After Swatek, (1967)].

Along the direction of loading, there are two modes of deformation that taken place; compression (passive) at the front side and expansion (active) at the back side. As stated by many authors **[Terzaghi, (1945)]**, the active failure is soon taken place while the passive failure requires much more displacement to generate. The cell resisting in this respect is mainly dependent on the soil passive resistance. Since the later passive resistance, is strongly dependent on the depth of point under consideration. Thus it may be anticipated that a progressive passive failure is taken place into the soil mass after each load increment. That is; a new location of the passive failure surface is generated after each load increment, therefore, if the sheetpile elements are well connected, and can safely withstand loading the only possible failure will be an external failure, that is; sliding, overturning or shear failure in the foundation. Local failure between sheet elements under the influence of hoop tension may also be anticipated when these elements are poorly interlocked. However, the displacement of any point along the cell depth, which consists of translation and

rotation, is strongly related to the applied bending moment. That is; when the load is applied at the ground surface (no bending moment) the cell will be subjected to a pure translation. The cell failure in this case will be pure shear failure.

4.4 EFFECT OF LOADING HEIGHT

To show the effect of loading height, the resistance along circular cell filled with five different types of soil (sand passing sieve No.4, sand passing sieve No.8, subbase, river sand, clayey sand) is drawn against the height of the applied loading as illustrated in Figs. (4-28) to (4-32).

All the cells considered in this study was placed on the ground surface. It is clear that the load resistance decreased as the loading height increased. The relative decreasing of resistance between the cells is according to the density of soil and its angle of friction. It is worth mentioned that a pure translation failure has taken place for all cells if the load exerted close to the base while an overturning failure was taken place under (300 mm) height of loading. Thus, the results may indicate that the sliding resistance of cell is generally greater than that of the overturning. The sliding resistance should be:

$$P = W * tan\emptyset \qquad (4\text{-}1)$$

where:

P = the lateral load.

W = the weight of the cell,

$\emptyset$ = the angle of friction of the cell fill.

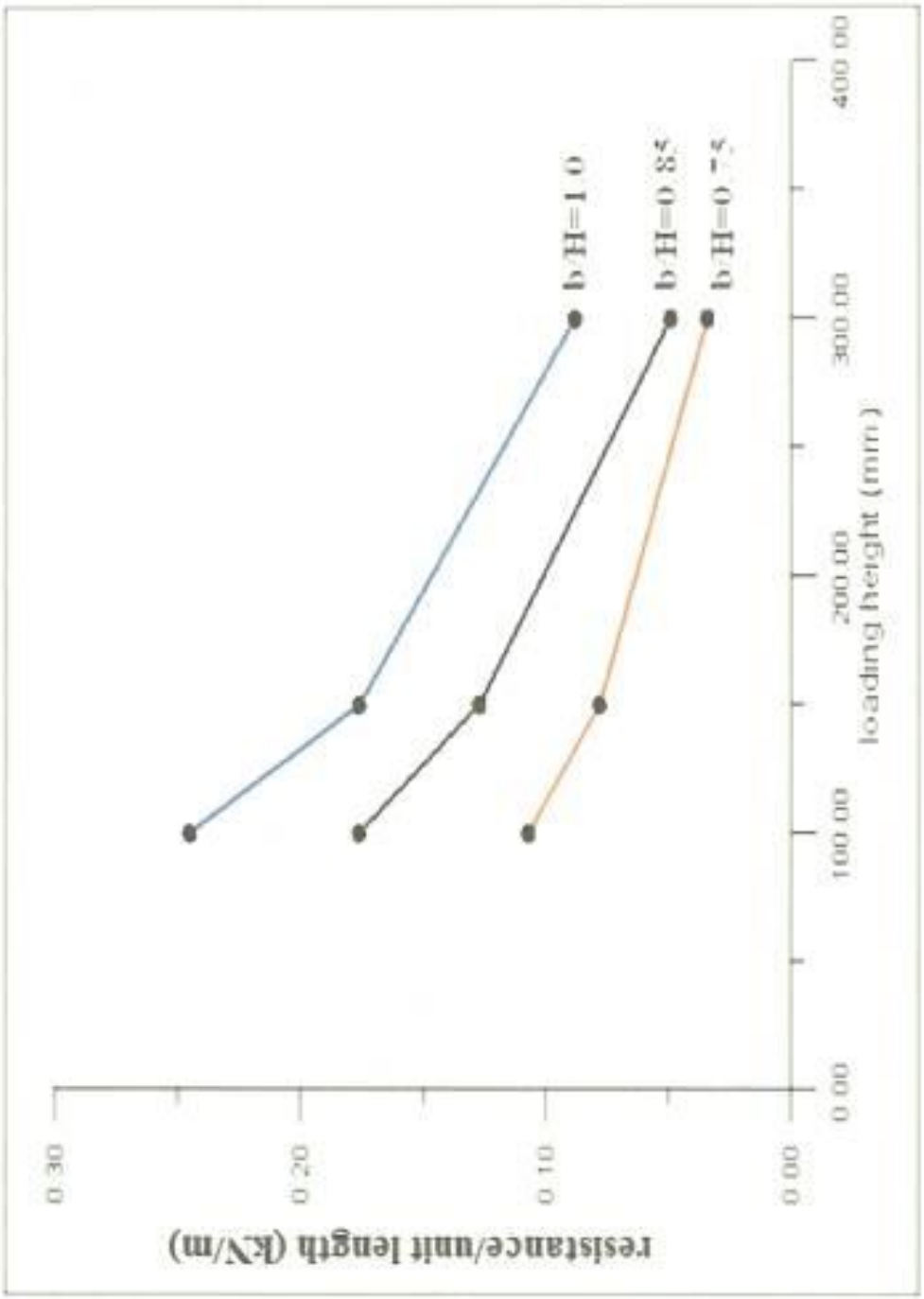

Fig. (4-28): Effect of loading height on the resistance for cells filled with subbase.

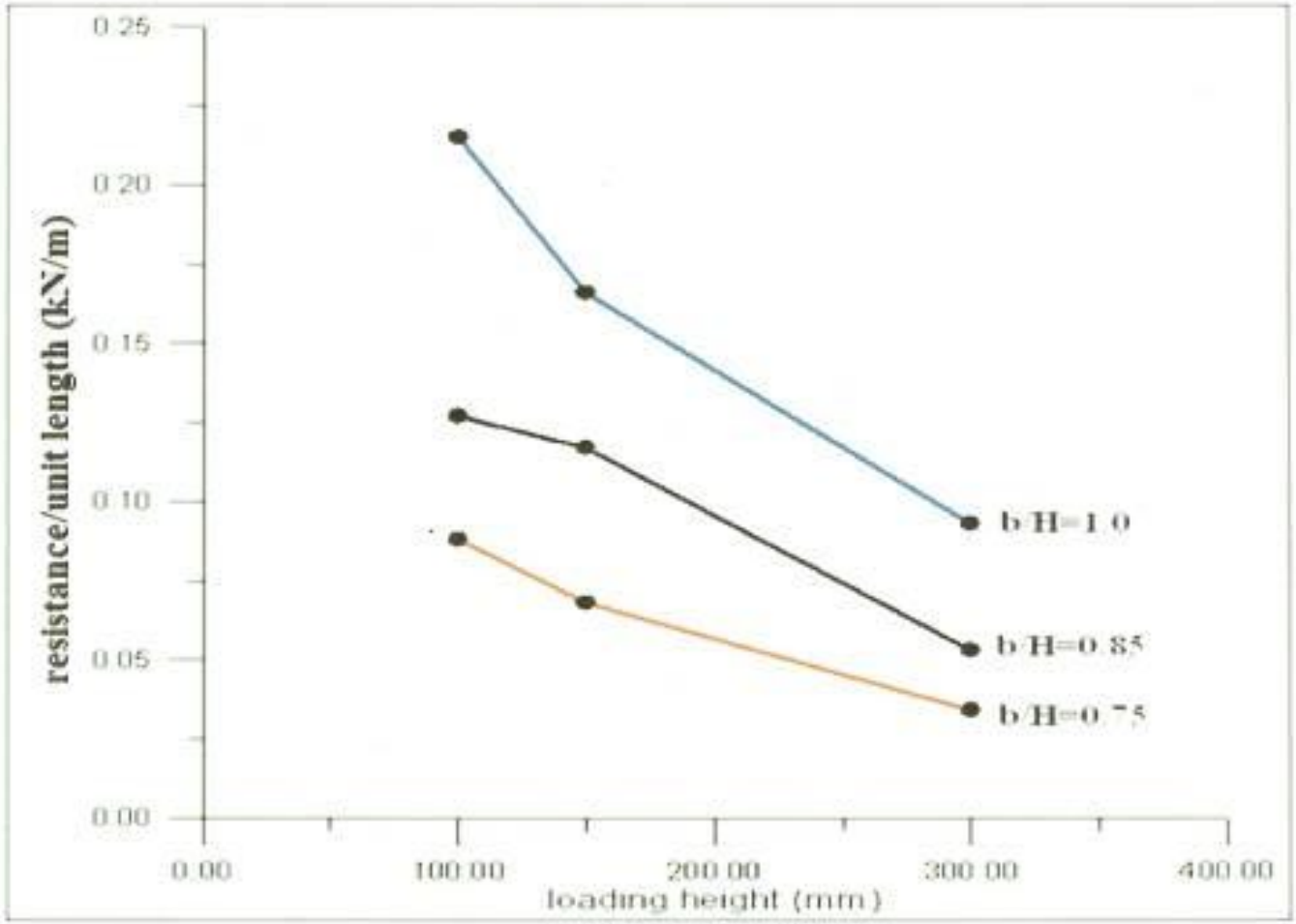

Fig. (4-29): Effect of loading height on the resistance for cells filled with sand passing No.4.

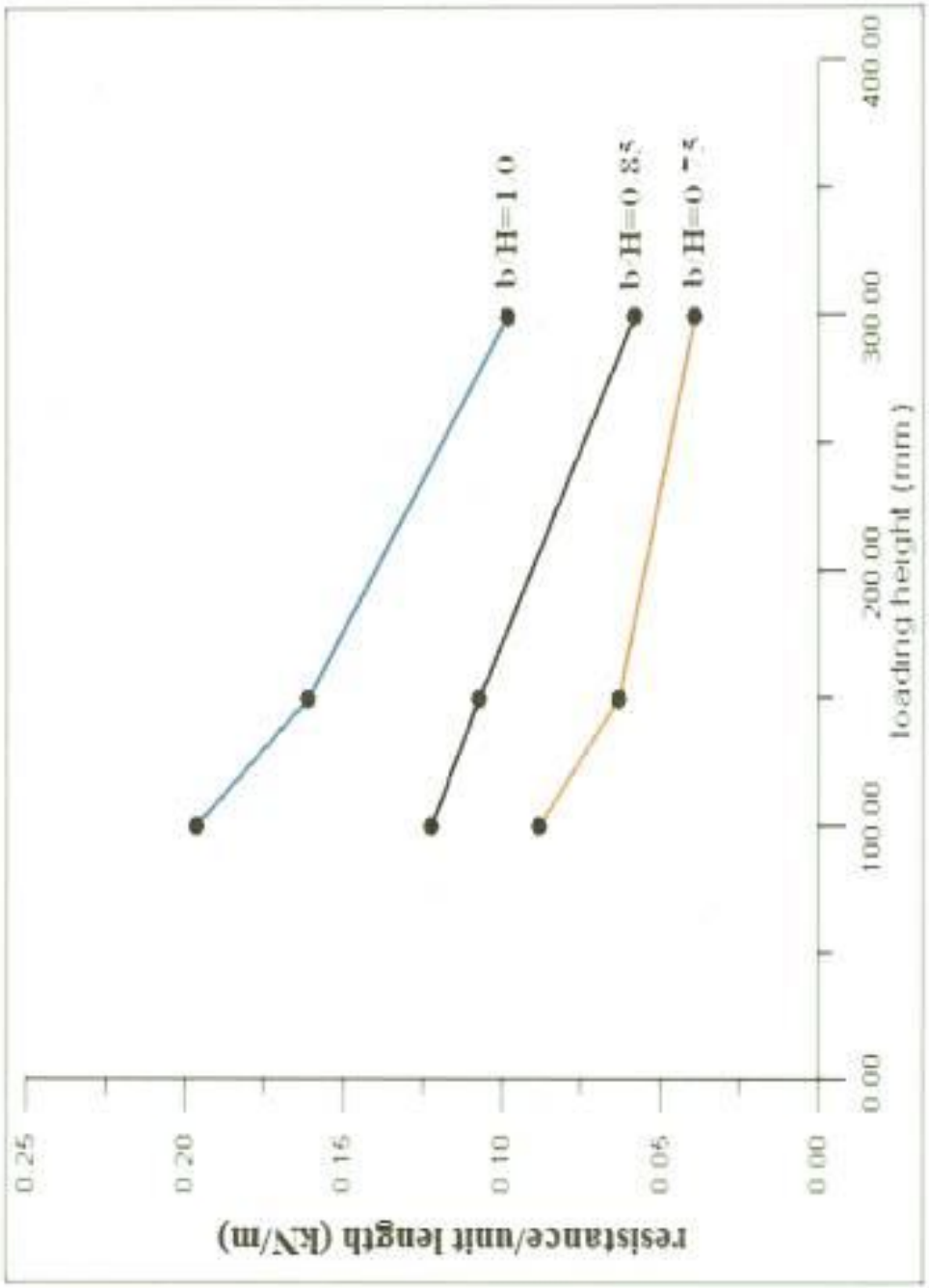

Fig. (4-30): Effect of loading height on the resistance for cells filled with sand passing No.8.

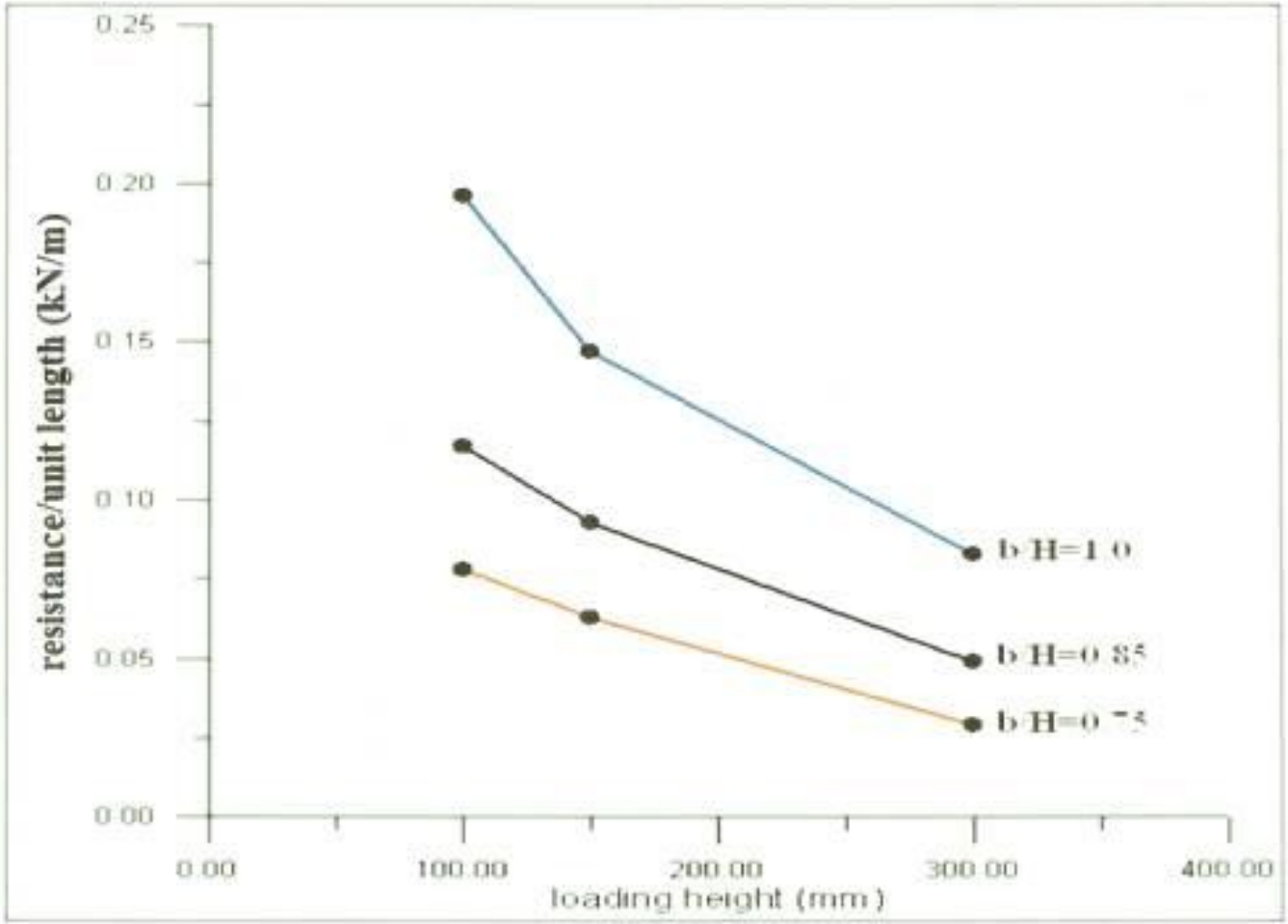

Fig. (4-31): Effect of loading height on the resistance for cells filled with river sand.

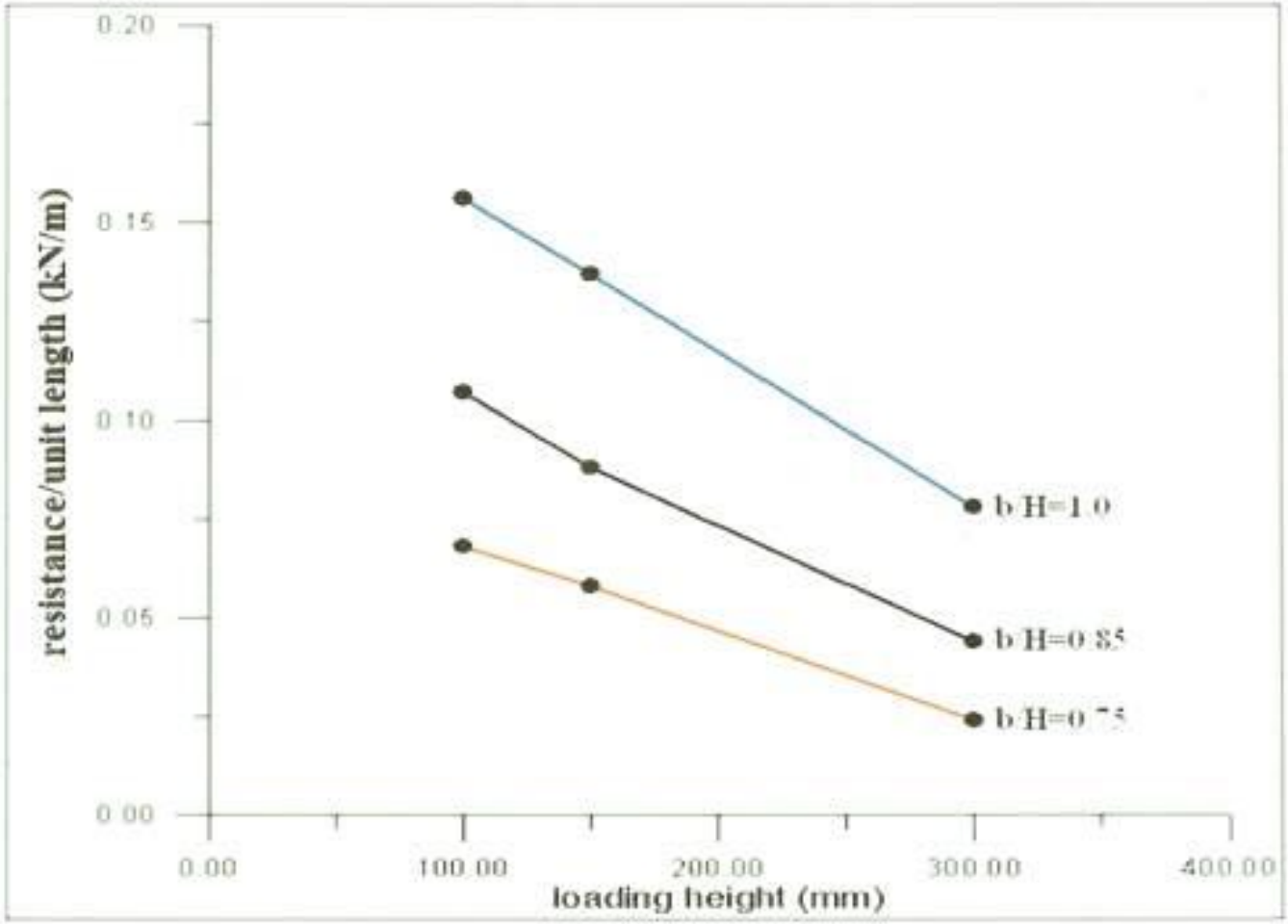

Fig. (4-32): Effect of loading height on the resistance for cells filled with clayey sand.

on the other hand, the ultimate load that cause overturning failure may be estimated as:

$$P.y = W * \frac{b}{2} \quad (4\text{-}2)$$

thus, $$P = W * \frac{b}{2y} \quad (4\text{-}3)$$

where:

y = height of lateral load.

b = the cell width.

For the cases under consideration where (Ø, b and y) are known, a comparison between the values of (P) resulted from eq. (4-1) and eq. (4-3) was listed in table (4-1). This table indicate that the sliding resistance should be greater than that of the overturning resistance except in case of a clayey sand that was used in the filling of cell had (b/H) ratio equal to (0.85), and (0.75), where the overturning resistance greater than the sliding resistance.

In an attempt to define the critical height above which an overturning failure is taken place, the value of (P) obtained from equation (4-1) is equated to that of equation (4-3).

$$W * tan\emptyset = W * \frac{b}{2y} \quad (4\text{-}4)$$

$$\therefore y_{cr} = \frac{b}{2tan\emptyset}$$

the (y_{cr})values for all tests are listed in Table (4-2).

Table (4-1): The theoretical values of cellular resistance.

Soil type		$(\frac{b}{H} = 1.0)$	$(\frac{b}{H} = 0.85)$	$(\frac{b}{H} = 0.75)$
Subbase	*Sliding resistance*	0.78*W	0.78*W	0.78*W
	Overturning resistance	0.5*W	0.425*W	0.375*W
Sand passing sieve No.4	*Sliding resistance*	0.661*W	0.661*W	0.661*W
	Overturning resistance	0.5*W	0.425*W	0.375*W
Sand passing sieve No.8	*Sliding resistance*	0.624*W	0.624*W	0.624*W
	Overturning resistance	0.5*W	0.425*W	0.375*W
River sand	*sliding resistance*	0.612*W	0.612*W	0.612*W
	Overturning resistance	0.5*W	0.425*W	0.375*W
Clayey sand	*Sliding resistance*	0.383*W	0.383*W	0.383*W
	Overturning resistance	0.5*W	0.425*W	0.375*W

Table (4-2): The y_{cr}(mm) values for all tested models.

Type of soil	Angle of friction	$\frac{b}{H} = 1.0$	$\frac{b}{H} = 0.85$	$\frac{b}{H} = 0.75$
Subbase	38	192	163	144
Sand passing sieve No.4	33.5	226.6	192.6	170
Sand passing sieve No.8	32	240	204	180
River sand	31.5	245	208	183.5
Clayey sand	21	>300	>300	293

From the table (4-2) could be see that the all values of (y_{cr}) greater than on half of cell height except one case, which the cell has ($\frac{b}{H}$ =0.75) and filled with subbase. Thus, a failure of sliding mode is more probable to take place in a cellular cofferdam subjected to an external water pressure. This is mainly because the resultant of such pressure lies below the lower half.

4.5 EFFECT OF ($\frac{b}{H}$) RATIO

To understand the effect of ($\frac{b}{H}$) ratio, three circular cells with different ratio (0.75, 0.85, 1.0) were tested under lateral load applied at one third of the cell height, mean while all the cells were placed at the ground surface, the effect of ($\frac{b}{H}$) ratio was illustrated in Fig. (4-33), through Fig. (4-37).

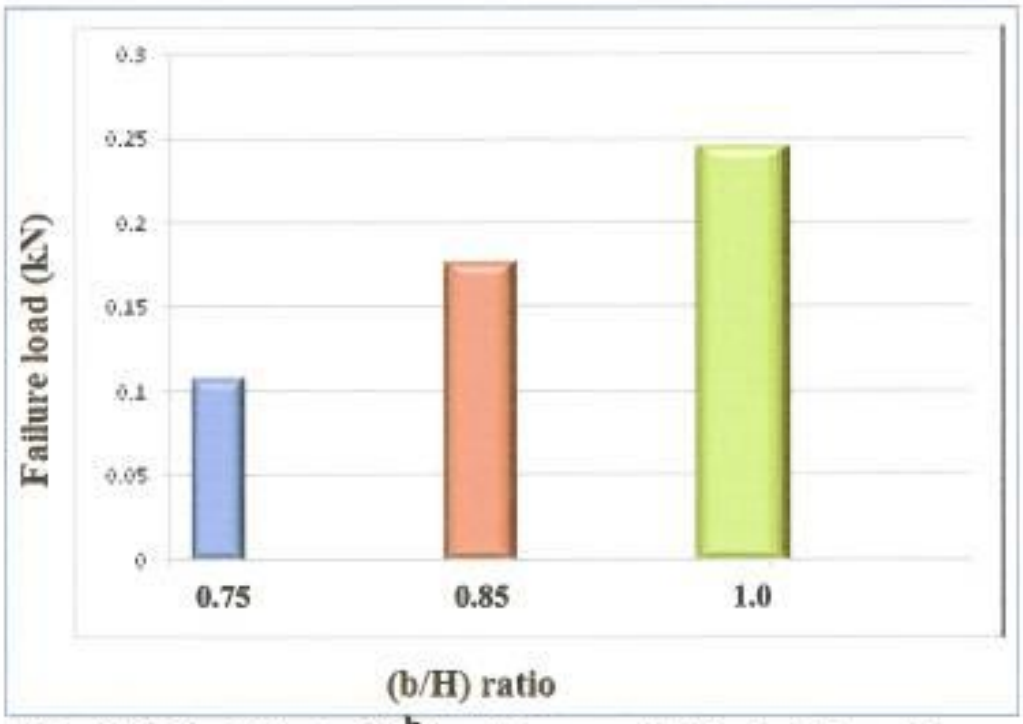

Fig. (4-33): Effect of $(\frac{b}{H})$ ratio on cell filled with subbase.

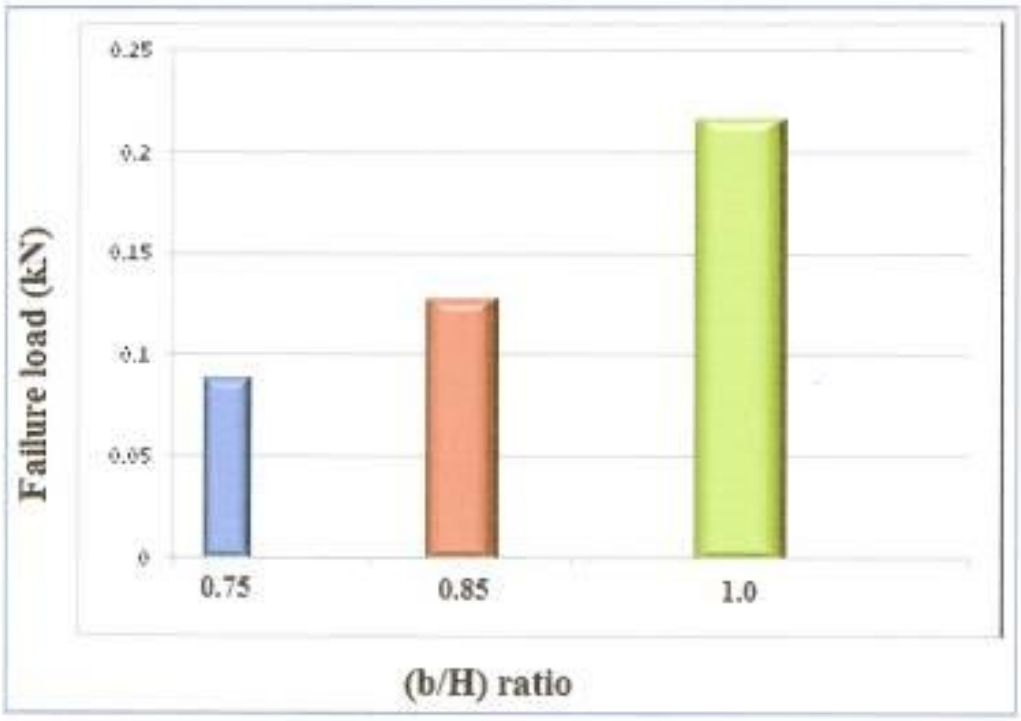

Fig. (4-34): Effect of $(\frac{b}{H})$ ratio on cell filled with sand passing No.4 .

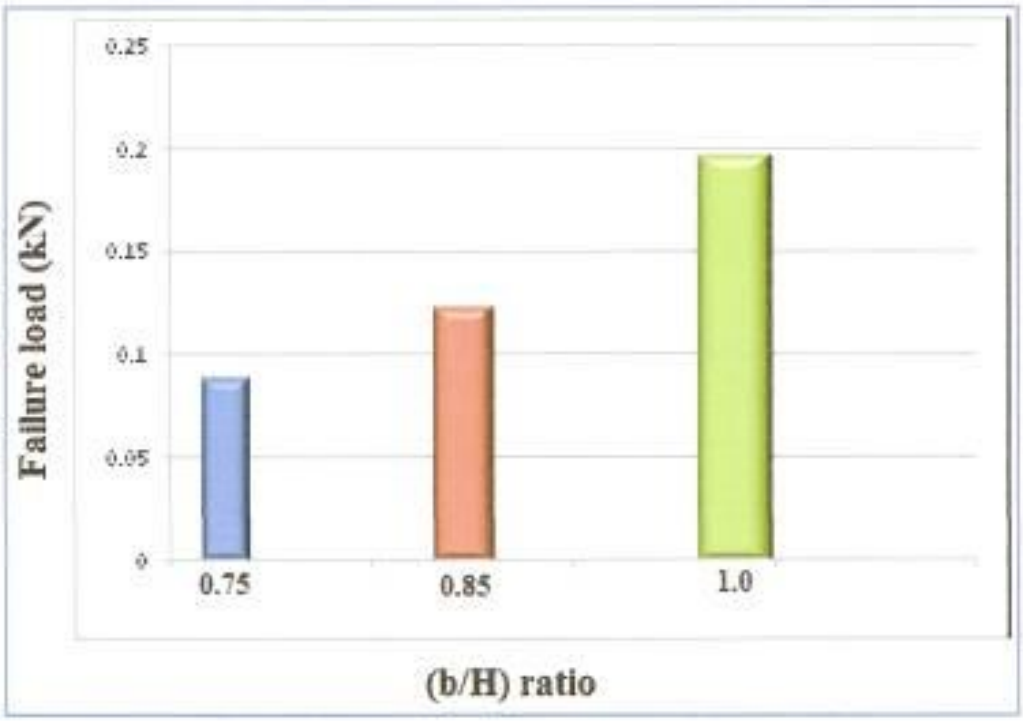

Fig. (4-35): Effect of $(\frac{b}{H})$ ratio on cell filled with sand passing No.8 .

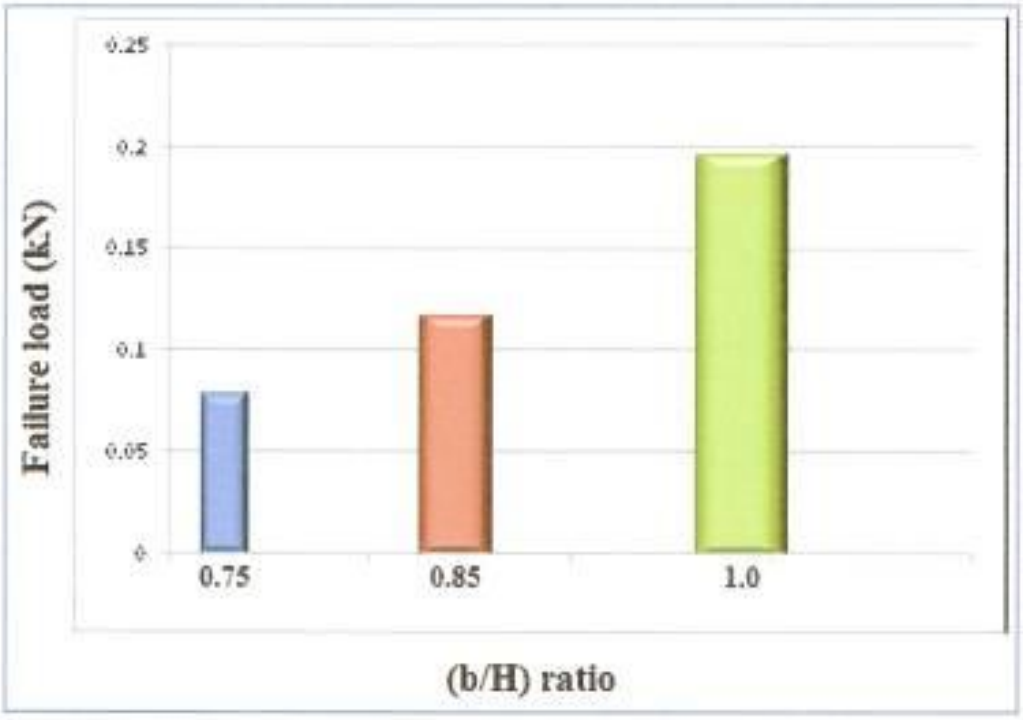

Fig. (4-36): Effect of $(\frac{b}{H})$ ratio on cell filled with river sand.

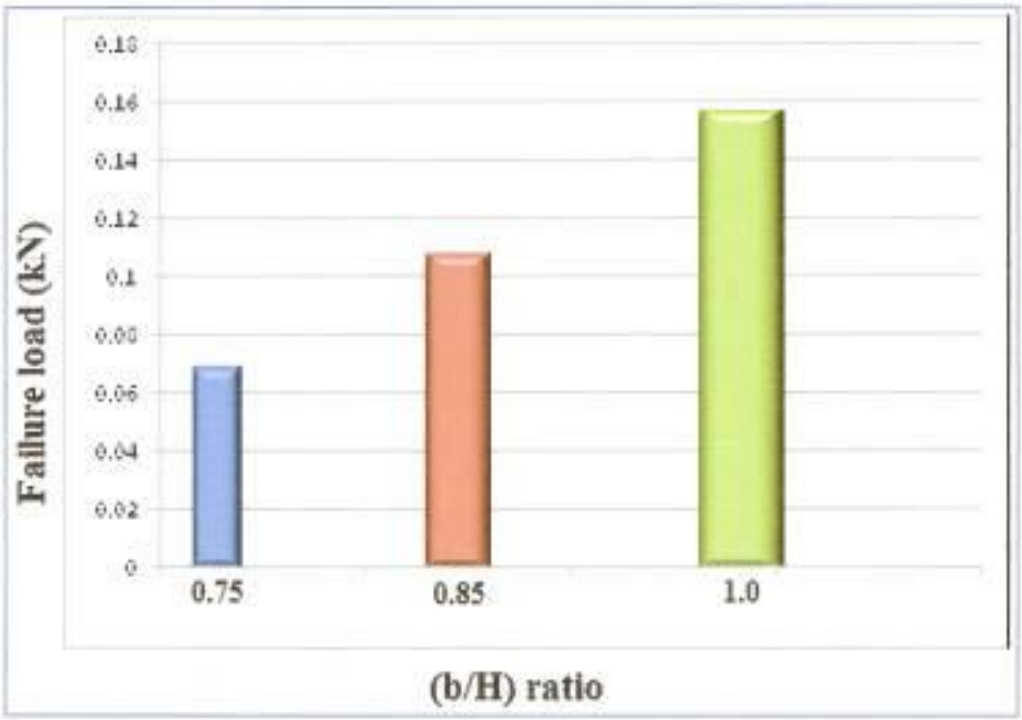

Fig. (4-37): Effect of $(\frac{b}{H})$ ratio on cell filled with clayey sand.

It is clear that the resistance decreases as the $(\frac{b}{H})$ ratio of the cell decreases. This is because in the cell $(\frac{b}{H})$ ratio result in a decrease in the weight of the cell and therefore a decrease in resistance. The ratio of decreasing illustrated in Table (4-3).

Table (4-3): Ratio of decreasing in resistance according to the $(\frac{b}{H})$ ratio.

Type of soil	Decreasing percentage of resistance from $\frac{b}{H}$ = 1.0 to 0.85	Decreasing percentage of resistance from $\frac{b}{H}$ = 0.85 to 0.75	Decreasing percentage of resistance from $\frac{b}{H}$ = 1.0 to 0.75
Subbase	28%	38.8%	56%
Sand passing No.4	40.9%	30.7%	59%
Sand passing No.8	37.5%	28%	55%
River sand	40%	33.3%	60%
Clayey sand	31.2%	36.3%	36.25%

4.6 EFFECT OF SOIL TYPE

To show the effect of soil type used in the cell fill, the cell resistance along circular cell with different $(\frac{b}{H})$ ratio is drawn against the height of the applied loading, as shown in Figs. (4-38), (4-39) and (4-40). It is clear that the cell resistance decreased as the unit weight and the angle of friction of fill decreased, when the load was applied at (100mm and 150mm), so that the cell resistance of the subbase is greater than the other soils. But when the load was applied at (300mm) the effect of angle of friction decreased and the stable of cell became dependent on the unit weight of the soil that was used in the fill, so that the cell resistance of sand passing No.8 was greater than that in the other soils fill because it has a big unit weight.

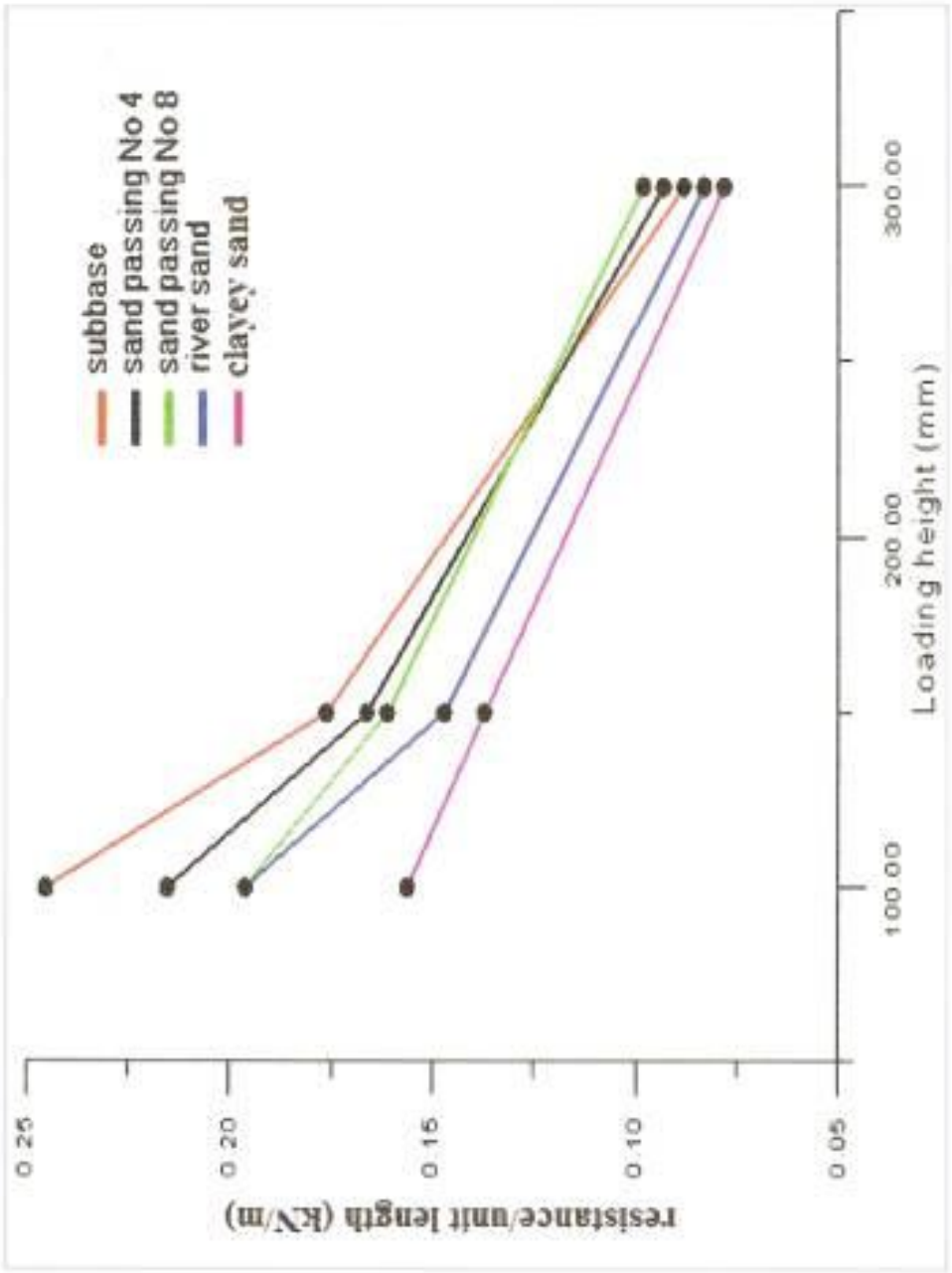

Fig. (4-38): Effect of soil type on cell resistance at $(\frac{b}{H})= 1.0$.

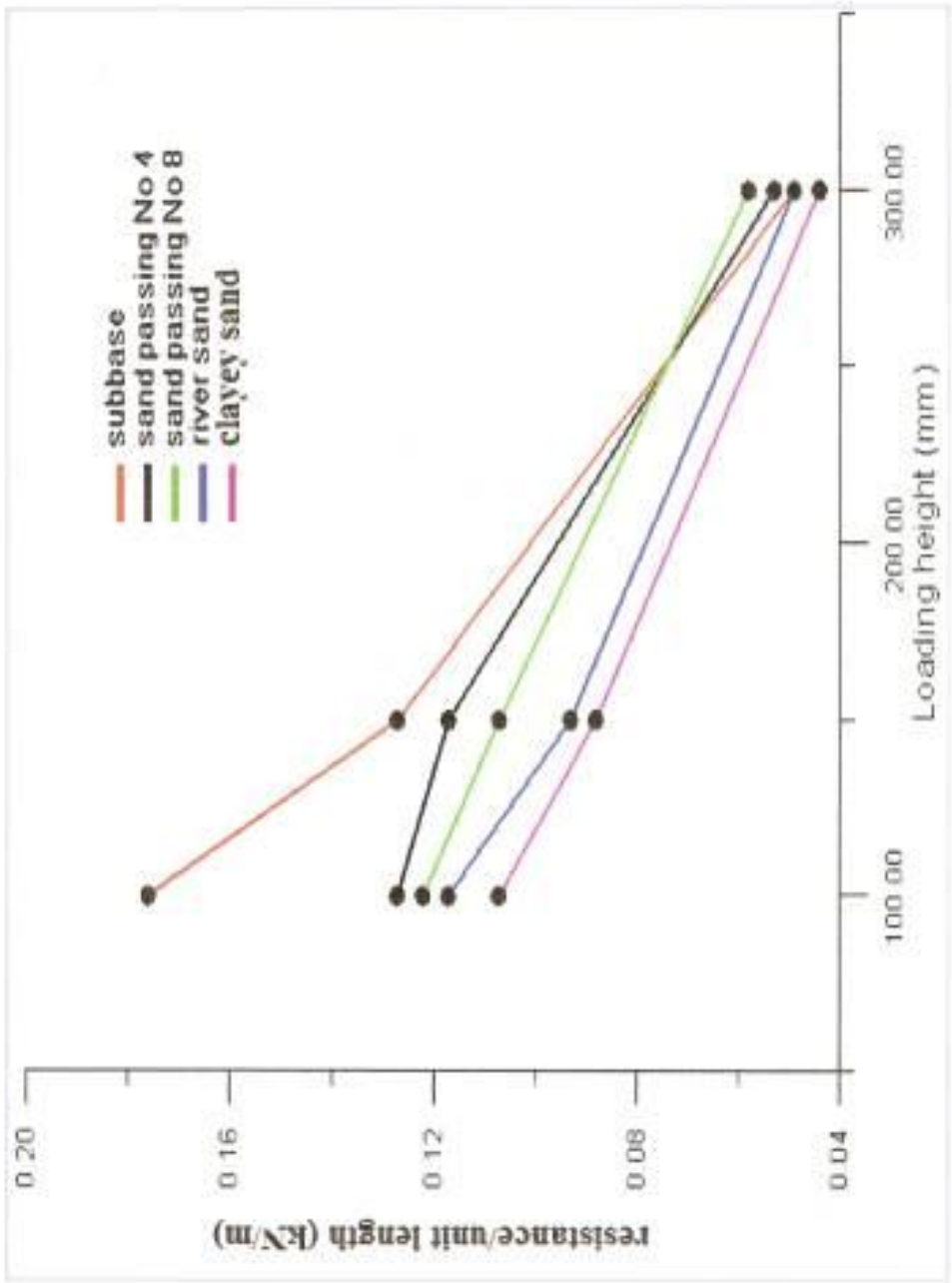

Fig. (4-39): Effect of soil type on cell resistance at $(\frac{b}{H})= 0.85$.

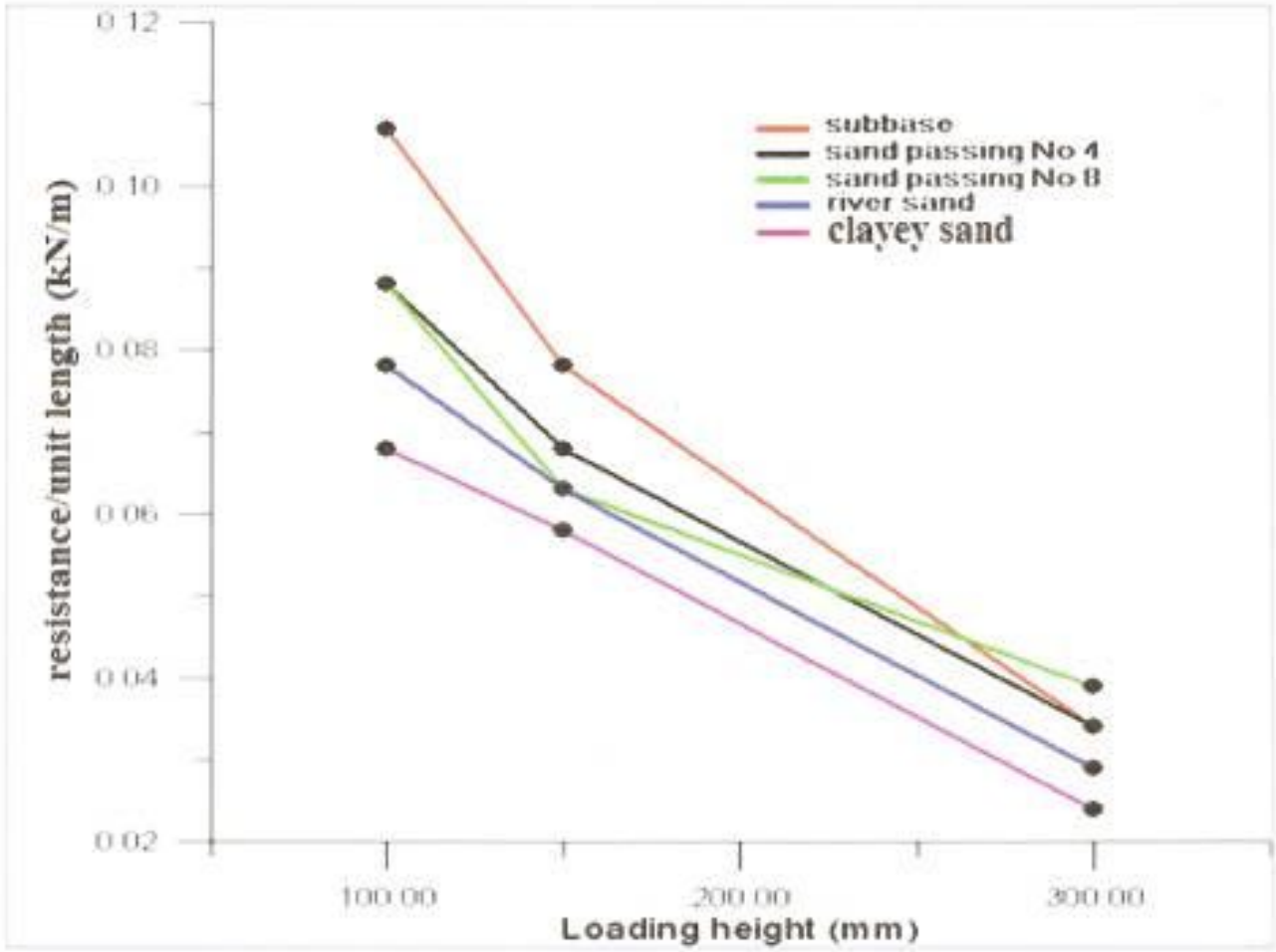

Fig. (4-40): Effect of soil type on cell resistance at $(\frac{b}{H})= 0.75$.

4.7 THE FAILURE DISPLACEMENT

Regarding the failure displacement, it was found that the behavior of the cell was divided into two cases, the cell had a big resistance with small displacement at first, and then failed suddenly. The second case, the cell was failed gradually until the total failure took place. The tests indicate that the range of failure displacement ranges between (1.03% to 2.17%) from cell height, as shown in table (4-4), where lateral load was applied at one third from cell height, and all cells put on the ground surface.

Table (4-4): Percentage of failure displacement.

Soil type \ $\frac{b}{H}$	1.0	0.85	0.75
Subbase	1.38%	1.92%	1.08%
Sand passing sieve No.4	1.77%	2.14%	1.03%
Sand passing sieve No.8	1.6%	1.1%	2.11%
River sand	1.26%	2.17%	1.34%
Clayey sand	1.75%	1.57%	1.18%

4.8 EVALUATION OF THE CURRENT DESIGN METHOD

Tables (4-5), (4-6), and (4-7), show comparison between the observed and calculated resistance of different circular cofferdams. The method of calculation has been considered for this purpose, the horizontal shear (Cummings) method. It is clear from the tables, that the Cummings method is overestimating capacity. The horizontal shear method gives a load capacity which is in not good agreement with the observed one.

Table (4-5): Comparison of the resistance observed and those calculated by horizontal shear method for cell with b=300mm, H=300mm, and y=100mm.

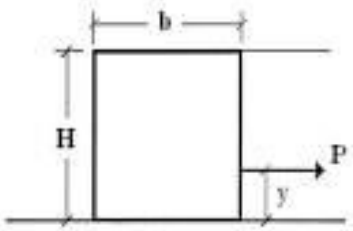

Soil type	Resistance KN/m		Difference %	Remark
	Observed	Calculated		
Subbase	0.82	0.91	-9.8%	in all cases, the load applied at one third of the cell height.
Sand passing No.4	0.719	0.82	-12.3%	
Sand passing No.8	0.65	0.8	-18.75%	
River sand	0.65	0.61	+6.5%	
Clayey sand	0.52	0.39	+33.3%	

Table (4-6): Comparison of the resistance observed and those calculated by horizontal shear method for cell with b=255mm, H=300mm, and y=100mm.

Soil type	Resistance KN/m		Difference %	Remark
	Observed	Calculated		
Subbase	0.69	0.76	-9.21%	in all cases, the load applied at one third of the cell height.
Sand passing No.4	0.5	0.69	-27.5%	
Sand passing No.8	0.48	0.67	-28.35%	
River sand	0.46	0.51	-9.8%	
Clayey sand	0.42	0.33	+27.27%	

Table (4-7): Comparison of the resistance observed and those calculated by horizontal shear method for cell with b=225mm, H=300mm, and y=100mm.

Soil type	Resistance KN/m		Difference %	Remark
	Observed	Calculated		
Subbase	0.47	0.69	-31.8%	in all cases, the load applied at one third of the cell height.
Sand passing No.4	0.39	0.65	-40%	
Sand passing No.8	0.39	0.61	-36%	
River sand	0.34	0.46	-26%	
Clayey sand	0.3	0.3	0	

CHAPTER FIVE

CONCLUSIONS AND RECOMMENDATIONS

CHAPTER FIVE
CONCLUSIONS AND RECOMMENDATIONS

5.1 CONCLUSIONS

1- The cells filled with subbase were more stable against sliding at different $(\frac{b}{H})$ ratio, the cells filled with sand passing No.8 were more stable against overturning at different $(\frac{b}{H})$ ratio.

2- Minimum ratio of decreasing in resistance of the cell if the $(\frac{b}{H})$ ratio decreasing from (1.0 to 0.85) is nearly (28%) when the cell filling with subbase, if the $(\frac{b}{H})$ ratio decreases from (0.85 to 0.75). The minimum ratio of decreasing in resistance is nearly (28%) when the cell filling with sand passing No.8, and if the $(\frac{b}{H})$ ratio decreases from (1.0 to 0.75) the minimum ratio of decreasing in resistance of the cell is nearly (36.25%) when the cell is filled with clayey sand.

3- The resistance of cell against lateral load decrease as the height of the applied load increases, due to the sliding resistance of cell is generally greater than that of the overturning load resistance.

4- Comparison of the experimental results with the calculated values indicates that the Cummings method not agreed with observed results.

5.2 RECOMMENDATIONS

1- The work has been based on three isolated circular cells. It should be more useful to investigate the stability of many circular cells connected with each other by arcs.

2- The effect of embedment depth with different depths of the performance is required.

3- The method of applying failure loads should be improved over the cable technique possibly with hydraulic pressure, to ensure a more realistic distribution of lateral forces.

4- The effect of the sheetpile flexibility should be studied.

REFERENCES

* **Alizadeh, M. M. [1973]:** "Circular land cofferdam for deep excavation". J. Construction, ASCE, Vol. 99, No.GT1, pp. 11-20.

* **Bowles, J. E. [1997]:** "Foundation analysis and design". McGraw-Hill, New York, U.S.A.

* **Burki, Naveed K. and Richards, R. Jr. [1975]:** "Photoelastic analysis of a cofferdam". J. Geotech., ASCE, Vol. 101, No. GT2, pp.129-145.

* **Al-Chalabi, K. T. [1959]:** "Stability of cellular cofferdams". Ph. D.Thesis, College of Engineering, University of Michigan, U.S.A.

* **Chen H., Guo G., Che Q. and Jiang Z. [2008]:** "Model test and numerical computation about cofferdam break of Jinghong hydroelectric station". Yangtze River Scientific Research Institute, Wuhan430010, China.

* **Cummings, E. M. [1957]:** "Cellular cofferdams and docks". Proceedings, ASCE, Vol. 83, No. WW3, pp. 13-45.

* **Dismuke, T. D. [1975]:** "Foundation Engineering Handbook". Litton Educational Publishing Inc., New York, U.S.A.

* **Esring, M. I. [1970]:** " Stability of cellular cofferdams against vertical shear". J. Soil Mechanics and Foundation, ASCE, Vol. 96, No. 6, pp. 1853-1862.

* **Horiuchi, S. , Taketsuka, M. , Takuro, O., and Kawasaki, H. [1992]:** "Fly-ash slurry island: I. Theoretical and experimental investigations". J. Materials. ASCE, Vol. 4, Paper No.2, pp. 117-133.

* **Kelly, P. B. [1969]:** "Design and evaluation of a foundation model testing device". M. Sc. Thesis, Oregon State University, U.S.A.

* **Krynine, D. P. [1945]:** "Discussion of stability and stiffness of cellular cofferdams". ASCE, Vol. 110, Paper No.2253, pp. 1175-1178.

* **Lacroix, Y., Esrig, M. I., and Lusher, U. [1970]:** "Design, construction, and performance of cellular cofferdams". Specialty Conf. Lateral Stresses in the Ground and Design of Earth-Retaining Structures, ASCE, pp. 271-328.

* **Maitland, J. K., and Schroeder, W. L. [1979]:** "Model study of circular sheetpile cells". J. Geotech. Div., ASCE, Vol. 105, Paper No. GT7, pp. 805-821.

* **Mohammod R. Amin Khan, Jiro T., Hiroki F. and Osamu K. [2001]:** "Behavior of double sheetpile wall cofferdam on sand observed in centrifuge tests". IJPMG-International Journal of Physical Moodelling in Geotechnics, Tokyo, Japan.

* **Peng Y., Chen W. and JI C. [2007]:** "Hydraulic calculation for overflow cofferdam in staged diversion". North China Electric Power University, Ministry of Education, Beijing, China.

* **Polivka, J. J. [1945]:** "Discussion of stability and stiffness of cellular cofferdams by K. Terzaghi". Transactions, ASCE, Vol. 110, pp. 1170-1187.

* **Rossow, Mark P. [1984]:** "Sheetpile interlock tension in cellular cofferdams". J. Geotech., ASCE, Vol. 110, No. GT10, pp. 1446-1458.

* **Al-Shamkhi M. A. Al-Mejeed [1992]:** " The stability of cellular dams". M. Sc. thesis, College of Engineering, University of Baghdad.

* **Schroeder, W. L. and Maitland, J. K. [1979]:** "Cellular bulkhead and cofferdams". J. Geotech, ASCE, Vol. 105, No. GT7, pp. 823-837.

* **Schroder, W. L. Marker. D. K. and Khuayjarempanishk, T. [1977]:** "Performance of a cellular wharf". J. Geotech. Eng. Div., ASCE, Vol. 103, No. GT3, pp. 153-168.

* **Sorota, Max. D. and Kinner, Edward B. [1981]:** "Cellular cofferdam for trident drydock: Design". J. Geotech. Div., ASCE, Vol. 107, No. GT12, pp. 1643-1655.

* **Swatek, E. P. [1967]:** "Cellular cofferdams design and practice". J. Wtrwys. and Hrbrs. Div., ASCE, Vol. 93, pp. 109-132.

* **Al-Taee, K.N. [1990]:** "Effect of geometry on stability of cellular cofferdams". M. Sc. thesis, College of Engineering, University of Baghdad.

* **Teng, W. C. [1962]:** "Foundation design". Prentic Hall, Inc., Englewood Cliffs N. J. .

* **Terzaghi, K. [1945]:** "Stability and stiffness of cellular cofferdams". Transactions, ASCE, Vol. 110, pp. 1083-1202.

* **Thomas, Harry E., Speaker, John J., and Miller, Eugene J. [1975]:** "Difficult dam problems - - Cofferdam failure". J. Geotech, ASCE, Vol.45, No.GT8, pp. 66-70.

* **TVA (Tennesse Valley Authority) [2003]:** "Steel sheetpile cellular cofferdams on rock". Technical Monograph 75, Pilebuck edition, U.S.A. .

* **USACE (U.S.Army Corps of Engineers) [1989]:** "Design of sheetpile cellular structures". Engineering Manual No. 1110-2-2503, Department of the Army, Washington.

* **USS (United State Steel). [1970]:** "USS sheetpiling design manual". www.eng-tips.com.

* **USS (United State Steel). [1974]:** "USS sheetpiling design manual". www.eng-tips.com.

* **White, A. , Cheney, J. A. , and Duke, M. [1963]:** "Field study of cellular bulkhead". Transactions, ASCE, Vol. 128, pp. 463-508.

* **Zhang L., Bian Z., Jing F. and Yang J. [2008]:** "Anchorage cable unloading technology in cofferdam of diversion tunnel inlet of some water power station". Laboratory of Geotechnical Mechanics and Engineering of the Ministry of Water Resources, Yangtze River Scientific Research Institute,Wuhan430010, China.

الخلاصة

تتضمن الدراسة إنشاء نماذج من السدود الخلوية الدائرية وإجراء الفحوصات المختبرية عليها لملاحظة مدى استقراريتها ضد فشل الانزلاق والانقلاب. حيث تم إنشاء ثلاث نماذج من السدود الخلوية الدائرية المنفردة، كل واحده تمتلك نسبة عرض إلى ارتفاع مختلفة، وفحص كل خليه منها وسط خمس أنواع مختلفة من التربة. كذلك الدراسة تضمنت تقييم طريقة (Cummings) في التصميم.

وقد تم التوصل في هذه الدراسة إلى:

الخلايا التي كان إملائها بالسبيس كانت أكثر مقاومه للانزلاق من الخلايا التي ملئت بالترب الأخرى عند نسبة عرض إلى ارتفاع مختلفة، في حين كانت الخلايا المملوئه بالرمل المار على المنخل No.8 أكثر إستقرارية ومقاومه للانقلاب من الخلايا التي ملئت بالترب الأخرى مهما تغيرت نسبة العرض إلى الارتفاع.

كانت اقل نسبه للنقصان في مقاومة الخلية مايقارب الـ (٢٨%) عندما قلت نسبة العرض إلى الارتفاع من (١ إلى ٠,٨٥) وتحدث عندما تكون الخلية مملوئه بالسبيس، في حين أن اقل نسبة للنقصان في مقاومة الخلية مايقارب الـ (٢٨%) أيضا عندما تقل نسبة العرض إلى الارتفاع من (٠,٨٥ إلى ٠,٧٥) وتحدث عندما تكون الخلية مملوئه بالرمل المار على المنخل No.8 ، وعندما تتغير نسبة العرض إلى الارتفاع من (١ إلى ٠,٧٥) يكون اقل فقدان من مقاومة الخلية مايقارب الـ (٣٦,٢٥%) ويحدث ذلك عندما تكون الخلية مملوئه بالرمل الطيني.

جمهورية العراق
وزارة التعليم العالي والبحث العلمي
جامعة بابل

دراسة مختبرية للتحري عن إستقرارية سدود الإنضاب الخلوية

الرسالة
مقدمة إلى كلية الهندسة، جامعة بابل
كجزء من متطلبات نيل شهادة الماجستير
في هندسة الموارد المائية

من قبل:
حيدر سامي محمد الخياط
(بكالوريوس هندسة مدنية)

تشرين الأول, ٢٠٠٩